

HAZARD MAPPING OF THE PHILIPPINES USING LIDAR (PHIL-LIDAR 1)

LiDAR Surveys and Flood Mapping of Rosario-Lobo River



University of the Philippines Training Center
for Applied Geodesy and Photogrammetry
Mapúa Institute of Technology

APRIL 2017



© University of the Philippines Diliman and Mapua Institute of Technology 2017

Published by the UP Training Center for Applied Geodesy and Photogrammetry (TCAGP)
College of Engineering
University of the Philippines – Diliman
Quezon City
1101 PHILIPPINES

This research project is supported by the Department of Science and Technology (DOST) as part of its Grants-in-Aid Program and is to be cited as:

E.C. Paringit and F.A. Uy (eds.) (2017), *LiDAR Surveys and Flood Mapping of Rosario-Lobo River*, Quezon City: University of the Philippines Training Center on Applied Geodesy and Photogrammetry-128pp.

The text of this information may be copied and distributed for research and educational purposes with proper acknowledgement. While every care is taken to ensure the accuracy of this publication, the UP TCAGP disclaims all responsibility and all liability (including without limitation, liability in negligence) and costs which might incur as a result of the materials in this publication being inaccurate or incomplete in any way and for any reason.

For questions/queries regarding this report, contact:

Dr. Francis Aldrine A. Uy
Project Leader, Phil-LiDAR 1 Program
MAPUA Institute of Technology
City of Manila, Metro Manila 1002
E-mail: faauy@mapua.edu.ph

Enrico C. Paringit, Dr. Eng.
Program Leader, Phil-LiDAR 1 Program
University of the Philippines Diliman
Quezon City, Philippines 1101
E-mail: ecparingit@up.edu.ph

National Library of the Philippines
ISBN: 978-621-430-061-7

TABLE OF CONTENTS

LIST OF TABLES.....	v
LIST OF FIGURES.....	vii
LIST OF ACRONYMS AND ABBREVIATIONS.....	x
CHAPTER 1: OVERVIEW OF THE PROGRAM AND ROSARIO-LOBO RIVER.	1
1.1 Background of the Phil-LiDAR 1 Program.	1
1.2 Overview of the Rosario-Lobo River Basin.	1
CHAPTER 2: LIDAR DATA ACQUISITION OF THE ROSARIO-LOBO FLOODPLAIN.....	3
2.1 Flight Plans.	3
2.2 Ground Base Stations.	5
2.3 Flight Missions.	7
2.4 Survey Coverage.	8
CHAPTER 3: LIDAR DATA PROCESSING OF THE ROSARIO-LOBO FLOODPLAIN.....	10
3.1 Overview of the LiDAR Data Pre-Processing.	10
3.2 Transmittal of Acquired LiDAR Data.	11
3.3 Trajectory Computation.	11
3.4 LiDAR Point Cloud Computation.	13
3.5 LiDAR Data Quality Checking.	14
3.6 LiDAR Point Cloud Classification and Rasterization.	18
3.7 LiDAR Image Processing and Orthophotograph Rectification.	20
3.8 DEM Editing and Hydro-Correction.	21
3.9 Mosaicking of Blocks.	23
3.10 Calibration and Validation of Mosaicked LiDAR DEM.	25
3.11 Integration of Bathymetric Data into the LiDAR Digital Terrain Model.	28
3.12 Feature Extraction.	30
3.12.1 Quality Checking of Digitized Features' Boundary.	30
3.12.2 Height Extraction.	31
3.12.3 Feature Attribution.	31
3.12.4 Final Quality Checking of Extracted Features.	32
CHAPTER 4: LIDAR VALIDATION SURVEY AND MEASUREMENTS OF THE ROSARIO-LOBO RIVER BASIN...33	33
4.1 Summary of Activities.	33
4.2 Control Survey.	34
4.3 Baseline Processing.	39
4.4 Network Adjustment.	40
4.5 Cross-section and Bridge As-Built survey and Water Level Marking.	43
4.6 Validation Points Acquisition Survey.	47
4.7 River Bathymetric Survey.	49
CHAPTER 5: FLOOD MODELING AND MAPPING.....	52
5.1 Data Used for Hydrologic Modeling.	52
5.1.1 Hydrometry and Rating Curves.	52
5.1.2 Precipitation.	52
5.1.3 Rating Curves and River Outflow.	53
5.2 RIDF Station.	55
5.3 HMS Model.	56
5.4 Cross-section Data.	59
5.5 Flo 2D Model.	61
5.6 Results of HMS Calibration.	63
5.7 Calculated outflow hydrographs and discharge values for different rainfall return periods.	65
5.7.1 Hydrograph using the Rainfall Runoff Model.	65
5.8 River Analysis (RAS) Model Simulation.	66
5.9 Flow Depth and Flood Hazard.	66
5.10 Inventory of Areas Exposed to Flooding.	73
5.11 Flood Validation.	80
REFERENCES.....	82
ANNEXES.....	83
Annex 1. Technical Specifications of the LiDAR Sensors used in the Rosario-Lobo Floodplain Survey....	83
Annex 2. NAMRIA Certification of Reference Points Used in the LiDAR Survey.	84
Annex 3. Baseline Processing Reports of Control Points used in the LiDAR Survey.	85
Annex 4. The LiDAR Survey Team Composition.	86
Annex 5. Data Transfer Sheet for Rosario-Lobo Floodplain.	87

Annex 6. Flight logs for the flight missions.	89
Annex 7. Flight status reports.	91
Annex 8. Mission Summary Reports.	95
Annex 9. Rosario-Lobo Model Basin Parameters.	105
Annex 10. Rosario-Lobo Model Reach Parameters.	108
Annex 11. Rosario-Lobo Field Validation Points.	110
Annex 12. Educational Institutions Affected by flooding in Rosario-Lobo Floodplain.	117
Annex 13. Health Institutions affected by flooding in Rosario-Lobo Floodplain.	118

LIST OF TABLES

Table 1. Flight planning parameters for Pegasus LiDAR system.....	3
Table 2. Details of the recovered NAMRIA horizontal control point BTG-30 used as base station for the LiDAR acquisition. 6	6
Table 3. Details of the established horizontal control point BTG-30A used as base station for the LiDAR Acquisition with established coordinates.	7
Table 4. Ground control points used during LiDAR data acquisition.....	7
Table 5. Flight missions for LiDAR data acquisition in Rosario-Lobo Floodplain.....	8
Table 6. Actual parameters used during LiDAR data acquisition	8
Table 7. List of municipalities and cities surveyed during Rosario-Lobo Floodplain LiDAR survey.....	8
Table 8. Self-Calibration Results values for Rosario-Lobo flights.	13
Table 9. List of LiDAR blocks for Rosario-Lobo Floodplain.	14
Table 10. Rosario-Lobo classification results in TerraScan.	18
Table 11. LiDAR blocks with its corresponding area.	21
Table 12. Shift Values of each LiDAR Block of Rosario-Lobo Floodplain.	23
Table 13. Calibration Statistical Measures.	27
Table 14. Validation Statistical Measures.	28
Table 15. Quality Checking Ratings for Rosario-Lobo Building Features.	30
Table 16. Building Features Extracted for Rosario-Lobo Floodplain.	31
Table 17. Total Length of Extracted Roads for Rosario-Lobo Floodplain.	31
Table 18. Number of Extracted Water Bodies for Pandanan Floodplain.	32
Table 19. List of Reference and Control Points occupied for Rosario-Lobo River Survey.....	35
Table 20. Baseline Processing Summary Report for Rosario-Lobo River Basin Static Survey.....	39
Table 21. Control Point Constraints	40
Table 22. Adjusted Grid Coordinates	40
Table 23. Adjusted Geodetic Coordinates	42
Table 24. Reference and control points used and its location (Source: NAMRIA, UP-TCAGP)	42
Table 25. RIDF values for Ambulong Rain Gauge computed by PAGASA	55
Table 26. Range of Calibrated Values for Rosario-Lobo	63
Table 27. Summary of the Efficiency Test of Rosario-Lobo HMS Model	64
Table 28. Peak values of the Rosario-Lobo HECHMS Model outflow using the Ambulong RIDF.....	65
Table 29. Municipalities affected in Rosario-Lobo Floodplain	66
Table 30. Affected areas in Lobo, Batangas during a 5-Year Rainfall Return Period	73
Table 31. Affected areas in Lobo, Batangas during a 5-Year Rainfall Return Period	73
Table 32. Affected Areas in Lobo, Batangas during 25-Year Rainfall Return Period	75
Table 33. Affected Areas in Lobo, Batangas during 25-Year Rainfall Return Period	75
Table 34. Affected Areas in Lobo, Batangas during 100-Year Rainfall Return Period	77
Table 35. Affected Areas in Lobo, Batangas during 100-Year Rainfall Return Period	77
Table 36. Areas covered by each warning level with respect to the rainfall scenarios	79
Table 37. Actual flood vs simulated flood depth at different levels in the Rosario-Lobo River Basin.	81
Table 38. Summary of the Accuracy Assessment in the Rosario-Lobo River Basin Survey	81

LIST OF FIGURES

Figure 1. Map of Rosario-Lobo River Basin	2
Figure 2. Flight plans for Pegasus System used for Rosario-Lobo Floodplain	4
Figure 3. Flight plans and base stations for Rosario-Lobo Floodplain.	5
Figure 4. GPS set-up over BTG-30 in the vicinity of Brgy. Pallocan, Batangas City along the E side dike of Calumpang River, on the N side of Calumpang Bridge (a) and NAMRIA reference point BTG-30 (b) as recovered by the field team.	6
Figure 5. Actual LiDAR survey coverage for Rosario-Lobo Floodplain.	9
Figure 6. Schematic Diagram for Data Pre-Processing Component	10
Figure 7. Smoothed Performance Metric Parameters of Rosario-Lobo Flight 3381P.	11
Figure 8. Solution Status Parameters of Rosario-Lobo Flight 3381P.	12
Figure 9. Best Estimated Trajectory for Rosario-Lobo Floodplain.	13
Figure 10. Boundary of the processed LiDAR data over Rosario-Lobo Floodplain	14
Figure 11. Image of data overlap for Rosario-Lobo Floodplain.	15
Figure 12. Pulse density map of merged LiDAR data for Rosario-Lobo Floodplain.	16
Figure 13. Elevation difference map between flight lines for Rosario-Lobo Floodplain.	17
Figure 14. Quality checking for Rosario-Lobo flight 3381P	18
Figure 15. Tiles for Rosario-Lobo Floodplain (a) and classification results (b) in TerraScan.	19
Figure 16. Point cloud before (a) and after (b) classification.	19
Figure 17. The production of last return DSM (a) and DTM (b), first return DSM (c) and secondary DTM (d) in some portion of Rosario-Lobo Floodplain.	20
Figure 18. Portions in the DTM of Rosario-Lobo Floodplain – a bridge before	22
(a) and after (b) manual editing; mountain ridges before (c) and after (d) data retrieval; and a building before (e) and after (f) manual editing.	
Figure 19. Map of Processed LiDAR Data for Rosario-Lobo Floodplain.	24
Figure 20. Map of Rosario-Lobo Floodplain with validation survey points in green.	26
Figure 21. Correlation plot between calibration survey points and LiDAR data.	27
Figure 22. Correlation plot between validation survey points and LiDAR data.	28
Figure 23. Map of Rosario-Lobo Floodplain with bathymetric survey points shown in blue.	29
Figure 24. QC blocks for Rosario-Lobo building features.	30
Figure 25. Extracted features for Rosario-Lobo Floodplain.	32
Figure 26. Rosario-Lobo River Survey Extent	33
Figure 27. GNSS Network of Rosario-Lobo River field survey	34
Figure 28. GNSS receiver, Trimble® SPS 985, set-up at BG-207 at Palico Bridge,	35
Brgy. Luntal, Nasugbu, Batangas	
Figure 29. GNSS receiver, Trimble® SPS 985, set-up at BTG-7 in Dela Paz Lighthouse in	36
Brgy. Dela Paz, Batangas City, Batangas	
Figure 30. GNSS receiver, Trimble® SPS 882, set-up at UP-ASN at San Nicholas Bridge,	36
Brgy. Poblacion, San Nicholas, Batangas	
Figure 31. GNSS base receiver, Trimble® SPS 852, set-up at UP-BTN at Bantilan Bridge,	37
Brgy. Manggalang Banitilan, Sariaya, Quezon	
Figure 32. GNSS base receiver, Trimble® SPS 852, set-up at UP-CLG1 in Calumpang Bridge,	37
Brgy. Cumintang Ibaba, Batangas City, Batangas	
Figure 33. GNSS base receiver, Trimble® SPS 882, set-up at UP-LOBO, in Lobo Bridge,	38
Brgy. Lagadlarin, Lobo, Batangas	
Figure 34. GNSS receiver, Trimble® SPS 882, set-up at UP-LWY1 at Lawaye Bridge,	38
Brgy. Calitcalit-Mabalanoy, San Juan, Batangas	
Figure 35. Cross-section survey conducted on Rosario-Lobo River in Brgy. Lagadlarin,	43
Municipality of Lobo	
Figure 36. Location map of Rosario-Lobo Bridge cross-section	44
Figure 37. Rosario-Lobo Bridge cross-section diagram	45
Figure 38. Marking of MSL-based elevation on the pier on the left side facing downstream	46
(A) and right side (B) at the Lobo Bridge, Lobo Batangas	
Figure 39. Validation points acquisition survey set up along Rosario-Lobo River Basin	47
Figure 40. LiDAR validation points acquisition survey for Rosario-Lobo River Basin	48
Figure 41. Manual bathymetric survey along Rosario Lobo River from the mouth of the river	49
up to the Lobo Bridge	
Figure 42. Bathymetric points gathered from Rosario-Lobo River	50
Figure 43. Centerline riverbed profile of Rosario-Lobo River	51

Figure 44. Location map of Rosario-Lobo HEC-HMS model used for calibration	52
Figure 45. Cross-Section Plot of Rosario-Lobo Bridge	53
Figure 46. Rating curve at Lobo Bridge, Batangas City, Batangas Province	54
Figure 47. Rainflow and outflow data at Rosario-Lobo River used for modeling	54
Figure 48. Ambulong RIDF location relative to Rosario-Lobo River Basin	55
Figure 49. Synthetic storm generated for a 24-hr period rainfall for various return periods.	56
Figure 50. Soil map of the Rosario-Lobo River Basin	56
Figure 51. Land cover map of Rosario-Lobo River Basin	57
Figure 52. Slope map of Rosario-Lobo River Basin	57
Figure 53. Stream delineation map of Rosario-Lobo River Basin	58
Figure 54. HEC-HMS generated Rosario-Lobo River Basin Model.	59
Figure 55. River cross-section of Rosario-Lobo River generated through Arcmap HEC GeoRAS tool	60
Figure 56. Screenshot of subcatchment with the computational area to be modeled	61
in FLO-2D GDS Pro	
Figure 57. Generated 100-year rain return hazard map from FLO-2D Mapper	62
Figure 58. Generated 100-year rain return flow depth map from FLO-2D Mapper	62
Figure 59. Outflow Hydrograph of Rosario-Lobo produced by the HEC-HMS model compared	63
with observed outflow.	
Figure 60. Outflow hydrograph at Rosario-Lobo Station generated using Ambulong RIDF	65
simulated in HEC-HMS	
Figure 61. Sample output of Rosario-Lobo RAS Model	66
Figure 62. 100-year Flood Hazard Map for Rosario-Lobo Floodplain overlaid on Google Earth imagery.....	67
Figure 63. 100-year Flow Depth Map for Rosario-Lobo Floodplain overlaid on Google Earth imagery.....	68
Figure 64. 25-year Flood Hazard Map for Rosario-Lobo Floodplain overlaid on Google Earth imagery.....	69
Figure 65. 25-year Flow Depth Map for Rosario-Lobo Floodplain overlaid on Google Earth imagery.....	70
Figure 66. 5-year Flood Hazard Map for Rosario-Lobo Floodplain overlaid on Google Earth imagery.....	71
Figure 67. 5-year Flow Depth Map for Rosario-Lobo Floodplain overlaid on Google Earth imagery.....	72
Figure 68. Affected areas in Lobo, Batangas during a 5-Year Rainfall Return Period.	74
Figure 69. Affected areas in Lobo, Batangas during a 5-Year Rainfall Return Period.	74
Figure 70. Affected Areas in Lobo, Batangas during 25-Year Rainfall Return Period	76
Figure 71. Affected Areas in Lobo, Batangas during 25-Year Rainfall Return Period	76
Figure 72. Affected Areas in Lobo, Batangas during 100-Year Rainfall Return Period	78
Figure 73. Affected Areas in Lobo, Batangas during 100-Year Rainfall Return Period	78
Figure 74. Rosario-Lobo Flood Validation Points	80
Figure 75. Flood map depth vs. actual flood depth	81

LIST OF ACRONYMS AND ABBREVIATIONS

AAC	Asian Aerospace Corporation	IMU	Inertial Measurement Unit
Ab	abutment	kts	knots
ALTM	Airborne LiDAR Terrain Mapper	LAS	LiDAR Data Exchange File format
ARG	automatic rain gauge	LC	Low Chord
ATQ	Antique	LGU	local government unit
AWLS	Automated Water Level Sensor	LiDAR	Light Detection and Ranging
BA	Bridge Approach	LMS	LiDAR Mapping Suite
BM	benchmark	m AGL	meters Above Ground Level
CAD	Computer-Aided Design	MMS	Mobile Mapping Suite
CN	Curve Number	MSL	mean sea level
CSRS	Chief Science Research Specialist	NSTC	Northern Subtropical Convergence
DAC	Data Acquisition Component	PAF	Philippine Air Force
DEM	Digital Elevation Model	PAGASA	Philippine Atmospheric Geophysical and Astronomical Services Administration
DENR	Department of Environment and Natural Resources	PDOP	Positional Dilution of Precision
DOST	Department of Science and Technology	PPK	Post-Processed Kinematic [technique]
DPPC	Data Pre-Processing Component	PRF	Pulse Repetition Frequency
DREAM	Disaster Risk and Exposure Assessment for Mitigation [Program]	PTM	Philippine Transverse Mercator
DRRM	Disaster Risk Reduction and Management	QC	Quality Check
DSM	Digital Surface Model	QT	Quick Terrain [Modeler]
DTM	Digital Terrain Model	RA	Research Associate
DVBC	Data Validation and Bathymetry Component	RIDF	Rainfall-Intensity-Duration-Frequency
FMC	Flood Modeling Component	RMSE	Root Mean Square Error
FOV	Field of View	SAR	Synthetic Aperture Radar
GiA	Grants-in-Aid	SCS	Soil Conservation Service
GCP	Ground Control Point	SRTM	Shuttle Radar Topography Mission
GNSS	Global Navigation Satellite System	SRS	Science Research Specialist
GPS	Global Positioning System	SSG	Special Service Group
HEC-HMS	Hydrologic Engineering Center - Hydrologic Modeling System	TBC	Thermal Barrier Coatings
HEC-RAS	Hydrologic Engineering Center - River Analysis System	UPC	University of the Philippines Cebu
HC	High Chord	UP-TCAGP	University of the Philippines – Training Center for Applied Geodesy and Photogrammetry
IDW	Inverse Distance Weighted [interpolation method]	UTM	Universal Transverse Mercator
		WGS	World Geodetic System

CHAPTER 1: OVERVIEW OF THE PROGRAM AND ROSARIO-LOBO RIVER

Enrico C. Paringit, Dr. Eng., Dr. Francis Aldrine Uy, and Engr. Fabor Tan

1.1 Background of the Phil-LIDAR 1 Program

The University of the Philippines Training Center for Applied Geodesy and Photogrammetry (UP-TCAGP) launched a research program entitled “Nationwide Hazard Mapping using LiDAR” or Phil-LiDAR 1, supported by the Department of Science and Technology (DOST) Grants-in-Aid (GiA) Program. The program was primarily aimed at acquiring a national elevation and resource dataset at sufficient resolution to produce information necessary to support the different phases of disaster management. Particularly, it targeted to operationalize the development of flood hazard models that would produce updated and detailed flood hazard maps for the major river systems in the country.

Also, the program was aimed at producing an up-to-date and detailed national elevation dataset suitable for 1:5,000 scale mapping, with 50 cm and 20 cm horizontal and vertical accuracies, respectively. These accuracies were achieved through the use of the state-of-the-art Light Detection and Ranging (LiDAR) airborne technology procured by the project through DOST.

The implementing partner university for the Phil-LiDAR 1 Program is the MAPUA Institute of Technology (MIT). MIT is in charge of processing LiDAR data and conducting data validation reconnaissance, cross section, bathymetric survey, validation, river flow measurements, flood height and extent data gathering, flood modeling, and flood map generation for the 26 river basins in the Cavite-Batangas-Rizal-Quezon (CABARZON) Region. The university is located in the City of Manila within Metro Manila in the National Capital Region.

1.2 Overview of the Rosario-Lobo River Basin

Rosario Lobo River Basin covers portions of Batangas City, Taysan, Rosario, and Lobo Municipalities. Based on the DENR-RBCO, it has a drainage area of 197 km² and an estimated 315 million cubic meter (MCM) annual run-off (RBCO, 2015).

Its main stem, the Rosario-Lobo River, is also known as Rosario River or Lobo River. The Rosario – Lobo River is the main tributary that drains the tributaries in the southern municipalities of Batangas. It is among the twenty-five (25) river basins in CABARZON Area. The river runs along eight (8) barangays in Municipality of Lobo with a total estimated population number of 12,368 people living within based on 2010 NSO census. Its waters according to its beneficial use, is categorized as Class A or Public Water Supply Class II, which is for primary contact recreation such as bathing, swimming, skin diving, etc., particularly those designated for tourism purposes.

In addition, the Rosario-Lobo River’s headwaters come from the municipality of Rosario, and flow down to the gently sloping lands in the municipality of Lobo. Thus, whenever heavy rains are brought by typhoons, low lying areas in Lobo are severely flooded, which makes flooding a perennial problem in the past years. For instance, in 1988, the approach of the Lobo Bridge collapsed after a strong typhoon swelled up the river. The municipality of Lobo was declared under a state of calamity on November 7, 2012 after being assessed to be the most affected number of families and damages when Typhoon Ofel hit the province. Recently, flooding from typhoon Glenda in 2014 damaged rice and corn plantations and forced several families to evacuate to prevent any loss of lives.

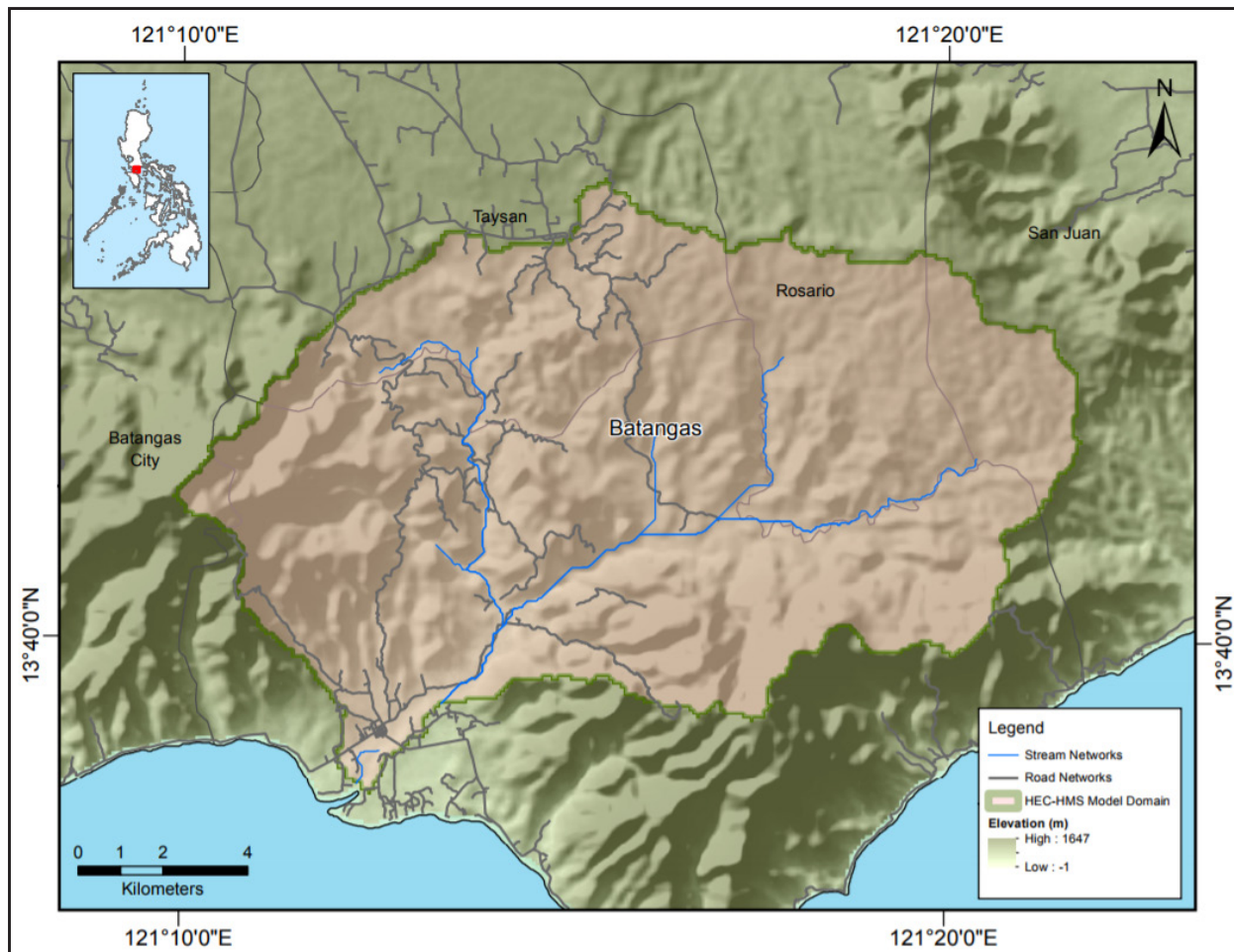


Figure 1. Map of Rosario-Lobo River Basin

In order to prevent or at least minimize the effects of flooding hazards among the people and crops in the river basin, a combination of several technologies have been employed to produce flood hazard maps. One of these is the introduction of LiDAR data, which primarily contains elevation used to derive the Digital Elevation Model or DEM. From elevation values, one can infer the presence and behavior of water bodies (such as rivers, streams, ponds, and lakes) and structures (such as roads, bridges, and buildings). Next, important data such as discharge and rainfall events gathered through fieldwork are used as inputs to the hydrological model. The gathered data is used to generate hydrographs that is used to create the calibrated model. These generated outputs, along with LiDAR data, will then be input for the river hydraulic model. The final output for these processes will be flood hazard maps of the river basin. The generated maps are used for urban planning and disaster risk reduction planning.

The flood hazard maps indicate the flood-prone areas within the river basin. With the accuracy and precision of LiDAR data, one can determine the flood height in a point or within a certain area. The local government unit of Lobo can now determine the appropriate locations for agriculture, businesses, and government projects. Thus, we can now make our wisest decisions based on the flood hazard maps – decisions that could save many lives and properties.

CHAPTER 2: LIDAR DATA ACQUISITION OF THE ROSARIO-LOBO FLOODPLAIN

Engr. Louie P. Balicanta, Engr. Christopher Cruz, Lovely Gracia Acuña, Engr. Gerome Hipolito, Ms. Pauline Joanne G. Arceo, and Engr. Gef F. Soriano

The methods applied in this Chapter were based on the DREAM methods manual (Sarmiento, et al., 2014) and further enhanced and updated in Paringit, et al. (2017).

2.1 Flight Plans

Plans were made to acquire LiDAR data within the delineated priority area for Rosario-Lobo floodplain in Batangas and Quezon. These missions were planned for 12 lines and ran for at most four and a half (4.5) hours including take-off, landing and turning time. The flight planning parameters for the LiDAR system is found in Table 1. Figure 2 shows the flight plan for Rosario-Lobo floodplain.

Table 1. Flight planning parameters for Pegasus LiDAR system.

Block Name	Flying Height (m AGL)	Overlap (%)	Field of view (ϕ)	Pulse Repetition Frequency (PRF) (kHz)	Scan Frequency (Hz)	Average Speed (kts)	Average Turn Time (Minutes)
BLK18O	1200	30	50	200	30	130	5
BLK18Q	1200	30	50	200	30	130	5
BLK18R	1200	30	50	200	30	130	5

¹ The explanation of the parameters used are in the volume "LiDAR Surveys and Flood Mapping in the Philippines: Methods."

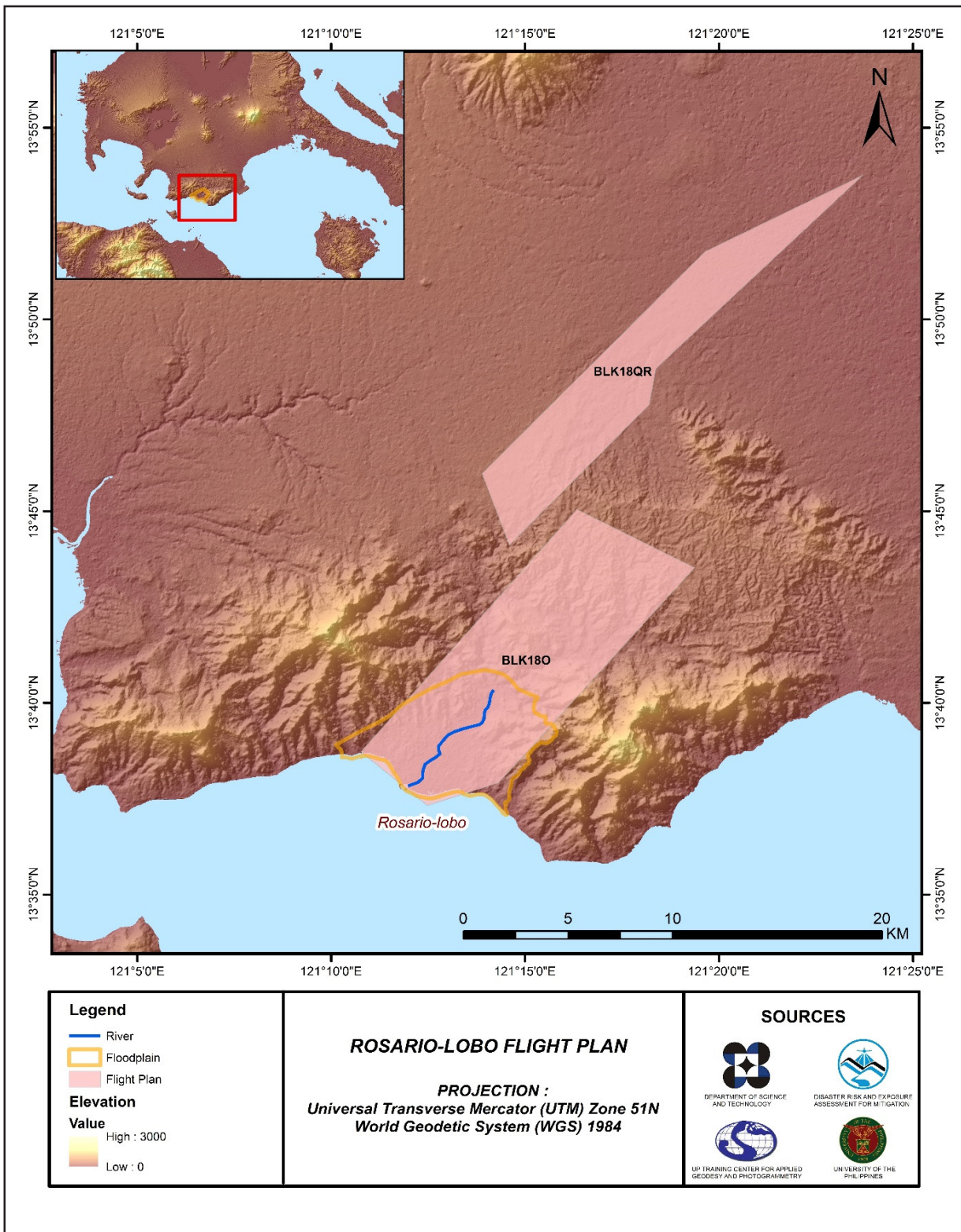


Figure 2. Flight plans for Pegasus System used for Rosario-Lobo Floodplain

2.2 Ground Base Stations

The project team was able to recover one (1) NAMRIA ground control point (GCP): BTG-30, with second (2nd) order accuracy. The project team also established one (1) GCP, BTG-30A. The certification for the NAMRIA reference point is found in Annex 2 while the baseline processing report for the established GCP is found in Annex 3. These were used as base stations during flight operations for the entire duration of the survey (August 29, 2016 and September 5, 2016). Base stations were observed using dual frequency GPS receivers, TRIMBLE SPS 882 and SPS 852. Flight plans and location of base stations used during the aerial LiDAR acquisition in Rosario-lobo floodplain are shown in Figure 3.

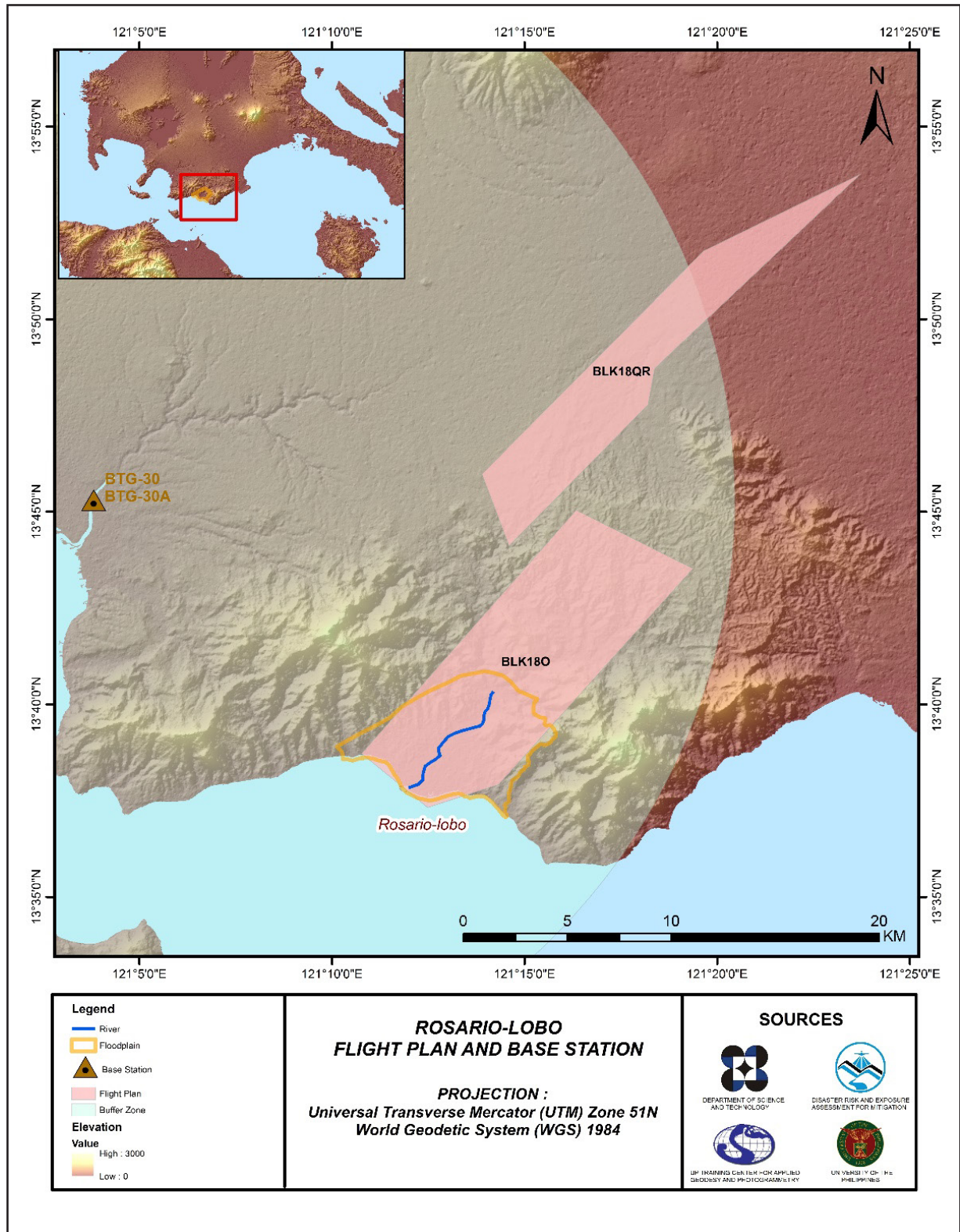


Figure 3. Flight plans and base stations for Rosario-Lobo Floodplain.

Figure 4 shows the recovered NAMRIA reference point within the area. In addition, Table 2 and Table 3 show the details about the NAMRIA control stations and the established point, while Table 4 shows the list of all GCPs occupied during the acquisition together with the corresponding dates of utilization.

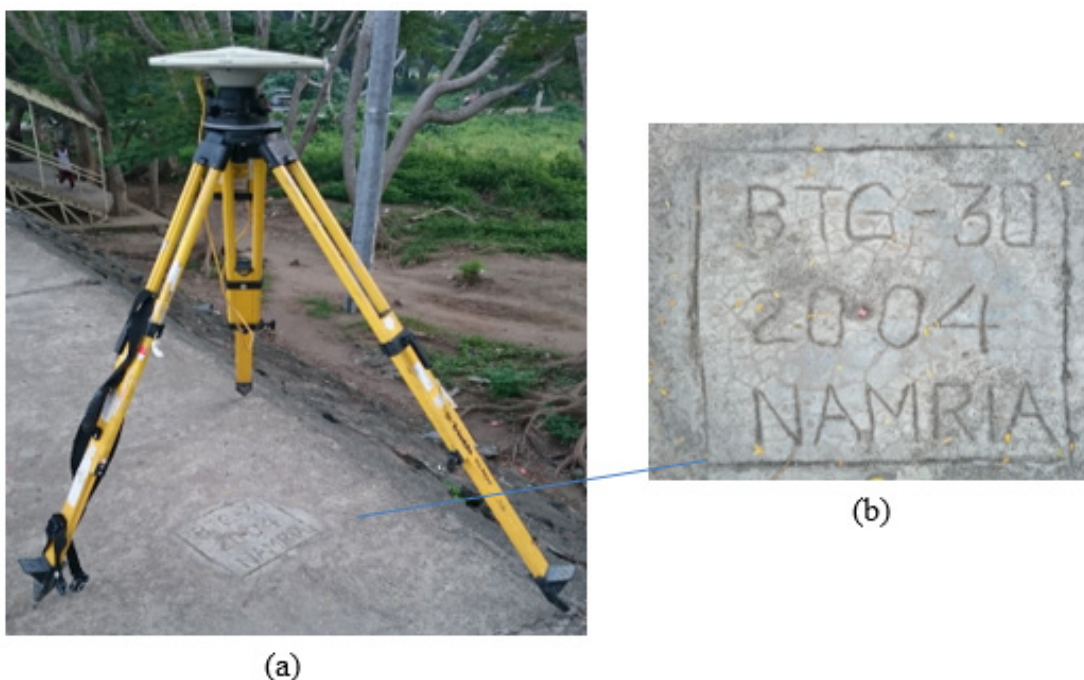


Figure 4. GPS set-up over BTG-30 in the vicinity of Brgy. Pallocan, Batangas City along the E side dike of Calumpang River, on the N side of Calumpang Bridge (a) and NAMRIA reference point BTG-30 (b) as recovered by the field team.

Table 2. Details of the recovered NAMRIA horizontal control point BTG-30 used as base station for the LiDAR acquisition.

Station Name	BTG-30	
Order of Accuracy	2nd	
Relative Error (Horizontal positioning)	1 in 50,000	
Geographic Coordinates, Philippine Reference of 1992 Datum (PRS 92)	Latitude Longitude Ellipsoidal Height	13° 45' 23.09640" North 121° 03' 43.87175" East 21.056 meters
Grid Coordinates, Philippine Transverse Mercator Zone 5 (PTM Zone 5 PRS 92)	Easting Northing	506735.366 meters 1521220.652 meters
Geographic Coordinates, World Geodetic System 1984 Datum (WGS 84)	Latitude Longitude Ellipsoidal Height	13° 45' 17.88182" North 121° 03' 48.83762" East 53.872 meters
Grid Coordinates, Universal Transverse Mercator Zone 51 North (UTM 51N PRS 1992)	Easting Northing	290477.094 meters 1521536.181 meters

Table 3. Details of the established horizontal control point BTG-30A used as base station for the LiDAR Acquisition with established coordinates.

Station Name	BTG-30A	
Order of Accuracy	2nd	
Relative Error (Horizontal positioning)	1:50,000	
Geographic Coordinates, Philippine Reference of 1992 Datum (PRS 92)	Latitude Longitude Ellipsoidal Height	13° 17' 20.53041" North 120° 37' 46.98588" East 54.35200 meters
Grid Coordinates, Philippine Transverse Mercator Zone 3 (PTM Zone 5 PRS 92)	Easting Northing	243198.172 meters 1470321.018 meters
Geographic Coordinates, World Geodetic System 1984 Datum (WGS 84)	Latitude Longitude Ellipsoidal Height	13° 17' 20.53041" North 120° 37' 46.98588" East 54.35200 meters

Table 4. Ground control points used during LiDAR data acquisition.

Date Surveyed	Flight Number	Mission Name	Ground Control Points
August 29, 2016	3353P	1BLK18QRS241A	BTG-30, BTG-30A
September 5, 2016	3381P	1BLK18OS248A	BTG-30, BTG-30A

2.3 Flight Missions

Two (2) missions were conducted to complete LiDAR data acquisition in Rosario-Lobo floodplain, for a total of eight hours (8+00) of flying time for RP-C9022. All missions were acquired using the Pegasus LiDAR system. Table 5 shows the total area of actual coverage and the corresponding flying hours per mission while Table 6 presents the actual parameters used during the LiDAR data acquisition.

Table 5. Flight missions for LiDAR data acquisition in Rosario-Lobo Floodplain

Date Surveyed	Flight Number	Flight Plan Area (km ²)	Surveyed Area (km ²)	Area Surveyed within the Floodplain (km ²)	Area Surveyed Outside the Floodplain (km ²)	No. of Images (Frames)	Flying Hours	
							Hr	Min
August 29, 2016	3353P	386.74	171.86	8.56	163.31	NA	3	55
September 5, 2016	3381P	287.25	200.93	7.21	193.72	NA	4	5
TOTAL		673.99	372.79	15.77	357.03	NA	8	0

Table 14. Actual parameters used during the LiDAR data acquisition

Flight Number	Flying Height (m AGL)	Overlap (%)	FOV (θ)	PRF (khz)	Scan Frequency (Hz)	Average Speed (kts)	Average Turn Time (Minutes)
3353P	1000	30	50	200	30	130	5
3381P	1100	20	50	200	30	130	5

2.4 Survey Coverage

Rosario-Lobo floodplain is located in the provinces of Batangas and Quezon. The list of municipalities and cities surveyed, with at least one (1) square kilometer coverage, is shown in Table 15. The actual coverage of the LiDAR acquisition for the Rosario-Lobo floodplain is presented in Figure 8. The flight status reports are available in Annex 7.

Table 15. List of municipalities/cities surveyed during the Rosario-Lobo Floodplain LiDAR survey

Province	Municipality/City	Area of Municipality/City (km ²)	Total Area Surveyed (km ²)	Percentage of Area Surveyed
Batangas	Lobo	199.87	97.14	49%
	Taysan	91.03	41.69	46%
	Rosario	197.03	70.83	36%
	San Juan	236.84	15.55	7%
Quezon	San Antonio	60.34	3.12	5%
	Candelaria	158.33	5.92	4%
	Tiaong	109.11	3.34	3%
TOTAL		1052.55	237.59	22.57%

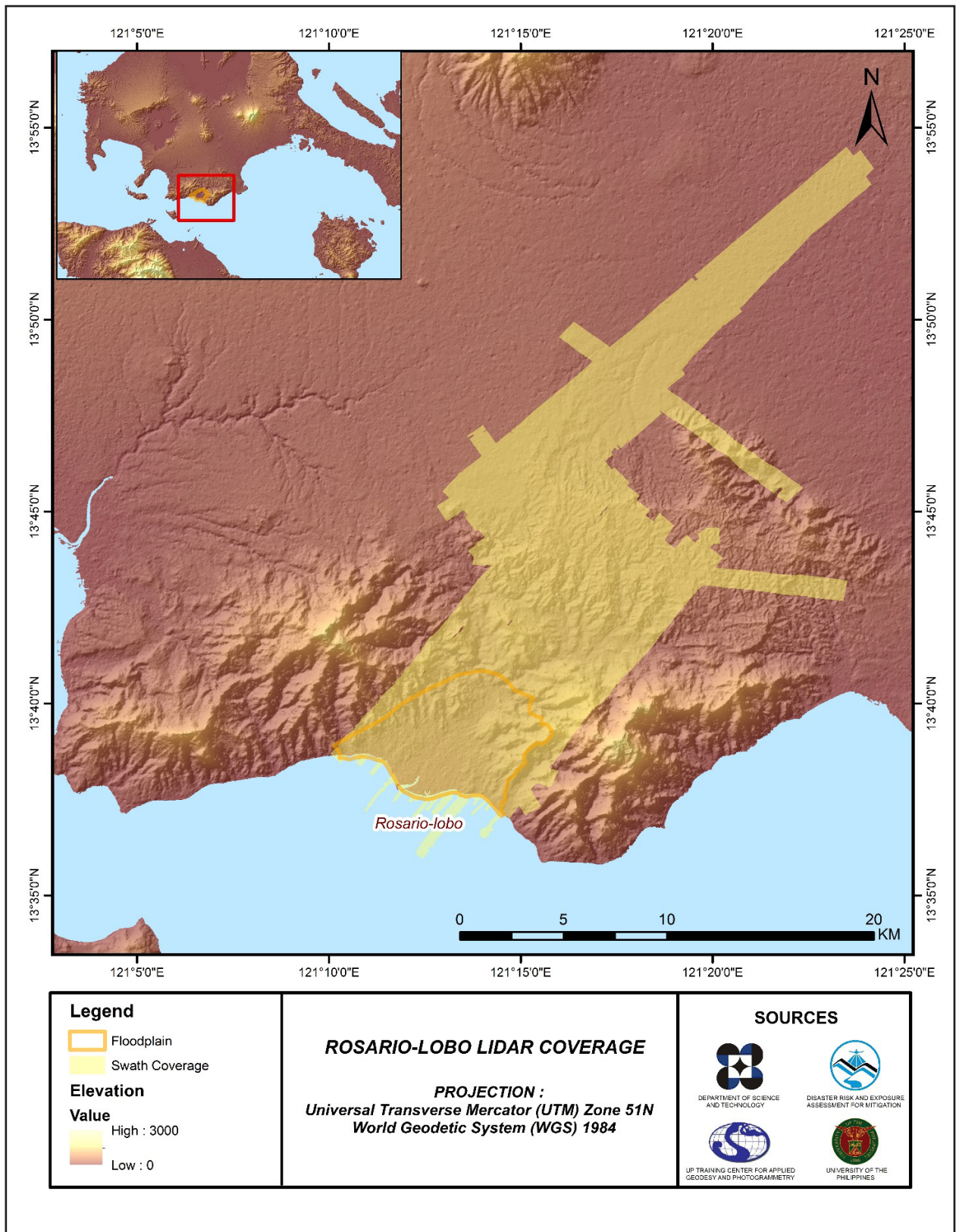


Figure 5. Actual LiDAR survey coverage for Rosario-Lobo Floodplain.

CHAPTER 3: LIDAR DATA PROCESSING OF THE ROSARIO-LOBO FLOODPLAIN

Engr. Ma. Rosario Concepcion O. Ang, Engr. John Louie D. Fabila, Engr. Sarah Jane D. Samalburro , Engr. Joida F. Prieto , Engr. Melissa F. Fernandez , Engr. Ma. Ailyn L. Olanda, Engr. Sheila-Maye F. Santillan, Engr. Antonio B. Chua, Jr. , Engr. Ezzo Marc C. Hibionada, and Ziarre Anne P. Mariposa

The methods applied in this Chapter were based on the DREAM methods manual (Ang, et al., 2014) and further enhanced and updated in Paringit, et al. (2017).

3.1 Overview of the LiDAR Data Pre-Processing

The data transmitted by the Data Acquisition Component are checked for completeness based on the list of raw files required to proceed with the pre-processing of the LiDAR data. Upon acceptance of the LiDAR field data, georeferencing of the flight trajectory is done in order to obtain the exact location of the LiDAR sensor when the laser was shot. Point cloud georectification is performed to incorporate correct position and orientation for each point acquired. The georectified LiDAR point clouds are subject for quality checking to ensure that the required accuracies of the program, which are the minimum point density, vertical and horizontal accuracies, are met. The point clouds are then classified into various classes before generating Digital Elevation Models such as Digital Terrain Model and Digital Surface Model.

Using the elevation of points gathered in the field, the LiDAR-derived digital models are calibrated. Portions of the river that are barely penetrated by the LiDAR system are replaced by the actual river geometry measured from the field by the Data Validation and Bathymetry Component. LiDAR acquired temporally are then mosaicked to completely cover the target river systems in the Philippines. Orthorectification of images acquired simultaneously with the LiDAR data is done through the help of the georectified point clouds and the metadata containing the time the image was captured.

These processes are summarized in the flowchart shown in Figure 6.

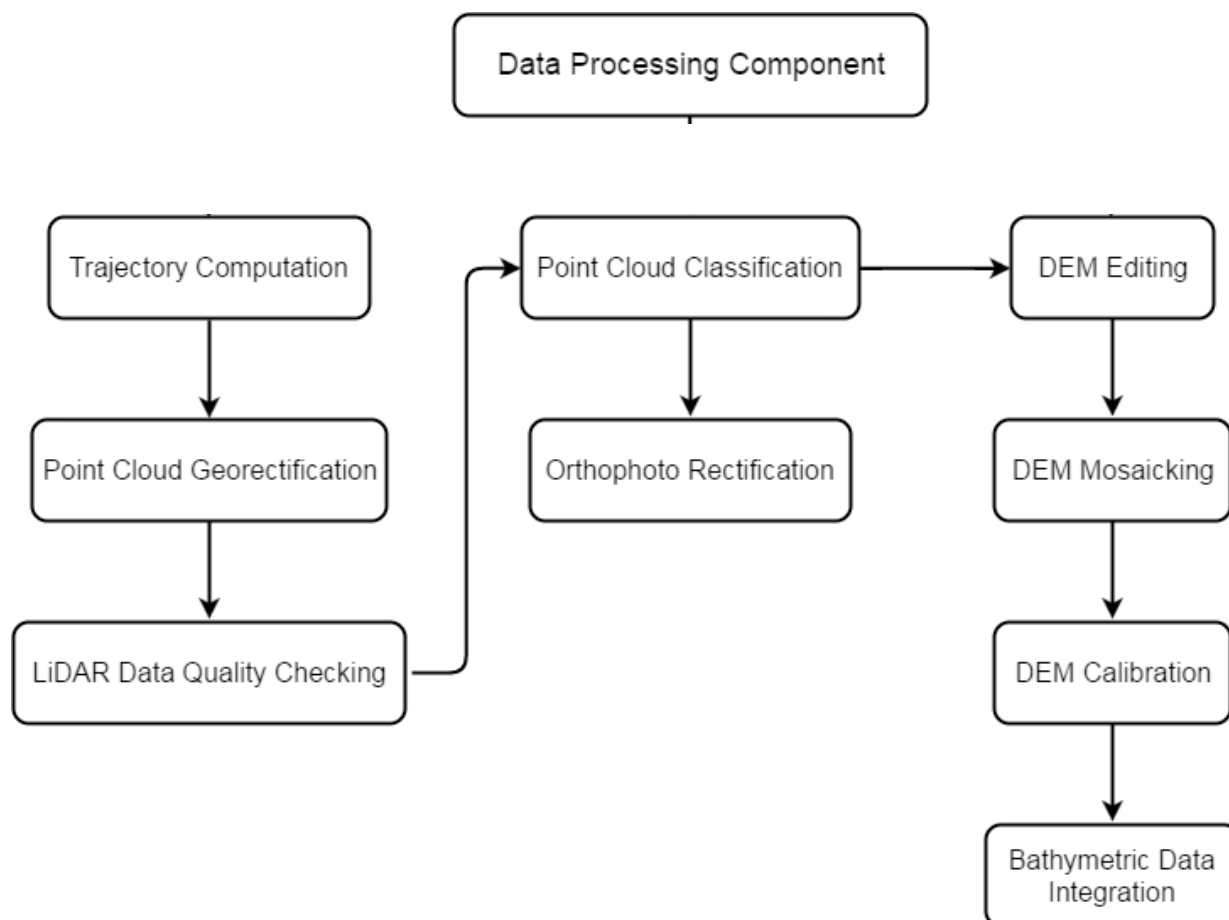


Figure 6. Schematic Diagram for Data Pre-Processing Component

3.2 Transmittal of Acquired LiDAR Data

Data transfer sheets for all the LiDAR missions for Rosario-Lobo floodplain can be found in Annex 5. Data Transfer Sheets. Missions flown during the first survey conducted on August and September 2015 used the Airborne LiDAR Terrain Mapper (ALTM™ Optech Inc.) Pegasus system over Lobo, Batangas.

The Data Acquisition Component (DAC) transferred a total of 39.40 Gigabytes of Range data, 502 Megabytes of POS data, 16.24 Megabytes of GPS base station data, and 0 Gigabytes of raw image data to the data server on September 8, 2015 for the first survey and September 11, 2015 for the second survey. The Data Pre-processing Component (DPPC) verified the completeness of the transferred data. The whole dataset for Rosario-Lobo was fully transferred on September 11, 2015, as indicated on the Data Transfer Sheets for Rosario-Lobo floodplain.

3.3 Trajectory Computation

The Smoothed Performance Metrics of the computed trajectory for flight 3381P, one of the Rosario-Lobo flights, which is the North, East, and Down position RMSE values are shown in Figure 7. The x-axis corresponds to the time of flight, which is measured by the number of seconds from the midnight of the start of the GPS week, which on that week fell on August 30, 2015 00:00AM. The y-axis is the RMSE value for that particular position.

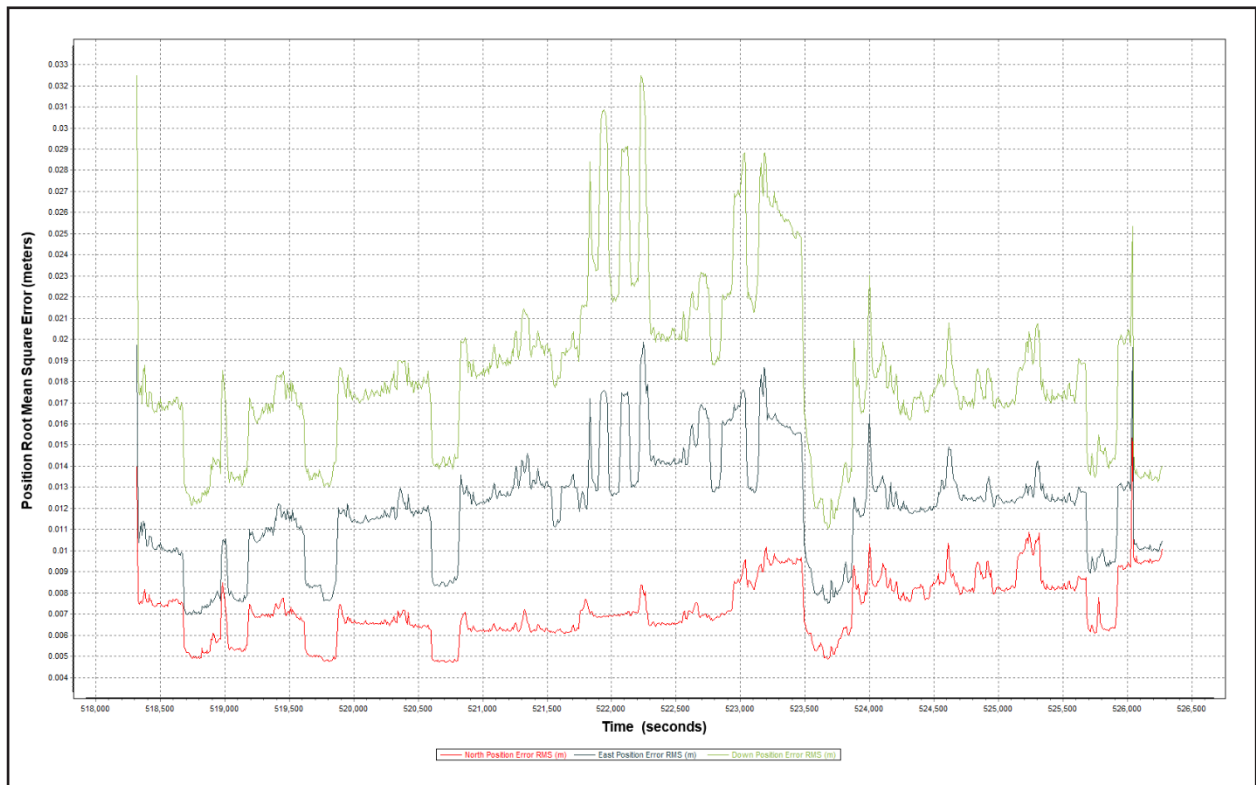


Figure 7. Smoothed Performance Metrics of Rosario-Lobo Flight 3381P.

The time of flight was from 518000 seconds to 526500 seconds, which corresponds to morning of September 5, 2015. The initial spike that is seen on the data corresponds to the time that the aircraft was getting into position to start the acquisition, and the POS system starts computing for the position and orientation of the aircraft.

Redundant measurements from the POS system quickly minimized the RMSE value of the positions. The periodic increase in RMSE values from an otherwise smoothly curving RMSE values correspond to the turn-around period of the aircraft, when the aircraft makes a turn to start a new flight line. Figure 7 shows that the North position RMSE peaks at 1.10 centimeters, the East position RMSE peaks at 2.00 centimeters, and the Down position RMSE peaks at 2.90 centimeters, which are within the prescribed accuracies described in the methodology.

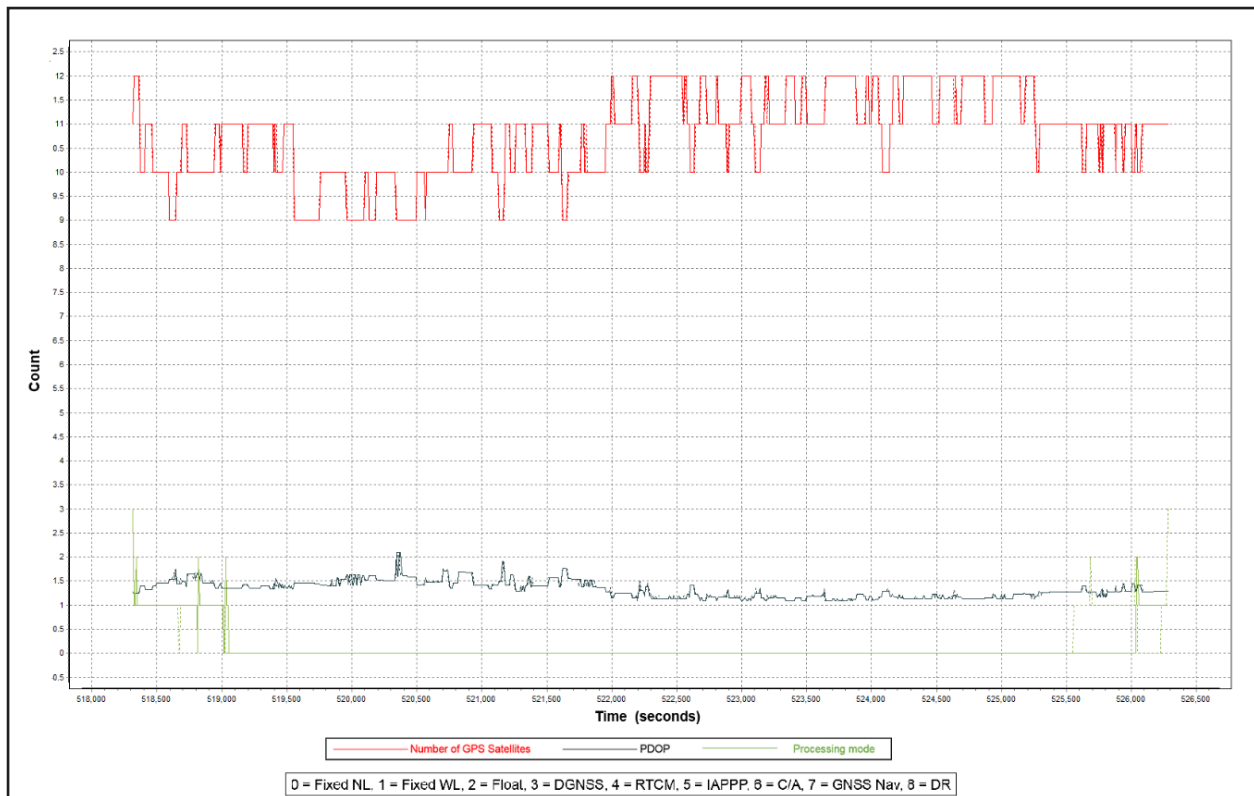


Figure 8. Solution Status Parameters of Rosario-Lobo Flight 3381P.

The Solution Status parameters of flight 3381P, one of the Rosario-Lobo flights, which are the number of GPS satellites, Positional Dilution of Precision (PDOP), and the GPS processing mode used, are shown in Figure 8. The graphs indicate that the number of satellites during the acquisition did not go down to 8. Majority of the time, the number of satellites tracked was between 9 and 12. The PDOP value also did not go above the value of 3, which indicates optimal GPS geometry. The processing mode stayed at the value of 0 for majority of the survey with some peaks up to 2 attributed to the turns performed by the aircraft. The value of 0 corresponds to a Fixed, Narrow-Lane mode, which is the optimum carrier-cycle integer ambiguity resolution technique available for POSPAC MMS. All of the parameters adhered to the accuracy requirements for optimal trajectory solutions, as indicated in the methodology. The computed best estimated trajectory for all Rosario-Lobo flights is shown in Figure 9.

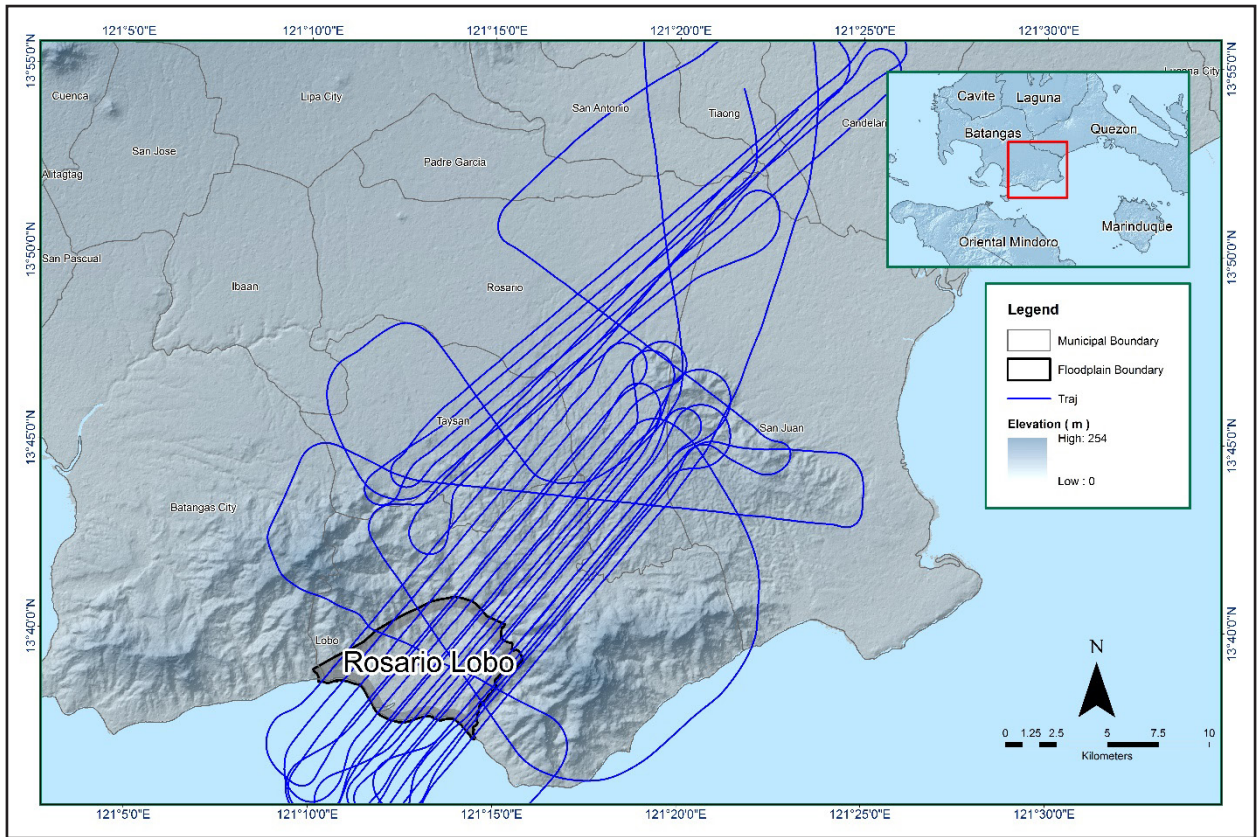


Figure 9. Best Estimated Trajectory for Rosario-Lobo Floodplain.

3.4 LiDAR Point Cloud Computation

The produced LAS data contains 24 flight lines, with each flight line containing two channels, since the Pegasus system contains two channels. The summary of the self-calibration results obtained from LiDAR processing in LiDAR Mapping Suite (LMS) software for all flights over Rosario-Lobo floodplain are given in Table 8.

Table 8. Self-Calibration Results values for Rosario-Lobo flights.

Parameter	Acceptable Value	Value
Boresight Correction stdev)	<0.001degrees	0.000232
IMU Attitude Correction Roll and Pitch Correction stdev)	<0.001degrees	0.000478
GPS Position Z-correction stdev)	<0.01meters	0.0073

The optimum accuracy is obtained for all Rosario-Lobo flights based on the computed standard deviations of the corrections of the orientation parameters. Standard deviation values for individual blocks are available in Annex 8. Mission Summary Reports

3.5 LiDAR Data Quality Checking

The boundary of the processed LiDAR data on top of a SAR Elevation Data over Rosario-Lobo Floodplain is shown in Figure 10. The map shows gaps in the LiDAR coverage that are attributed to cloud coverage.

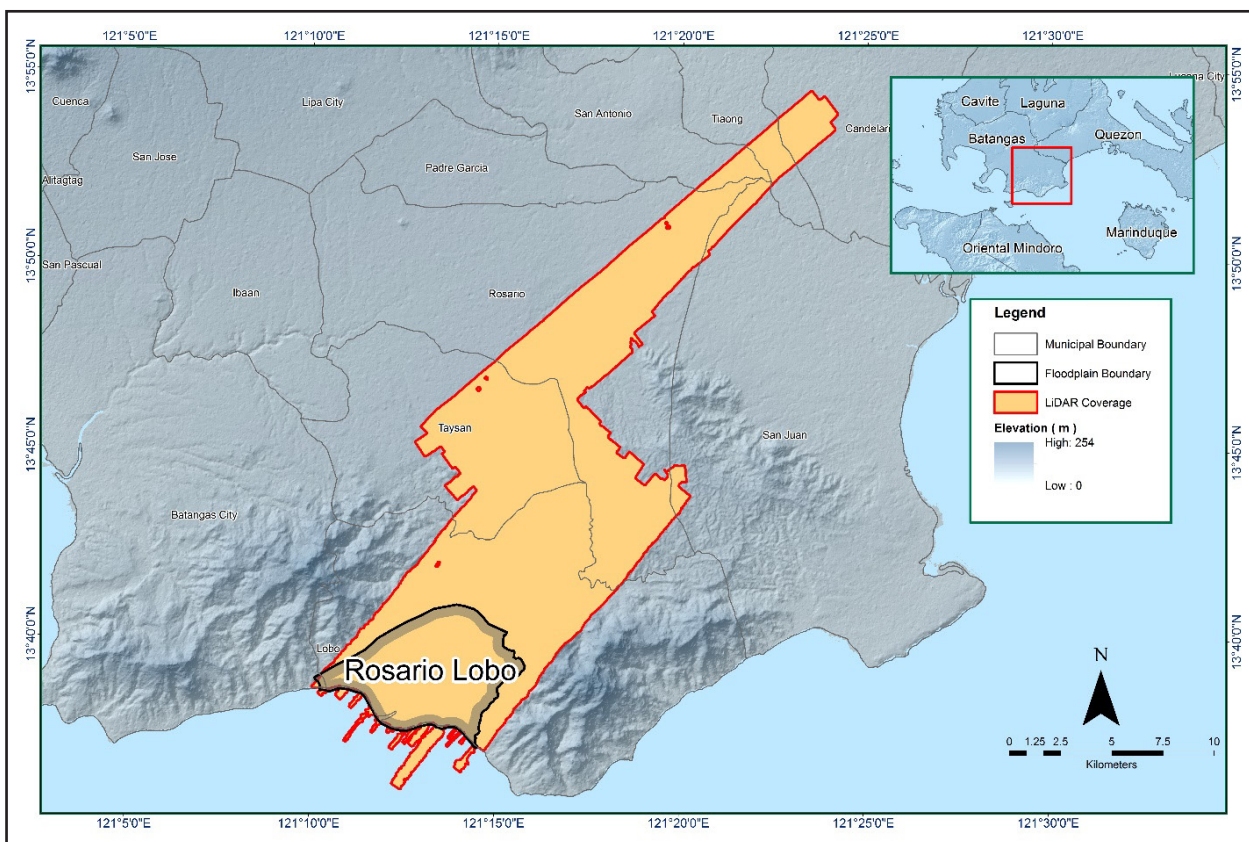


Figure 10. Boundary of the processed LiDAR data over Rosario-Lobo Floodplain

The total area covered by the Rosario-Lobo missions is 302.97 sq.km that is comprised of two (2) flight acquisitions grouped and merged into two (2) blocks as shown in Table 9.

Table 9. List of LiDAR blocks for Rosario-Lobo Floodplain.

LiDAR Blocks	Flight Numbers	Area (sq. km)
Calabarzon_Blk18U_supplement	3381G	181.43
Calabarzon_Blk18U_additional	3353G	80.45
TOTAL		261.88 sq.km

The overlap data for the merged LiDAR blocks, showing the number of channels that pass through a particular location is shown in Figure 11. Since the Pegasus system employs two channels, we would expect an average value of 2 (blue) for areas where there is limited overlap, and a value of 3 (yellow) or more (red) for areas with three or more overlapping flight lines.

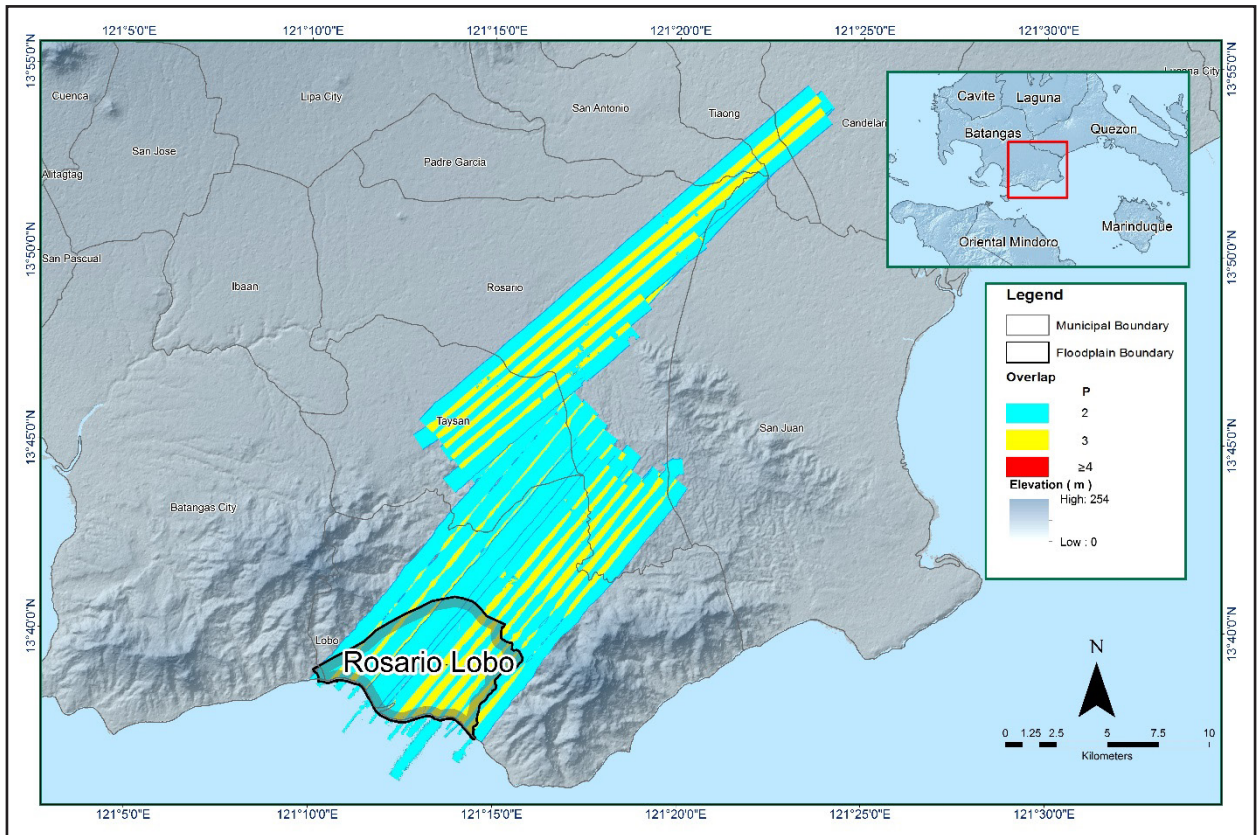


Figure 11. Image of data overlap for Rosario-Lobo Floodplain.

The overlap statistics per block for the Rosario-Lobo floodplain can be found in Annex B-1. Mission Summary Reports. It should be noted that one pixel corresponds to 25.0 square meters on the ground. For this area, the minimum and maximum percent overlaps are 33.91% and 34.18% respectively, which passed the 25% requirement.

The density map for the merged LiDAR data, with the red parts showing the portions of the data that satisfy the 2 points per square meter criterion is shown in Figure 12. It was determined that all LiDAR data for Rosario-Lobo floodplain satisfy the point density requirement, and the average density for the entire survey area is 3.06 points per square meter.

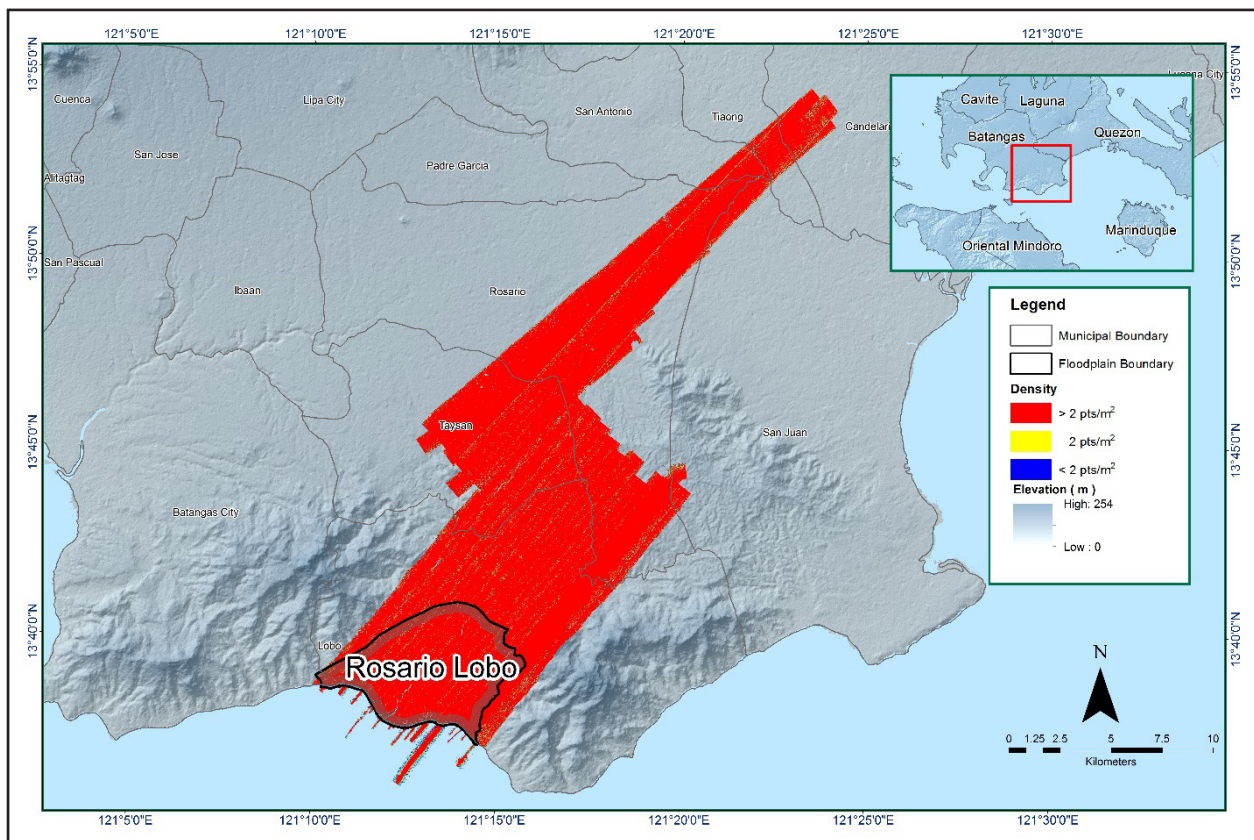


Figure 12. Pulse density map of merged LiDAR data for Rosario-Lobo Floodplain.

The elevation difference between overlaps of adjacent flight lines is shown in Figure 13. The default color range is from blue to red, where bright blue areas correspond to portions where elevations of a previous flight line, identified by its acquisition time, are higher by more than 0.20m relative to elevations of its adjacent flight line. Bright red areas indicate portions where elevations of a previous flight line are lower by more than 0.20m relative to elevations of its adjacent flight line. Areas with bright red or bright blue need to be investigated further using Quick Terrain Modeler software.

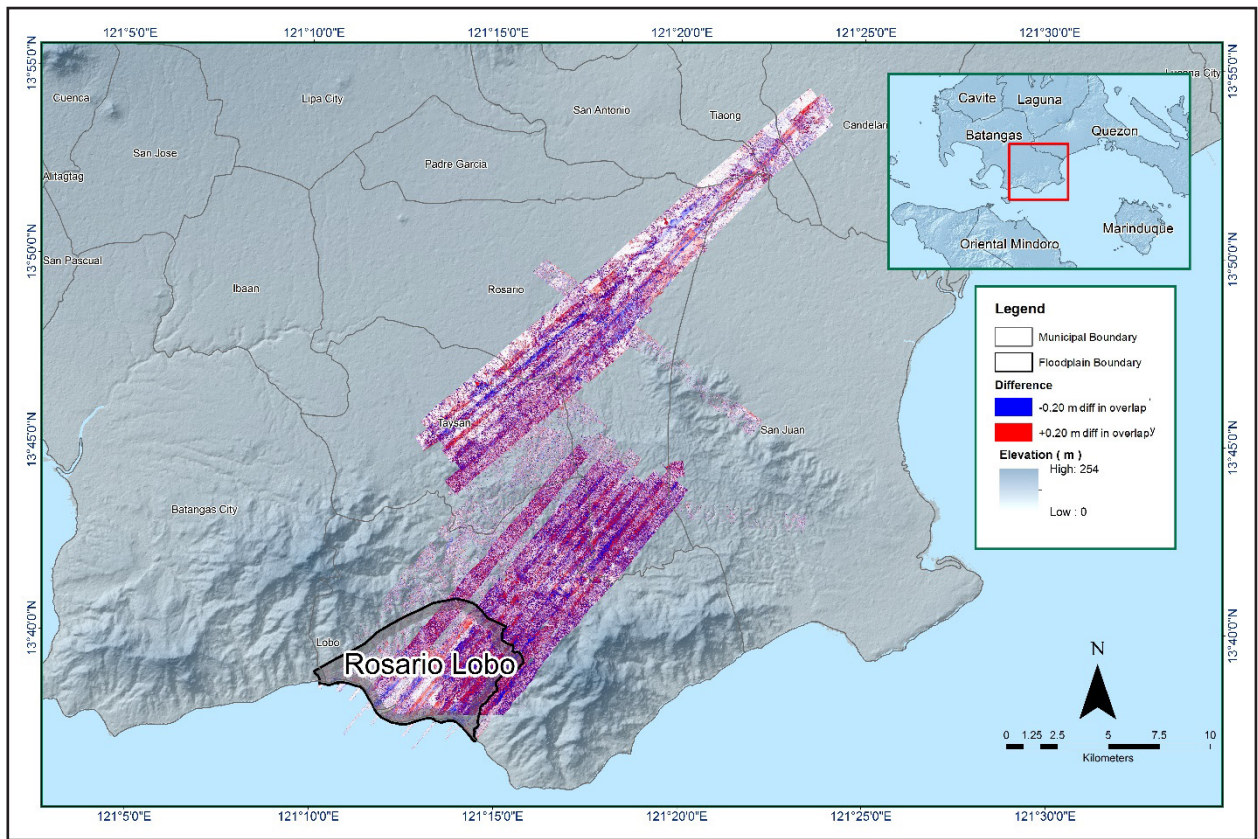


Figure 13. Elevation difference map between flight lines for Rosario-Lobo Floodplain.

A screen capture of the processed LAS data from a Rosario-Lobo flight 3381P loaded in QT Modeler is shown in Figure 14. The upper left image shows the elevations of the points from two overlapping flight strips traversed by the profile, illustrated by a dashed yellow line. The x-axis corresponds to the length of the profile. It is evident that there are differences in elevation, but the differences do not exceed the 20-centimeter mark. This profiling was repeated until the quality of the LiDAR data becomes satisfactory. No reprocessing was done for this LiDAR dataset.

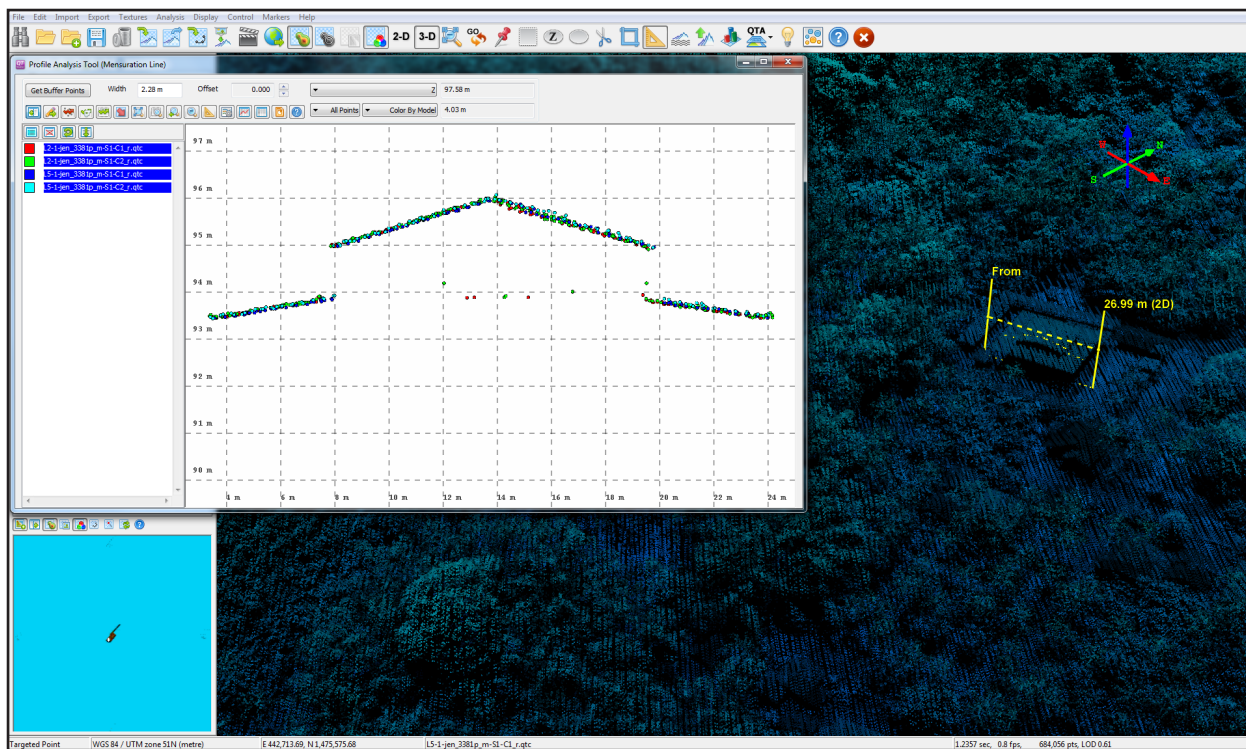


Figure 14. Quality checking for Rosario-Lobo flight 3381P

3.6 LiDAR Point Cloud Classification and Rasterization

Table 10. Rosario-Lobo classification results in TerraScan.

Pertinent Class	Total Number of Points
Ground	195,649,043
Low Vegetation	118,799,266
Medium Vegetation	378,938,973
High Vegetation	751,408,612
Building	22,987,317

The tile system that TerraScan employed for the LiDAR data and the final classification image for a block in Rosario-Lobo floodplain is shown in Figure 15. A total of 440 1km by 1km tiles were produced. The number of points classified to the pertinent categories is illustrated in Table 10. The point cloud has a maximum and minimum height of 749.60 meters and 48.73 meters respectively.

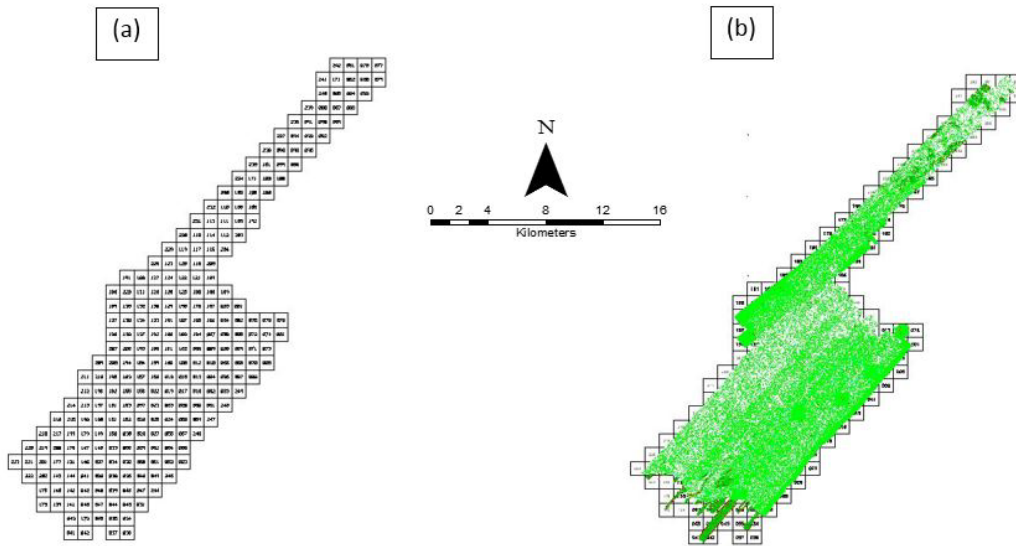


Figure 15. Tiles for Rosario-Lobo Floodplain (a) and classification results (b) in TerraScan.

An isometric view of an area before and after running the classification routines is shown in Figure 16. The ground points are in orange, the vegetation is in different shades of green, and the buildings are in cyan. It can be seen that residential structures adjacent or even below canopy are classified correctly, due to the density of the LiDAR data.

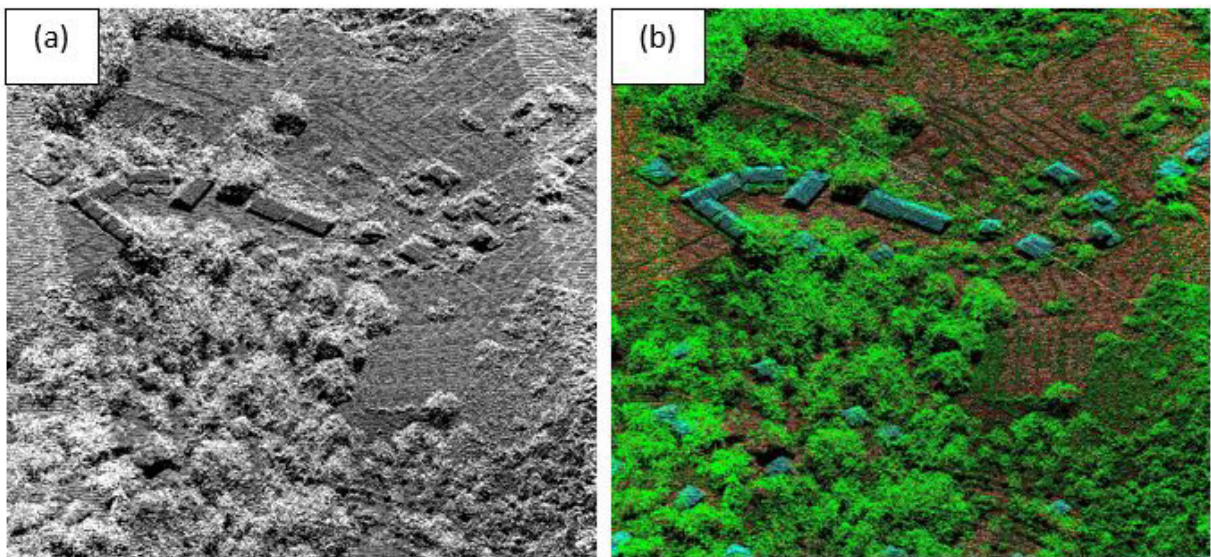


Figure 16. Point cloud before (a) and after (b) classification.

The production of last return (V_ASCII) and the secondary (T_ASCII) DTM, first (S_ASCII) and last (D_ASCII) return DSM of the area in top view display are shown in Figure 17. It shows that DTMs are the representation of the bare earth while on the DSMs, all features are present such as buildings and vegetation.

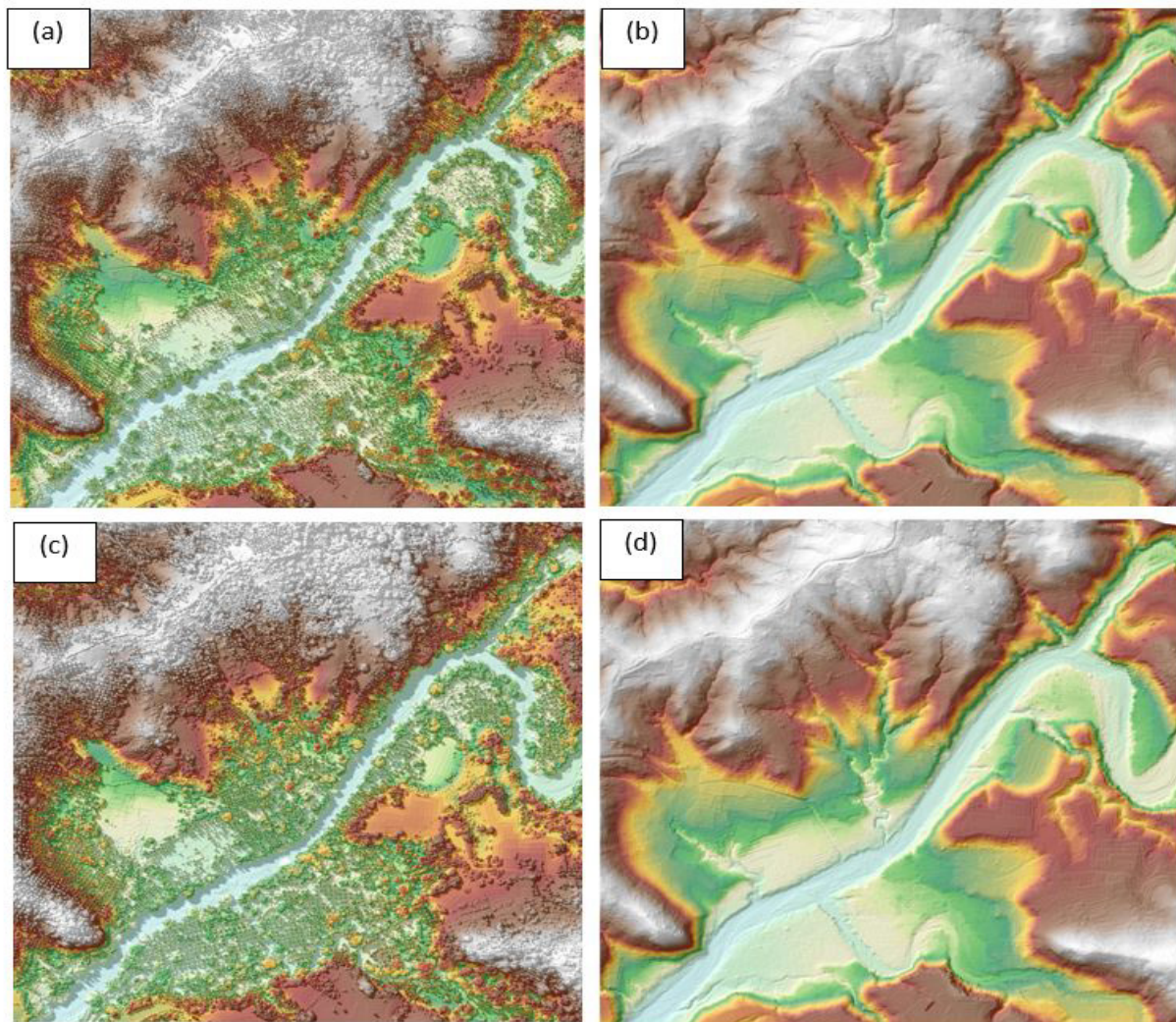


Figure 17. The production of last return DSM (a) and DTM (b), first return DSM (c) and secondary DTM (d) in some portion of Rosario-Lobo Floodplain.

3.7 LiDAR Image Processing and Orthophotograph Rectification

There are no available orthophotographs for the Rosario-Lobo floodplain.

3.8 DEM Editing and Hydro-Correction

Two (2) mission blocks were processed for Rosario-Lobo flood plain. These blocks are composed only of Calabarzon blocks with a total area of 261.88 square kilometers. Table 11 shows the name and corresponding area of each block in square kilometers.

Table 11. LiDAR blocks with its corresponding area.

LiDAR Blocks	Area (sq.km)
Calabarzon_Bl18U_supplement	181.43
Calabarzon_Bl18U_additional	80.45
TOTAL	261.88 sq.km

Portions of DTM before and after manual editing are shown in Figure 18. The bridge (Figure 18a) is also considered to be an impedance to the flow of water along the river and has to be removed has been misclassified and removed during classification process and has to be retrieved to complete the surface (Figure 18b) to allow the correct flow of water. The mountain ridges (Figure 18c) is also considered to be an impedance to the flow of water along the river and has to be removed (Figure 18d) in order to hydrologically correct the river. Another example is a building that is still present in the DTM after classification (Figure 18e) and has to be removed through manual editing (Figure 18f).

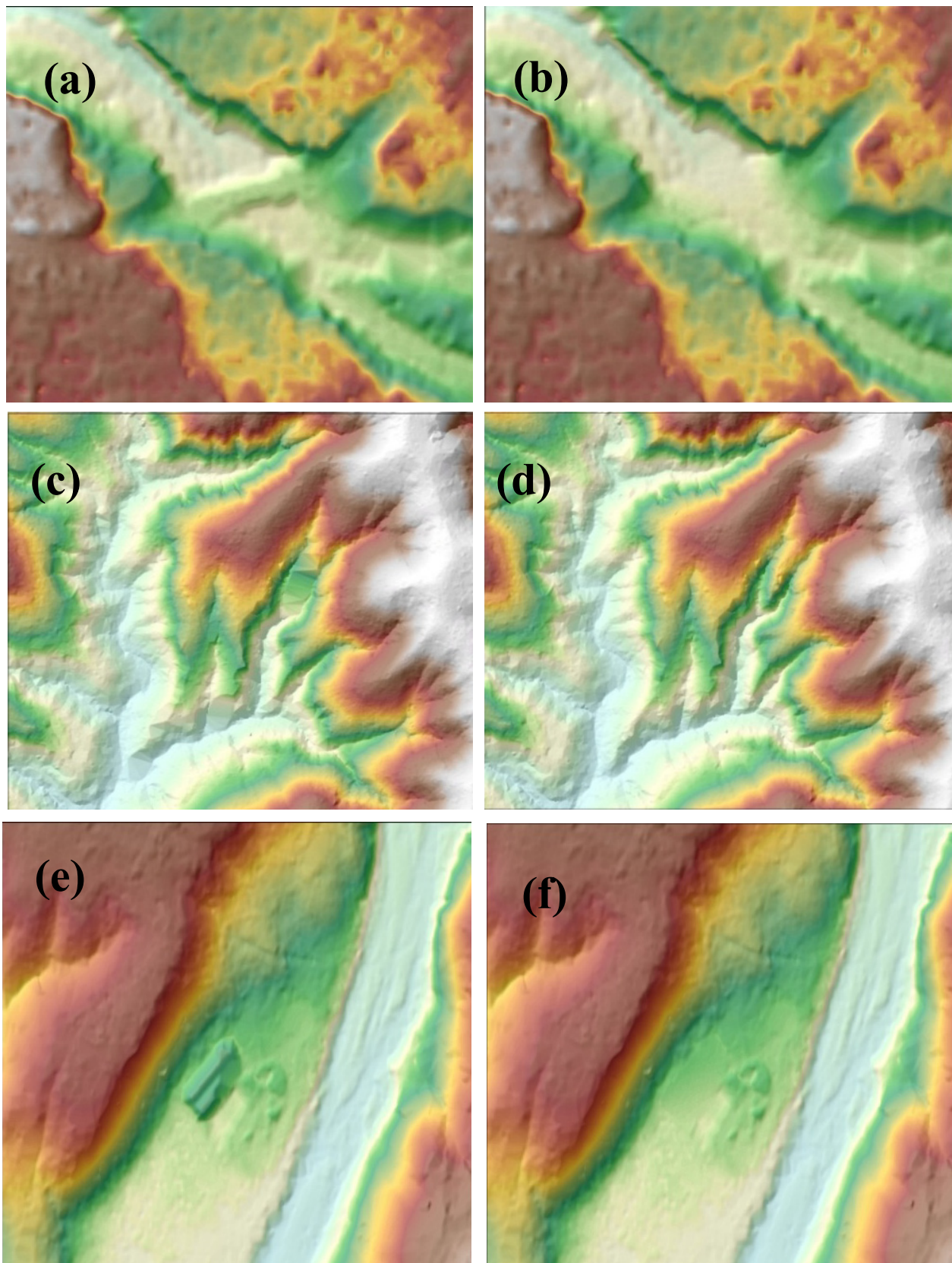


Figure 18. Portions in the DTM of Rosario-Lobo Floodplain – a bridge before (a) and after (b) manual editing; mountain ridges before (c) and after (d) data retrieval; and a building before (e) and after (f) manual editing.

3.9 Mosaicking of Blocks

No assumed reference block was used in mosaicking because the identified reference for shifting was an existing calibrated Bolbok_DTM overlapping with the blocks to be mosaicked. Table 12 shows the area of each LiDAR block and the shift values applied during mosaicking.

Mosaicked LiDAR DTM for Rosario-Lobo floodplain is shown in Figure 19. It can be seen that the entire Rosario-Lobo floodplain is 100% covered by LiDAR data.

Table 12. Shift Values of each LiDAR Block of Rosario-Lobo Floodplain.

Mission Blocks	Shift Values (meters)		
	x	y	z
Calabarzon_Bl18U_supplement	0.00	0.00	+0.38
Calabarzon_Bl18U_additional	+0.65	-1.51	+0.40

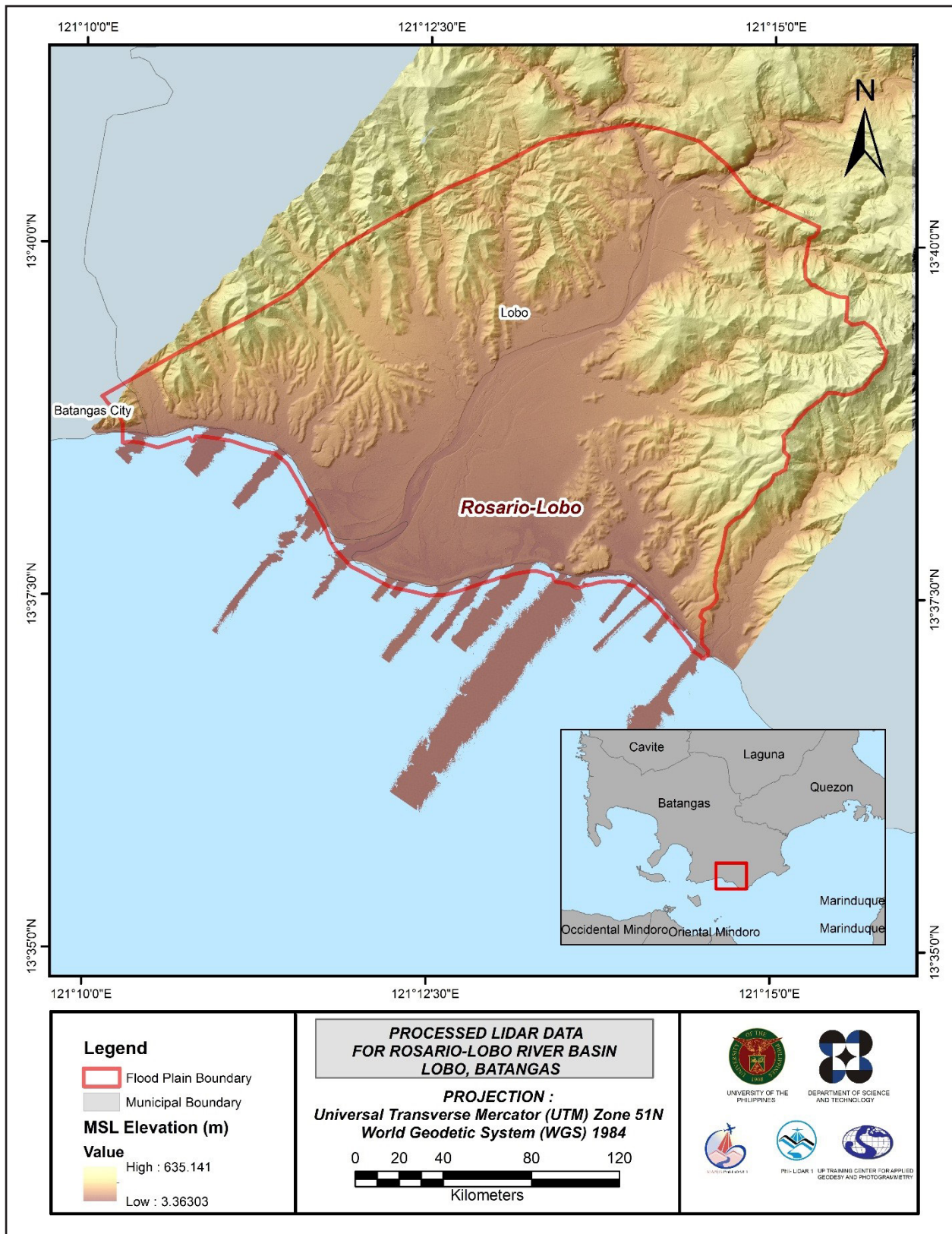


Figure 24. Map of the processed LiDAR data for the Rosario-Lobo Floodplain

3.10 Calibration and Validation of Mosaicked LiDAR DEM

The extent of the validation survey done by the Data Validation and Bathymetry Component (DVBC) in Rosario-Lobo to collect points with which the LiDAR dataset is validated is shown in Figure 25. A total of 24,251 survey points were gathered for all the flood plains within the provinces of CALABARZON wherein the Rosario-Lobo floodplain is located. Random selection of 80% of the survey points, resulting to 19,401 points, was used for calibration.

A good correlation between the uncalibrated mosaicked LiDAR DTM and ground survey elevation values is shown in Figure 26. Statistical values were computed from extracted LiDAR values using the selected points to assess the quality of data and obtain the value for vertical adjustment. The computed height difference between the LiDAR DTM and calibration points is 2.97 meters with a standard deviation of 0.20 meters. Calibration of the LiDAR data was done by subtracting the height difference value, 2.97 meters, to the mosaicked LiDAR data. Table 13 shows the statistical values of the compared elevation values between the LiDAR data and calibration data.

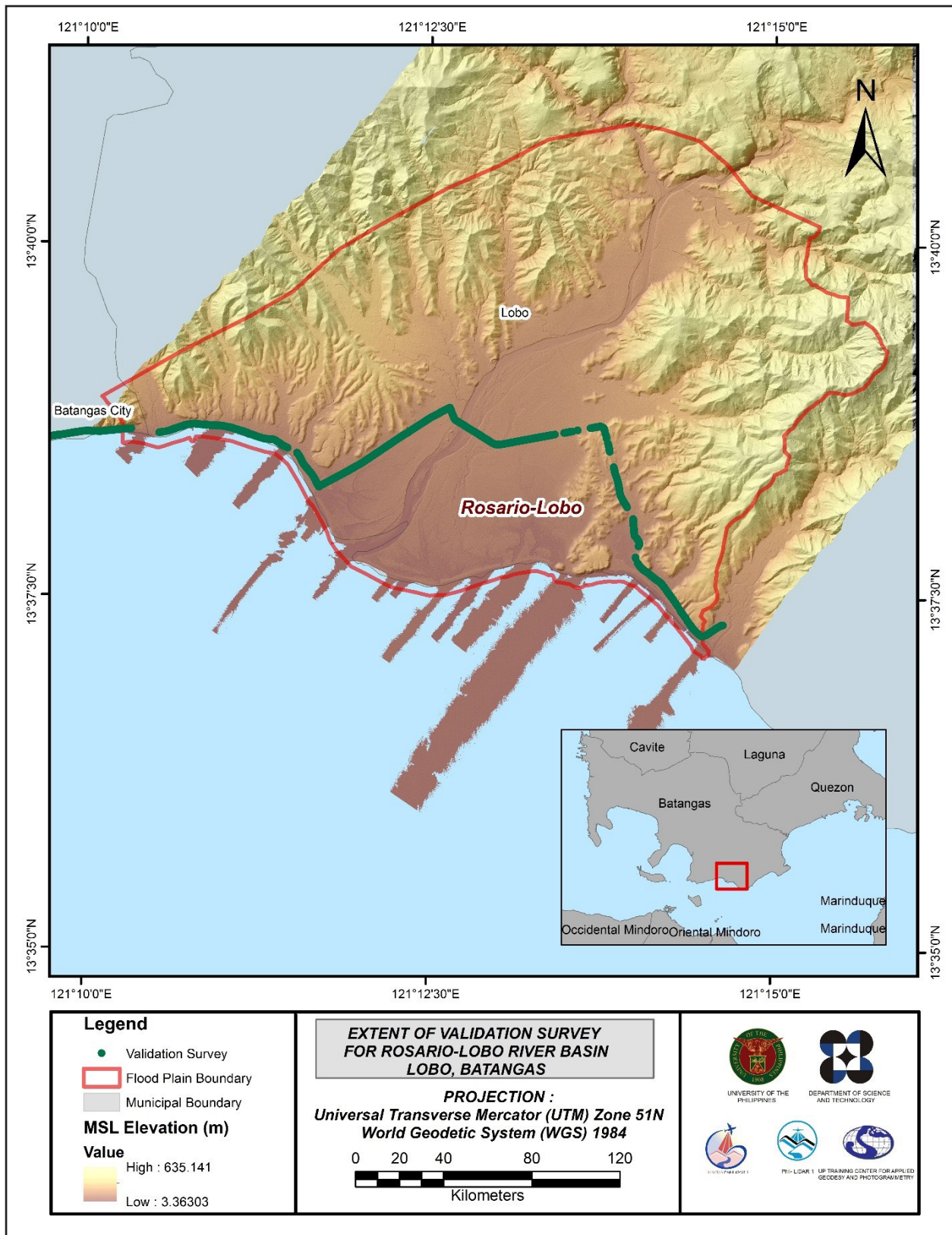


Figure 20. Map of Rosario-Lobo Floodplain with validation survey points in green.

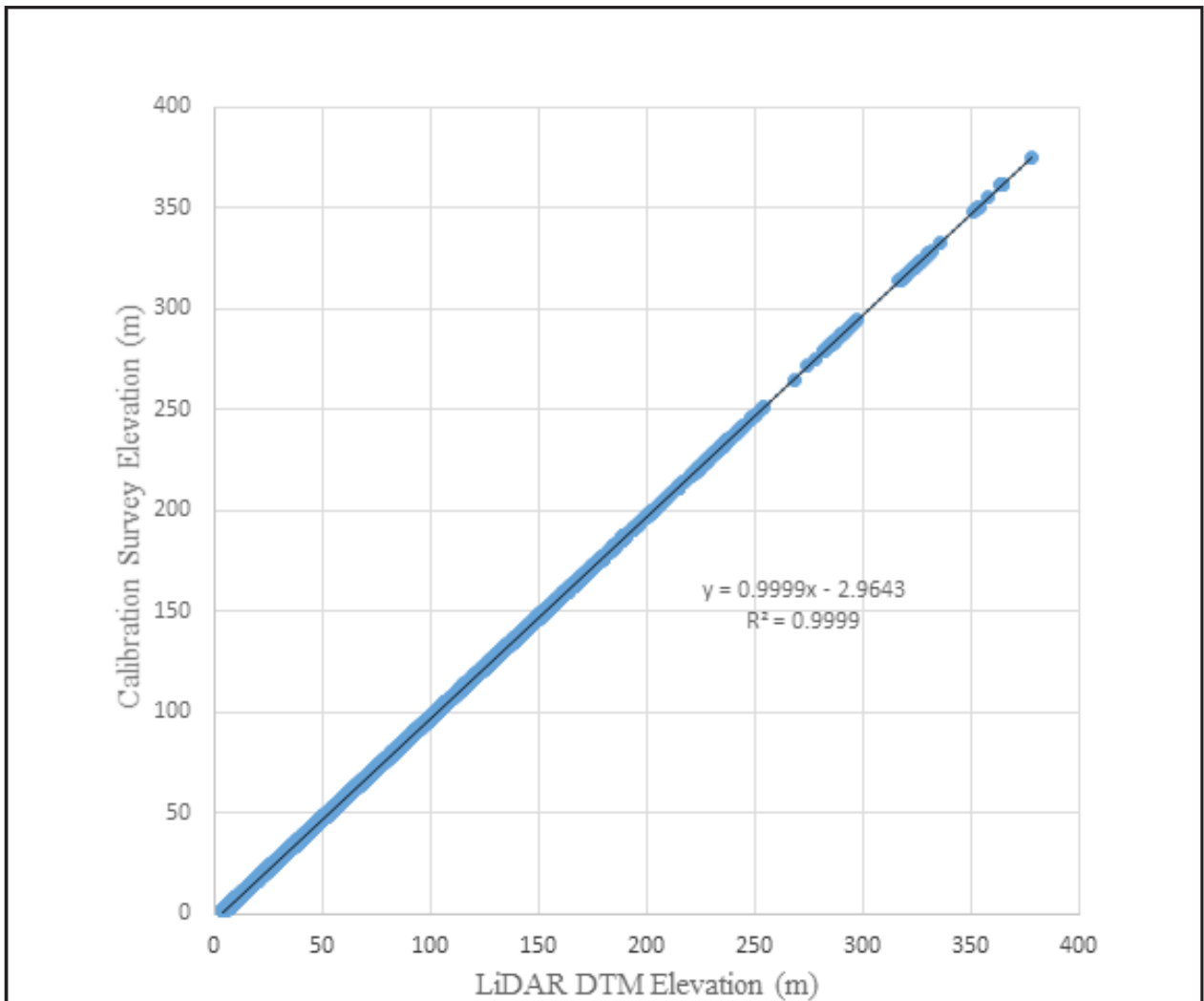


Figure 21. Correlation plot between calibration survey points and LiDAR data.

Table 13. Calibration Statistical Measures.

Calibration Statistical Measures	Value (meters)
Height Difference	2.97
Standard Deviation	0.20
Average	-2.97
Minimum	-3.48
Maximum	-2.40

The remaining 20% of the total survey points were intersected to the flood plain, resulting to 178 points, were used for the validation of calibrated Rosario-Lobo DTM. A good correlation between the calibrated mosaicked LiDAR elevation values and the ground survey elevation, which reflects the quality of the LiDAR DTM, is shown in Figure 22. The computed RMSE between the calibrated LiDAR DTM and validation elevation values is 0.18 meters with a standard deviation of 0.12 meters, as shown in Table 14.

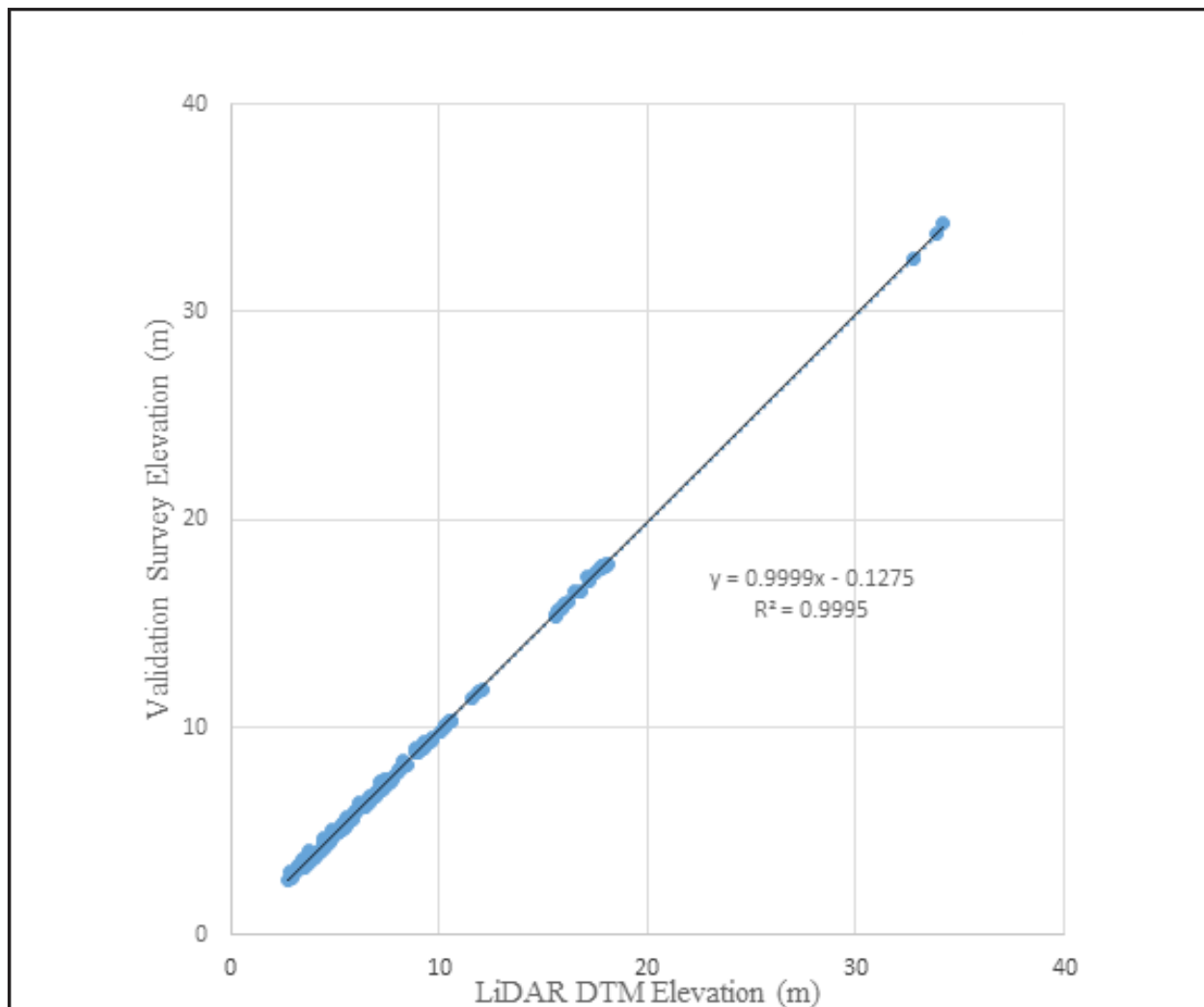


Figure 22. Correlation plot between validation survey points and LiDAR data.

Table 14. Validation Statistical Measures.

Validation Statistical Measures	Value (meters)
RMSE	0.18
Standard Deviation	0.12
Average	-0.13
Minimum	-0.27
Maximum	0.27

3.11 Integration of Bathymetric Data into the LiDAR Digital Terrain Model

For bathy integration, only centerline data was available for Rosario-Lobo with 724 bathymetric survey points. The resulting raster surface produced was done by Inverse Distance Weighted (IDW) interpolation method. After burning the bathymetric data to the calibrated DTM, assessment of the interpolated surface is represented by the computed RMSE value of 0.004 meters. The extent of the bathymetric survey done by the Data Validation and Bathymetry Component (DVBC) in Rosario-Lobo integrated with the processed LiDAR DEM is shown in Figure 23.

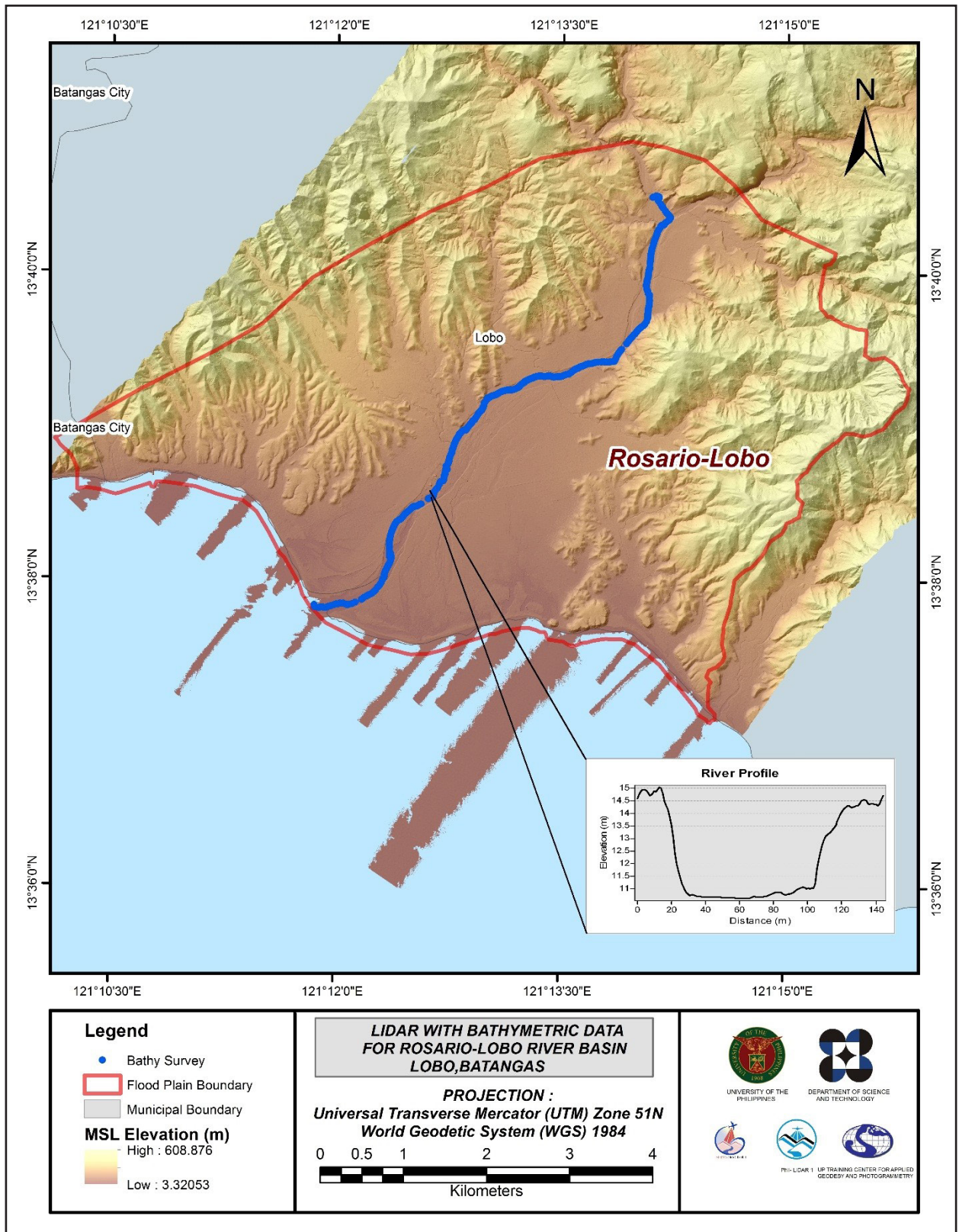


Figure 23. Map of Rosario-Lobo Floodplain with bathymetric survey points shown in blue.

3.12 Feature Extraction

The features salient in flood hazard exposure analysis include buildings, road networks, bridges and water bodies within the floodplain area with 200 m buffer zone. Mosaicked LiDAR DEM with 1 m resolution was used to delineate footprints of building features, which consist of residential buildings, government offices, medical facilities, religious institutions, and commercial establishments, among others. Road networks comprise of main thoroughfares such as highways and municipal and barangay roads essential for routing of disaster response efforts. These features are represented by a network of road centerlines.

3.12.1 Quality Checking of Digitized Features' Boundary

Rosario-Lobo floodplain, including its 200 m buffer, has a total area of 43.91 sq km. For this area, a total of 5.0 sq km, corresponding to a total of 870 building features, are considered for QC. Figure 24 shows the QC blocks for Rosario-Lobo floodplain.

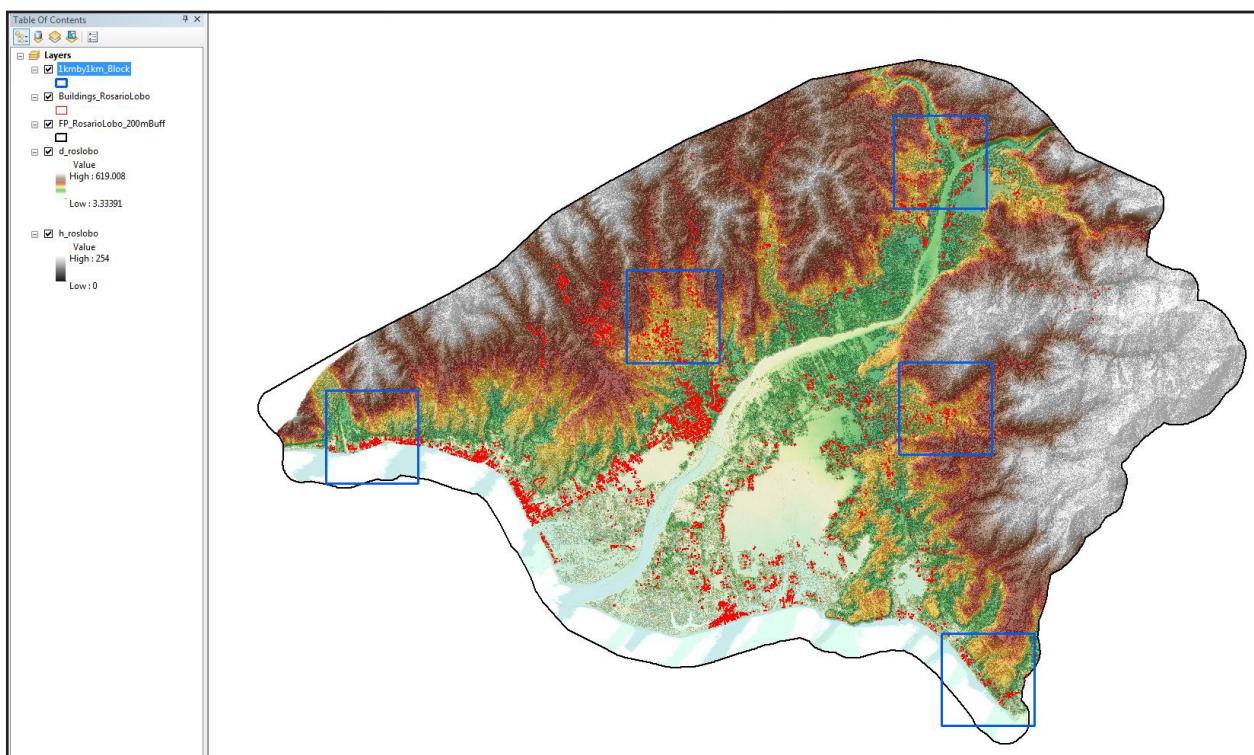


Figure 24. QC blocks for Rosario-Lobo building features.

Quality checking of Rosario-Lobo building features resulted in the ratings shown in Table 15.

Table 15. Quality Checking Ratings for Rosario-Lobo Building Features.

FLOODPLAIN	COMPLETENESS	CORRECTNESS	QUALITY	REMARKS
Rosario-Lobo	91.14	99.31	82.87	PASSED

3.12.2 Height Extraction

Height extraction was done for 4,942 building features in Rosario-Lobo floodplain. Of these building features, 12 buildings were filtered out after height extraction, resulting to 4,930 buildings with height attributes. The lowest building height is at 2.00 m, while the highest building is at 8.18 m.

3.12.3 Feature Attribution

The attributes were obtained by field data gathering. GPS devices were used to determine the coordinates of important features. These points are uploaded and overlaid in ArcMap and are then integrated with the shapefiles.

Table 16 summarizes the number of building features per type. On the other hand, Table 17 shows the total length of each road type, while Table 18 shows the number of water features extracted per type.

Table 16. Building Features Extracted for Rosario-Lobo Floodplain.

Facility Type	No. of Features
Residential	4742
School	83
Market	9
Agricultural/Agro-Industrial Facilities	4
Medical Institutions	8
Barangay Hall	10
Military Institution	0
Sports Center/Gymnasium/Covered Court	1
Telecommunication Facilities	1
Transport Terminal	1
Warehouse	3
Power Plant/Substation	0
NGO/CSO Offices	2
Police Station	1
Water Supply/Sewerage	2
Religious Institutions	25
Bank	2
Factory	0
Gas Station	3
Fire Station	0
Other Government Offices	5
Other Commercial Establishments	28
Total	4,930

Table 17. Total Length of Extracted Roads for Rosario-Lobo Floodplain.

Floodplain	Road Network Length (km)					Total
	Barangay Road	City/Municipal Road	Provincial Road	National Road	Others	
Rosario-Lobo	59.94	1.00	13.70	0	0.00	74.64

Table 18. Number of Extracted Water Bodies for Rosario-Lobo Floodplain.

Floodplain	Water Body Type					Total
	Rivers/Streams	Lakes/Ponds	Sea	Dam	Fish Pen	
Rosario-Lobo	4	4	0	0	1	9

A total of 8 bridges and culverts over small channels that are part of the river network were also extracted for the floodplain.

3.12.4 Final Quality Checking of Extracted Features

All extracted ground features were completely given the required attributes. All these output features comprise the flood hazard exposure database for the floodplain. This completes the feature extraction phase of the project.

Figure 25 shows the Digital Surface Model (DSM) of Rosario-Lobo floodplain overlaid with its ground features.

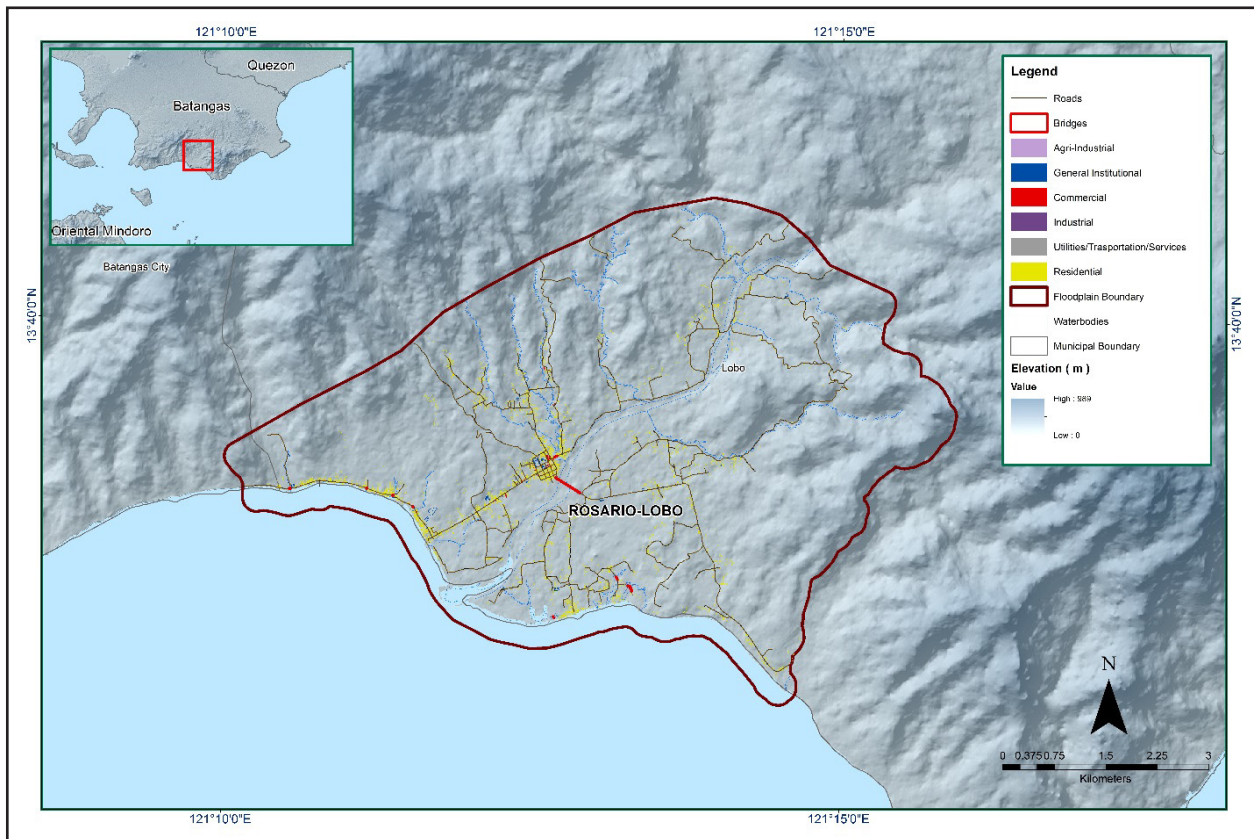


Figure 25. Extracted features for Rosario-Lobo Floodplain.

CHAPTER 4: LIDAR VALIDATION SURVEY AND MEASUREMENTS OF THE ROSARIO-LOBO RIVER BASIN

Engr. Louie P. Balicanta, Engr. Joemarie S. Caballero, Ms. Patrizia Mae. P. dela Cruz, Engr. Dexter T. Lozano, For. Dona Rina Patricia C. Tajora, Elaine Bennet Salvador, For. Rodel C. Alberto, Cybil Claire Atacador, and Engr. Lorenz R. Taguse

The methods applied in this Chapter were based on the DREAM methods manual (Balicanta, et al., 2014) and further enhanced and updated in Paringit, et al. (2017).

4.1 Summary of Activities

The Data Validation and Bathymetry Component (DVBC) conducted field surveys on May 14 – 22, 2014 for control survey, bridge cross-section and water level marking; August 26-30, 2014 for bathymetric survey of approximately 6.80 kilometers using GNSS PPK survey technique; and March 5-6, 2016 for the LiDAR validation survey (Figure 26).

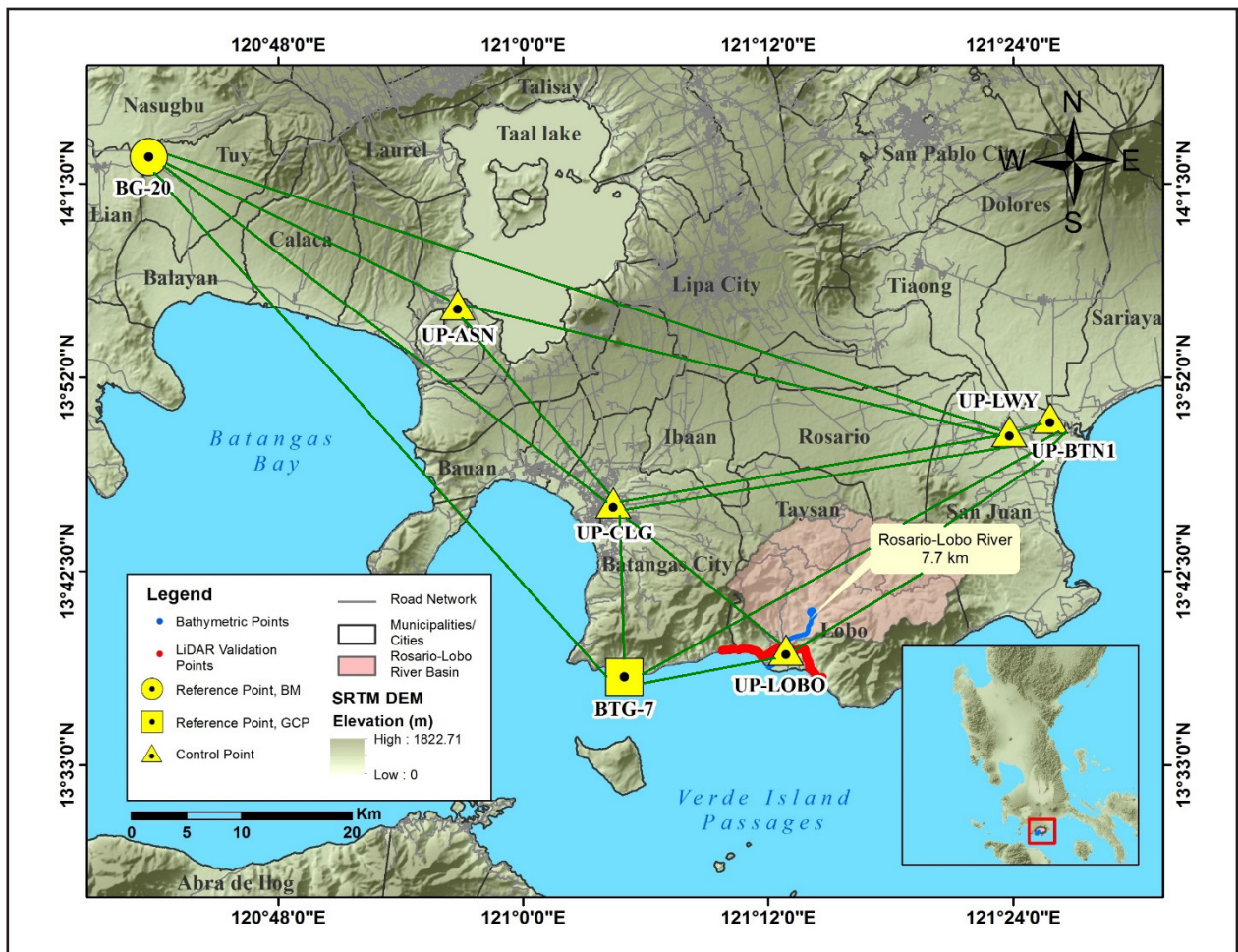


Figure 26. Rosario-Lobo River Survey Extent

4.2 Control Survey

The GNSS network for this survey is composed of six (6) loops established on May 14 – 22, 2016 occupying the following reference points: BG-207, a first order BM in Brgy. Sabang, Municipality of Tuy; and BTG-7, a first order GCP located in Brgy. Dela Paz, Batangas City.

Five (5) control points were established at the approach of bridges namely UP-BTN at Bantilan Bridge in Brgy. UP-LOBO at Lobo Bridge in Brgy. Lagadlarin, Municipality of Lobo; UP-ASN at San Nicholas Bridge in Brgy. Poblacion, Municipality of San Nicholas, UP-CLG at Calumpang Bridge in Brgy. Kumintang Ibaba, Batangas City and UP-LWY at Lawaye Bridge in Brgy. Calitalit, Municipality of San Juan.

The summary of reference and control points and its location is summarized in Table 19 while the GNSS network established is illustrated in Figure 27.

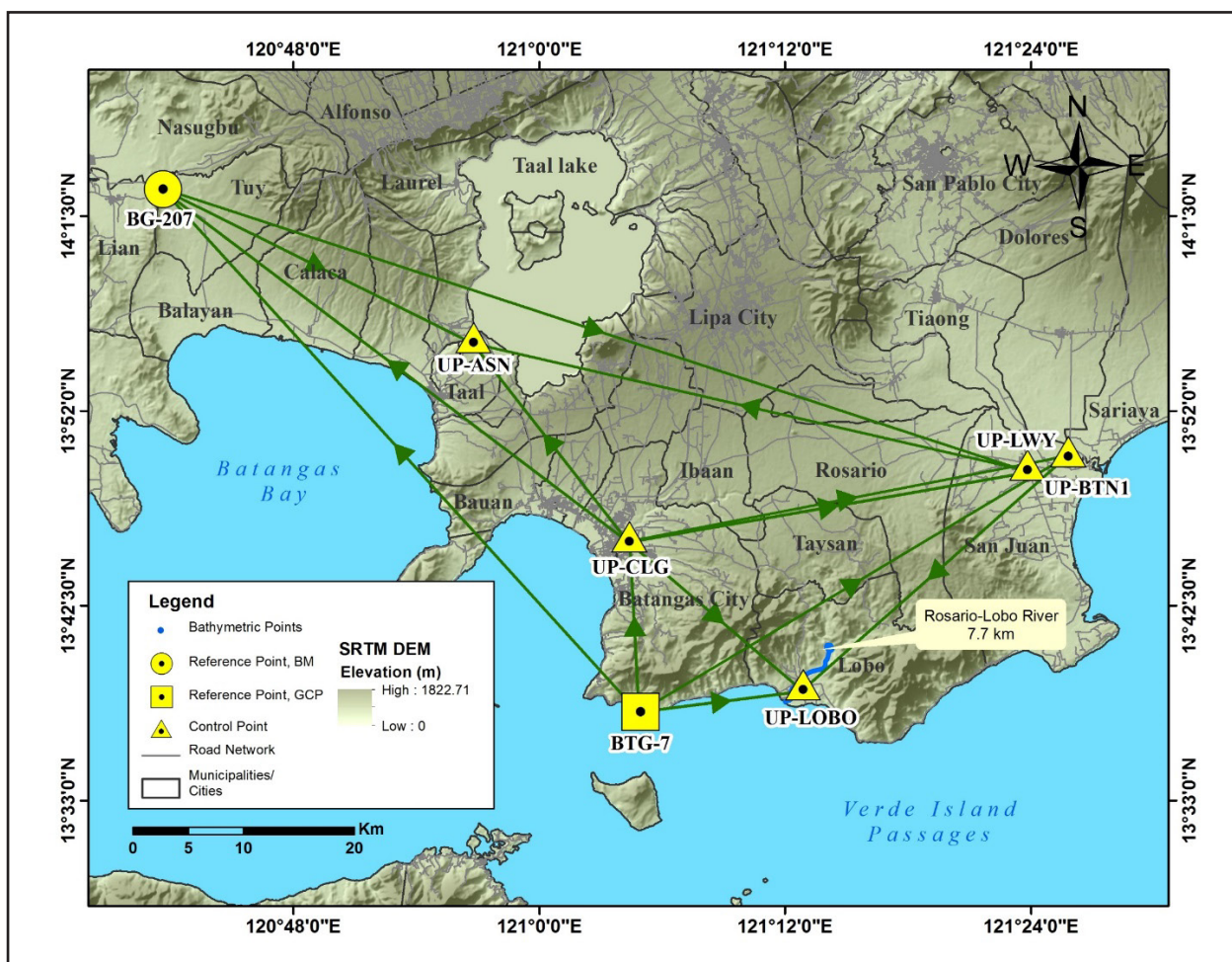


Figure 27. GNSS Network of Rosario-Lobo River field survey

Table 19. List of Reference and Control Points occupied for Rosario-Lobo River Survey
(Source: NAMRIA; UP-TCAGP)

Control Point	Order of Accuracy	Geographic Coordinates (WGS 84)				
		Latitude	Longitude	Ellipsoidal Height (Meter)	Elevation in MSL (Meter)	Date Established
BG207	1st Order	-	-	67.969	22.502	2008
BTG-7	1st Order	13°37'19.49611"	121°04'56.32756"	66.166	-	1992
UP-ASN	UP Established	-	-	-	-	5-22-2014
UP-BTN	UP Established	-	-	-	-	5-21-2014
UP-CLG1	UP Established	-	-	-	-	5-21-2014
UP-LOBO	UP Established	-	-	-	-	5-21-2014
UP-LWY1	UP Established					5-22-2014

The GNSS set up on reference and established control points in Batangas are shown on Figure 28 to Figure 34.



Figure 28. GNSS receiver, Trimble® SPS 985, set-up at BG-207 at Palico Bridge, Brgy. Luntal, Nasugbu, Batangas



Figure 29. GNSS receiver, Trimble® SPS 985, set-up at BTG-7 in Dela Paz Lighthouse in Brgy. Dela Paz, Batangas City, Batangas



Figure 30. GNSS receiver, Trimble® SPS 882, set-up at UP-ASN at San Nicholas Bridge, Brgy. Poblacion, San Nicholas, Batangas



Figure 31. GNSS base receiver, Trimble® SPS 852, set-up at UP-BTN at Bantilan Bridge, Brgy. Manggalang Banitilan, Sariaya, Quezon



Figure 32. GNSS base receiver, Trimble® SPS 852, set-up at UP-CLG1 in Calumpang Bridge, Brgy. Cumintang Ibaba, Batangas City, Batangas

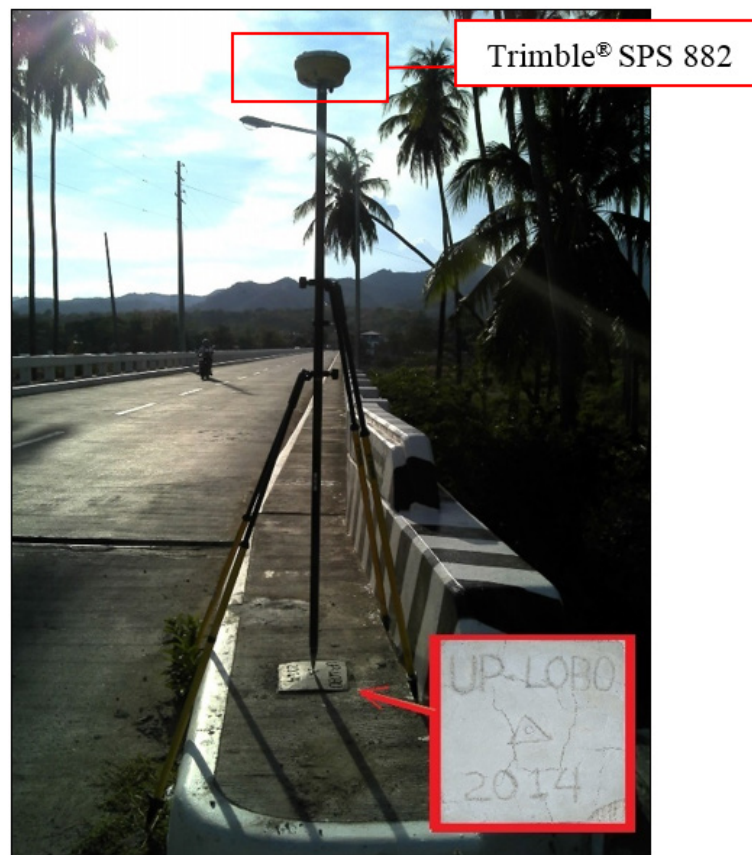


Figure 33. GNSS base receiver, Trimble® SPS 882, set-up at UP-LOBO, in Lobo Bridge, Brgy. Lagadlarin, Lobo, Batangas



Figure 34. GNSS receiver, Trimble® SPS 882, set-up at UP-LWY1 at Lawaye Bridge, Brgy. Calitcalit-Mabalanoy, San Juan, Batangas

4.3 Baseline Processing

GNSS Baselines were processed simultaneously in TBC by observing that all baselines have fixed solutions with horizontal and vertical precisions within +/- 20 cm and +/- 10 cm requirement, respectively. In case where one or more baselines did not meet all of these criteria, masking is performed. Masking is done by removing/masking portions of these baseline data using the same processing software. It is repeatedly processed until all baseline requirements are met. If the reiteration yields out of the required accuracy, resurvey is initiated. Baseline processing result of control points in Rosario-Lobo River Basin is summarized in Table 20 generated by TBC software.

Table 20. Baseline Processing Summary Report for Rosario-Lobo River Basin Static Survey

Observation	Date of Observation	Solution Type	H. Prec. (Meter)	V. Prec. (Meter)	Geodetic Az.	Ellipsoid Dist. (Meter)	ΔHeight (Meter)
UP-LWY --- UP-ASN	5-22-2014	Fixed	0.011	0.021	283°18'29"	50016.836	-12.285
BG-207 --- UP-ASN	5-22-2014	Fixed	0.005	0.021	115°58'50"	30324.836	-14.212
BG-207 --- UP-LWY	5-22-2014	Fixed	0.015	0.033	107°58'47"	79868.074	-1.872
UP-BTN --- UP-LOB	5-21-2014	Fixed	0.011	0.045	228°04'35"	31344.157	0.983
UP-CLG --- UP-LOB	5-21-2014	Fixed	0.006	0.026	131°01'52"	20253.373	-0.954
UP-CLG --- UP-BTN	5-21-2014	Fixed	0.004	0.018	78°44'11"	39325.813	-1.938
UP-CLG --- UP-ASN	5-22-2014	Fixed	0.004	0.006	322°34'54"	22553.645	-5.661
UP-CLG --- UP-LWY	5-22-2014	Fixed	0.004	0.005	79°31'48"	35577.341	6.630
UP-CLG --- BG-207	5-22-2014	Fixed	0.008	0.021	307°20'38"	51500.584	8.533
BTG-7 --- UP-LOB	5-22-2014	Fixed	0.008	0.011	80°16'20"	14501.812	-10.094
BTG-7 --- UP-BTN	5-22-2014	Fixed	0.004	0.005	58°03'54"	44287.330	-11.055
UP-CLG --- BTG-7	5-22-2014	Fixed	0.003	0.005	356°25'22"	15777.354	-9.093

As shown in Table 20, a total of twelve (12) baselines were processed with reference elevation of point BG-207 and coordinates of BTG-7 held fixed. All of them passed the required accuracy.

4.4 Network Adjustment

After the baseline processing procedure, network adjustment is performed using TBC. Looking at the Adjusted Grid Coordinates Table C-of the TBC generated Network Adjustment Report, it is observed that the square root of the sum of the squares of x and y must be less than 20 cm and z less than 10 cm or in equation form:

$$\sqrt{((x_e)^2 + (y_e)^2)} < 20cm \text{ and } z_e < 10 \text{ cm}$$

where:

- xe is the Easting Error,
- ye is the Northing Error, and
- ze is the Elevation Error

for each control point. See the Network Adjustment Report shown in Table 21 to Table 23 for the complete details.

The seven (7) control points, BG-207, BTG-7, UP-ASN, UP-BTN, UP-CLG, UP-LOBO and UP-LWY were occupied and observed simultaneously to form a GNSS loop. Coordinates of point BTG-7 and elevation value of BG-207 were held fixed during the processing of the control points as presented in Table 21. Through these reference points, the coordinates and elevation of the unknown control points will be computed.

Table 21. Control Point Constraints

Point ID	Type	East σ (Meter)	North σ (Meter)	Height σ (Meter)	Elevation σ (Meter)
BG-207	Grid				Fixed
BTG-7	Global	Fixed	Fixed		
Fixed = 0.000001 (Meter)					

The list of adjusted grid coordinates, i.e. Northing, Easting, Elevation and computed standard errors of the control points in the network is indicated in Table 22. The fixed control point BG-207 and BTG-7, has no values for standard elevation and coordinates error, respectively.

Table 22. Adjusted Grid Coordinates

Point ID	Easting (Meter)	Easting Error (Meter)	Northing (Meter)	Northing Error (Meter)	Elevation (Meter)	Elevation Error (Meter)	Constraint
BG-207	250979.763	0.013	1554083.401	0.008	22.502	?	e
BTG-7	292538.897	?	1506749.028	?	20.775	0.048	LL
UP-ASN	278117.295	0.012	1540530.571	0.007	7.417	0.047	
UP-BTN	330309.698	0.008	1529876.941	0.005	9.151	0.051	
UP-CLG	291679.221	0.007	1522505.094	0.005	12.120	0.046	
UP-LOB	306852.492	0.012	1509086.719	0.007	10.285	0.058	
UP-LWY	326716.783	0.012	1528689.760	0.007	17.801	0.047	

The network is fixed at reference points BG-207 and BTG-7 for elevation and coordinate values, respectively. With the mentioned equation $\sqrt{((x_e)^2+(y_e)^2)} < 20\text{cm}$ for horizontal accuracy, and $z_e < 10\text{ cm}$ for the vertical ; the computation for the accuracy for the controls are as follows:

- a. BG-207**
- | | | |
|---------------------|---|------------------------------|
| Horizontal Accuracy | = | $\sqrt{((1.3)^2 + (0.8)^2)}$ |
| | = | $\sqrt{1.69 + 0.64}$ |
| | = | 1.53 cm < 20 cm |
| Vertical Accuracy | = | Fixed |
- b. BTG-7**
- | | | |
|---------------------|---|--------|
| Horizontal Accuracy | = | Fixed |
| Vertical Accuracy | = | 4.8 cm |
- c. UP-ASN**
- | | | |
|---------------------|---|------------------------------|
| Horizontal Accuracy | = | $\sqrt{((1.2)^2 + (0.7)^2)}$ |
| | = | $\sqrt{1.44 + 0.49}$ |
| | = | 1.30 < 20 cm |
| Vertical Accuracy | = | 4.7 cm |
- d. UP-BTN**
- | | | |
|---------------------|---|------------------------------|
| Horizontal Accuracy | = | $\sqrt{((0.8)^2 + (0.5)^2)}$ |
| | = | $\sqrt{0.64 + 0.25}$ |
| | = | 0.94 cm < 20 cm |
| Vertical Accuracy | = | 5.1 cm |
- e. UP-CLG**
- | | | |
|---------------------|---|------------------------------|
| Horizontal Accuracy | = | $\sqrt{((0.7)^2 + (0.5)^2)}$ |
| | = | $\sqrt{0.49 + 0.25}$ |
| | = | 0.86 cm < 20 cm |
| Vertical Accuracy | = | 4.6 cm |
- f. UP-LOB**
- | | | |
|---------------------|---|------------------------------|
| Horizontal Accuracy | = | $\sqrt{((1.2)^2 + (0.7)^2)}$ |
| | = | $\sqrt{1.44 + 0.49}$ |
| | = | 1.39 cm < 20 cm |
| Vertical Accuracy | = | 5.8 cm |
- g. UP-LWY**
- | | | |
|---------------------|---|------------------------------|
| Horizontal Accuracy | = | $\sqrt{((1.2)^2 + (0.7)^2)}$ |
| | = | $\sqrt{1.44 + 0.49}$ |
| | = | 1.39 cm < 20 cm |
| Vertical Accuracy | = | 4.7 cm |

Following the given formula, the horizontal and vertical accuracy result of the seven occupied control points are within the required precision of the program.

Table 23. Adjusted Geodetic Coordinates

Point ID	Latitude	Longitude	Ellipsoid	Height	Constraint
BG-207	N14°02'47.32681"	E120°41'38.93590"	65.606	?	e
BTG-7	N13°37'19.49611"	E121°04'56.32756"	66.166	0.048	LL
UP-ASN	N13°55'34.60800"	E120°56'47.03866"	51.408	0.047	
UP-BTN	N13°50'00.87918"	E121°25'47.84863"	55.110	0.051	
UP-CLG	N13°45'51.87503"	E121°04'23.55772"	57.069	0.046	
UP-LOB	N13°38'39.10153"	E121°12'51.89915"	56.079	0.058	
UP-LWY	N13°49'21.47540"	E121°23'48.47087"	63.700	0.047	

The corresponding geodetic coordinates of the observed points are within the required accuracy as shown in Table 23. Based on the result of the computation, the accuracy condition is satisfied; hence, the required accuracy for the program was met.

The summary of reference and control points used is indicated in Table 24.

Table 24. Reference and control points used and its location (Source: NAMRIA, UP-TCAGP)

Control Point	Order of Accuracy	Geographic Coordinates (WGS 84)			UTM ZONE 51 N		
		Latitude	Longitude	Ellipsoidal Height (m)	Northing (m)	Easting (m)	BM Ortho (m)
BG-207	1st Order	14°02'47.32681"	120°41'38.93590"	65.606	1554083.401	250979.763	22.502
BTG-7	1st Order	13°37'19.49611"	121°04'56.32756"	66.166	1506749.028	292538.897	20.775
UP-ASN	UP Established	13°55'34.60800"	120°56'47.03866"	51.408	1540530.571	278117.295	7.417
UP-BTN	UP Established	13°50'00.87918"	121°25'47.84863"	55.110	1529876.941	330309.698	9.151
UP-CLG	UP Established	13°45'51.87503"	121°04'23.55772"	57.069	1522505.094	291679.221	12.120
UP-LOB	UP Established	13°38'39.10153"	121°12'51.89915"	56.079	1509086.719	306852.492	10.285
UP-LWY	UP Established	13°49'21.47540"	121°23'48.47087"	63.700	1528689.760	326716.783	17.801

4.5 Cross-section and Bridge As-Built survey and Water Level Marking

Bridge as-built and cross-section survey was conducted on May 21, 2014 at the downstream side of Lobo Bridge in Brgy. Lagadlarin, Municipality of Lobo, Batangas using GNSS receiver Trimble® SPS 882 in PPK survey technique with UP-LOBO and UP-CLG used as GNSS base station as shown in Figure 35.



Figure 35. Cross-section survey conducted on Rosario-Lobo River in Brgy. Lagadlarin, Municipality of Lobo

The cross-sectional line length of Lobo Bridge is about 412.31 m with 237 cross-sectional points acquired using UP-LOBO as the GNSS base station. The location map and cross section diagram are shown in Figure 36 and Figure 37, respectively.

Lobo Bridge
Rosario-Lobo River
LATITUDE = 13°38'39.10099" N
LONGITUDE = 121°12'51.89876" E

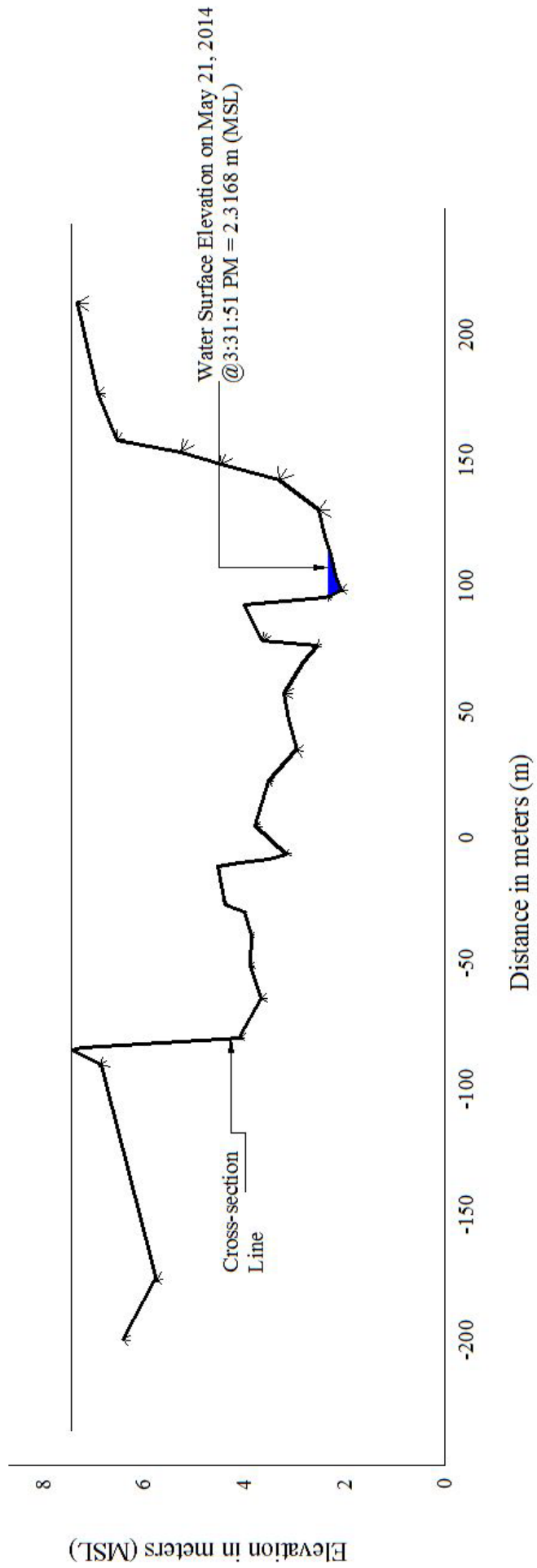


Figure 37. Rosario-Lobo Bridge cross-section diagram

Water surface elevation in MSL of Rosario-Lobo River was determined on May 21, 2014 at 3:31 PM using Trimble® SPS 882 in PPK mode with a value of 2.32 m in MSL. This value was translated onto marking on Lobo Bridge's pier using digital level which will be used by Mapua PHIL-LIDAR 1, as shown in Figure 38. The marking will serve as their reference for flow data gathering and depth gauge deployment for Rosario-Lobo River.



Figure 38. Marking of MSL-based elevation on the pier on the left side facing downstream (A) and right side (B) at the Lobo Bridge, Lobo Batangas

4.6 Validation Points Acquisition Survey

Validation points acquisition survey was conducted on March 5, 2016 using a survey-grade GNSS rover receiver, Trimble® SPS 882, mounted on a pole which was attached to the side of the vehicle as shown in Figure 39. It was secured with cable ties to ensure that it was horizontally and vertically balanced. The antenna height was 2.09 m measured from the ground up to the bottom of notch of the GNSS rover receiver. The PPK technique utilized for the conduct of the survey was set to continuous topo mode with UP-LOBO occupied as the GNSS base station all throughout the conduct of the survey.



Figure 39. Validation points acquisition survey set up along Rosario-Lobo River Basin

The validation points acquisition survey for the Rosario-Lobo River Basin traversed the Municipality of Lobo and Batangas City. The route of the survey aims to traverse LiDAR flight strips perpendicularly for the basin. A total of 2,694 points with an approximate length of 11.83 km was acquired for the validation point acquisition survey as shown in the map in Figure 40.



Figure 36. Location map of Rosario-Lobo Bridge cross-section

4.7 River Bathymetric Survey

Manual bathymetry survey using a Trimble® SPS882 GPS PPK survey technique was executed on August 28 and 29, 2014 as shown in Figure 41. The river was traversed by foot from the upstream in Brgy. Bignay, with coordinates 13°40'30.02" N and 121°14'06.28" E, down to Brgy. Lagadlarin, with coordinates 13°38'08.86"E and 121°12'21.81"N, Lobo Batangas because of the shallow depth of the river. A portable Cdepth sounder was used to get the depth for the deeper portion in the mouth of the river in Brgy. Lagadlarin. The control points and UP-LOBO were used as base station for the whole conduct of the survey.



Figure 41. Manual bathymetric survey along Rosario Lobo River from the mouth of the river up to the Lobo Bridge

The bathymetric survey coverage for Rosario-Lobo river is illustrated in Figure 42. A CAD drawing was also produced to illustrate the Rosario-Lobo riverbed centerline profile as shown in Figure 43. There is about a 17.22-m change in elevation observed within the entire extent of bathymetric data from its upstream in Brgy. Bignay down to the mouth of the river in Brgy. Lagadlarin, Municipality of Lobo.

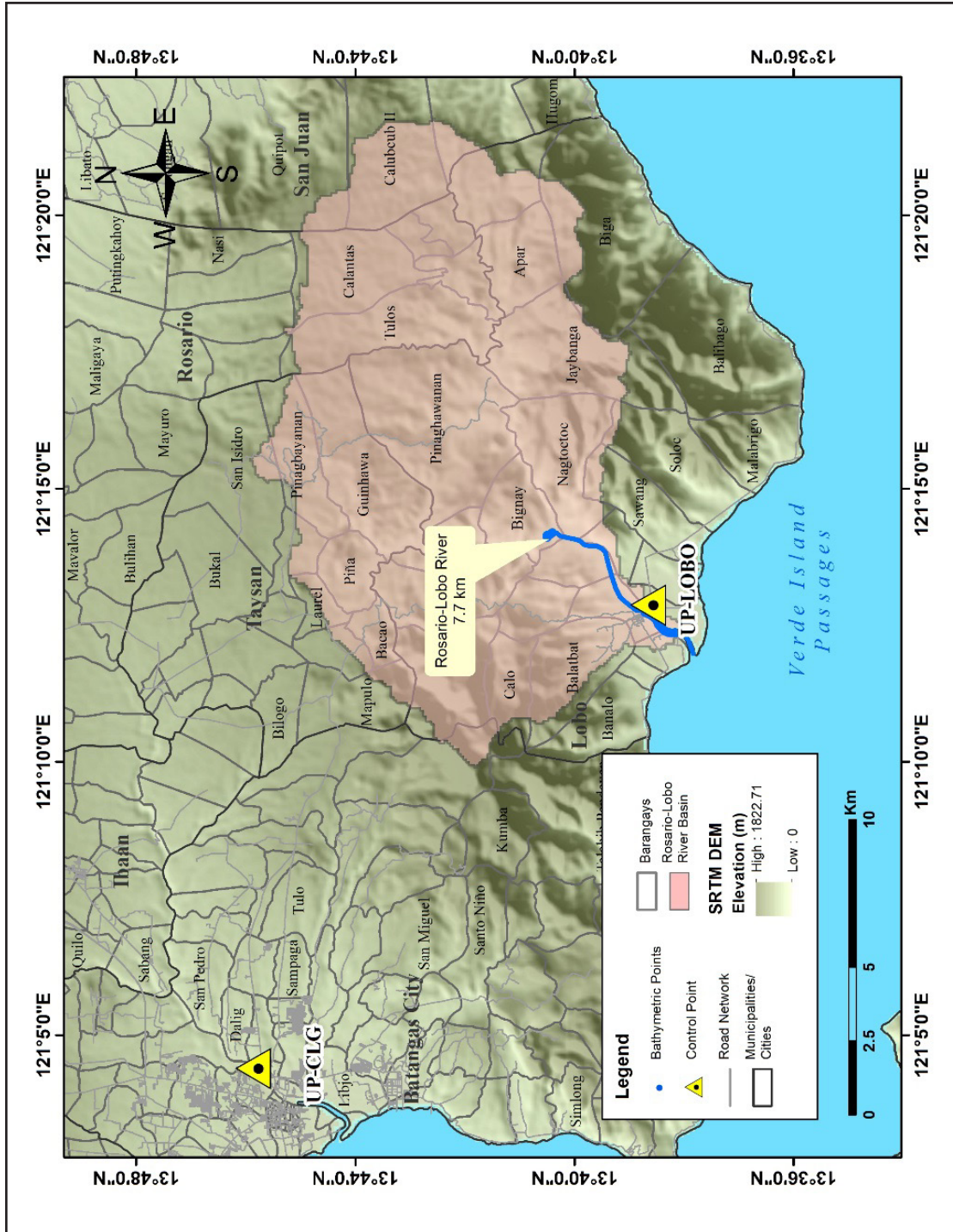
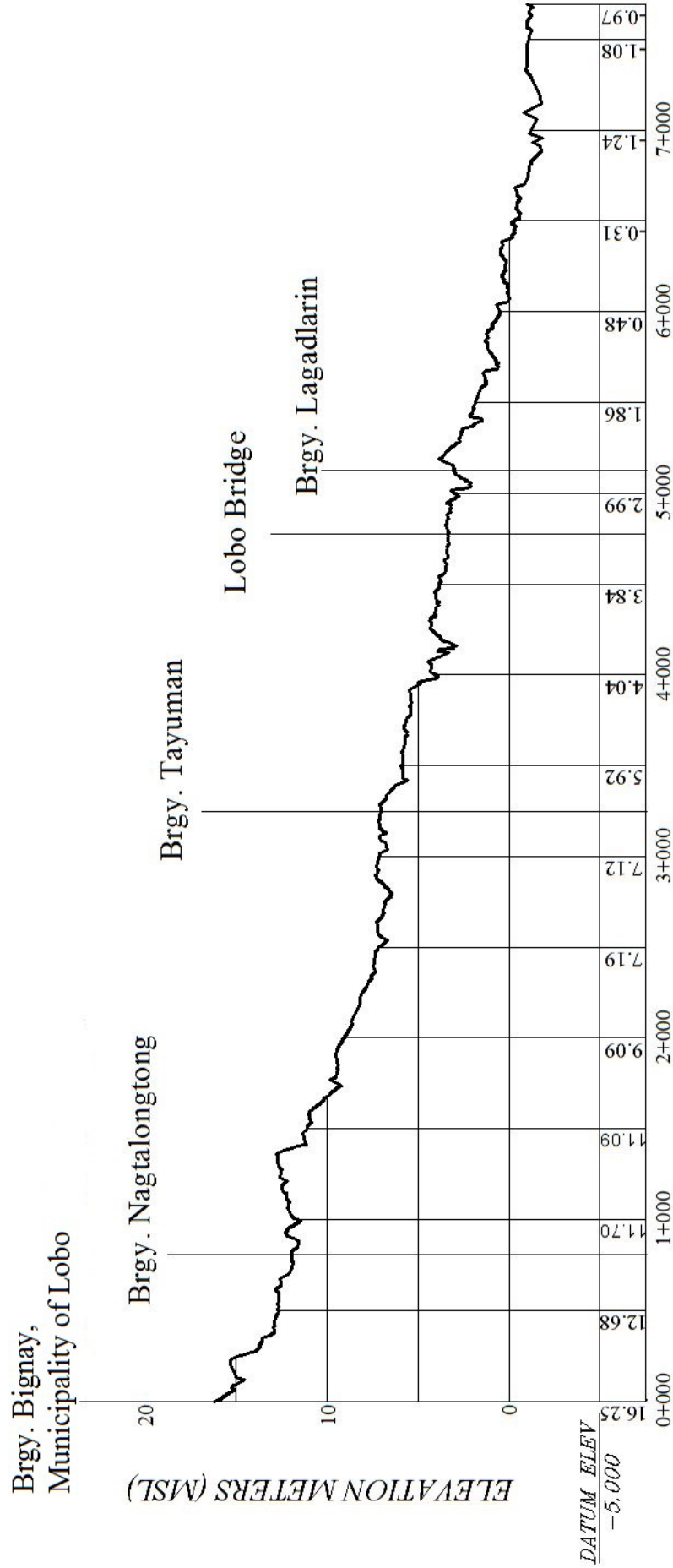


Figure 42. Bathymetric points gathered from Rosario-Lobo River

ROSARIO LOBO RIVERBED PROFILE



DISTANCE FROM UPSTREAM (m)

Figure 43. Centerline riverbed profile of Rosario-Lobo River

CHAPTER 5: FLOOD MODELING AND MAPPING

Dr. Alfredo Mahar Lagmay, Christopher Uichanco, Sylvia Sueno, Marc Moises, Hale Ines, Miguel del Rosario, Kenneth Punay, Neil Tingin, Pauline Racoma

The methods applied in this Chapter were based on the DREAM methods manual (Lagmay, et al., 2014) and further enhanced and updated in Paringit, et al. (2017).

5.1 Data Used for Hydrologic Modeling

5.1.1 Hydrometry and Rating Curves

All data that affect the hydrologic cycle of the Rosario-Lobo River Basin were monitored, collected, and analyzed. Rainfall, water level, and flow in a certain period of time, which may affect the hydrologic cycle of the Rosario-Lobo River Basin were monitored, collected, and analyzed.

5.1.2 Precipitation

Precipitation data was taken from two automatic rain gauges (ARGs) installed by the Department of Science and Technology – Advanced Science and Technology Institute (DOST-ASTI). The locations of the two (2) ARGs is in Lobo, Batangas. The location of one of the rain gauges is shown in Figure 44.

This specific rain gauge is the Lobo ARG (13°41'15.11"N, 121°12'32.47"E), located in Lobo, Batangas (Figure 44). The precipitation data collection started from October 18, 2015 at 00:00 AM to Octo 27, 2015 at 23:45AM with a 15-minute recording interval, as presented in Figure 47.

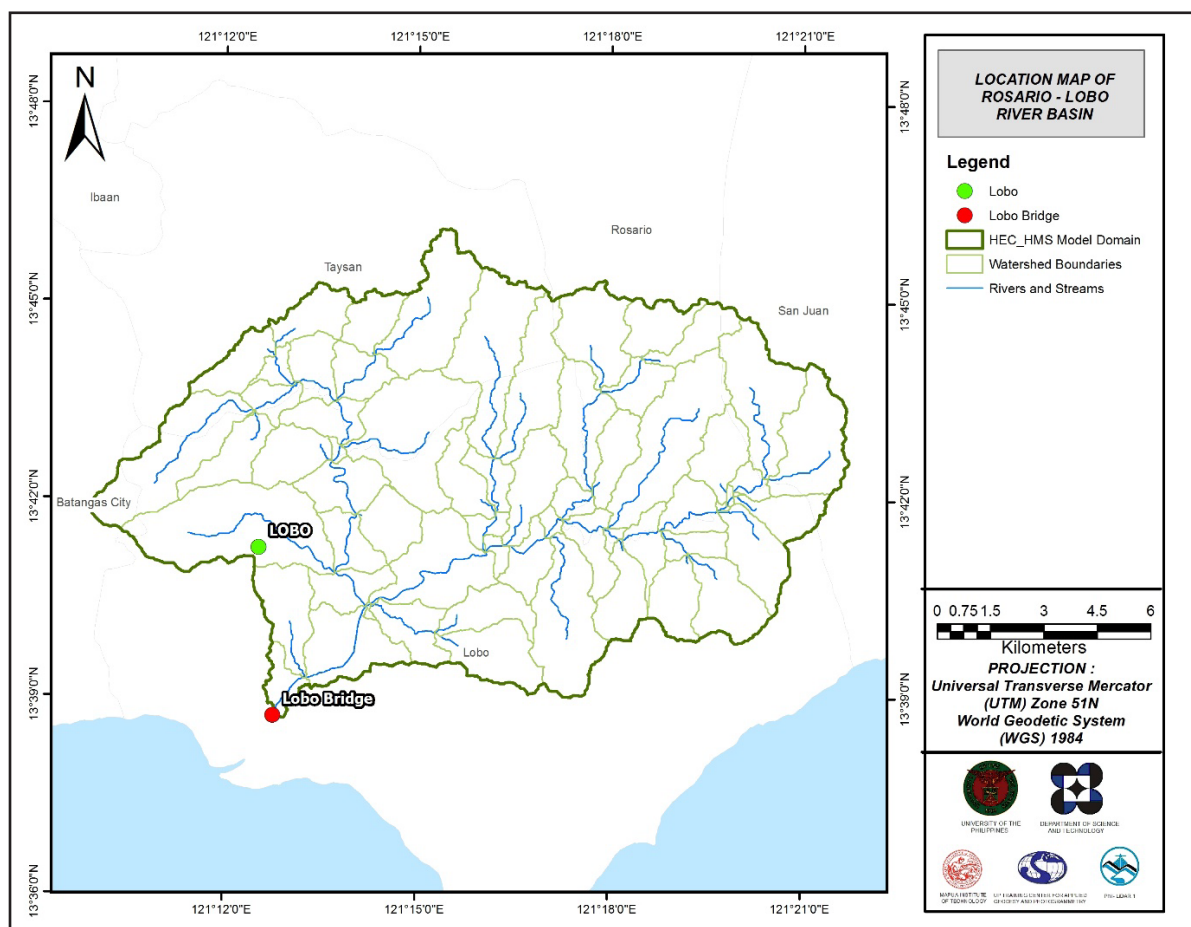


Figure 44. Location map of Rosario-Lobo HEC-HMS model used for calibration

For Lobo Rain Gauge, total rain for the event is 59.2 mm. Peak rain of 5.8 mm was recorded on 18 October 2015. The lag time between the peak rainfall and discharge is 13 hour, as seen in Figure 47.

5.1.3 Rating Curves and River Outflow

A rating curve was developed at Lobo Bridge, Lobo, Batangas Province (13°38'42.62"N, 121°12'46.10"E). It gives the relationship between the observed water levels from the Lobo Bridge using depth gage and outflow of the watershed got using the flow meter at this location. It is expressed in the form of the following equation:

$$Q=anh$$

where,

- Q : Discharge (m³/s),
- h : Gauge height, and
- a and n : Constants.

For the Bunga Bridge, the rating curve is expressed as $y = 2E-124e13.975x$, as demonstrated in Figure 52.

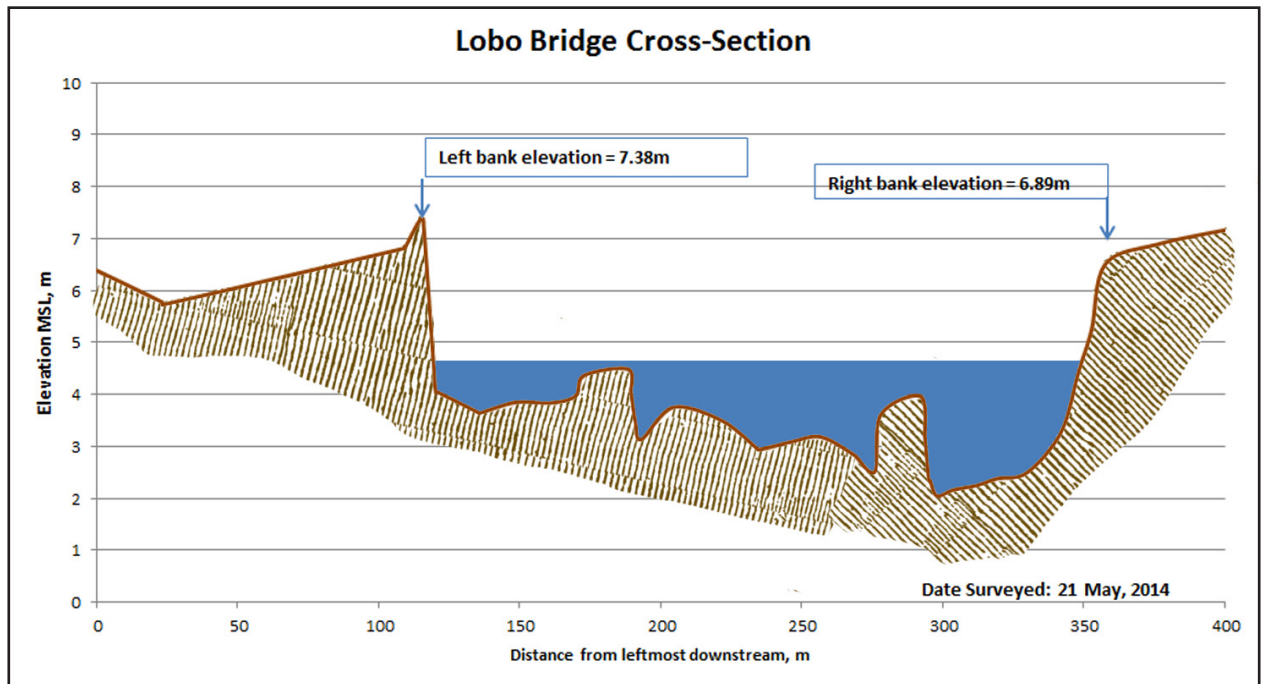


Figure 45. Cross-Section Plot of Rosario-Lobo Bridge

For Rosario-Lobo Bridge, the rating curve is expressed as $Q = 0.0002e^{5.8978h}$ as shown in Figure 46.

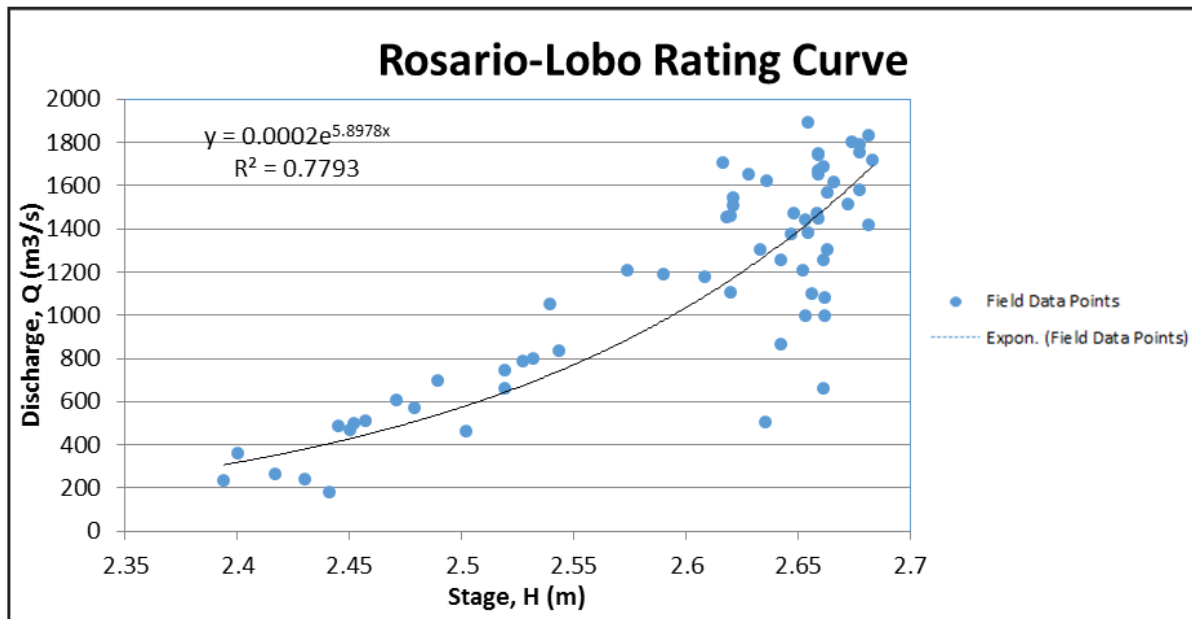


Figure 46. Rating curve at Lobo Bridge, Batangas City, Batangas Province

This rating curve equation was used to compute the river outflow at Lobo Bridge for the calibration of the HEC-HMS model shown in Figure 47. Peak discharge is 18.3 m³/s at 12:50, October 18, 2015.

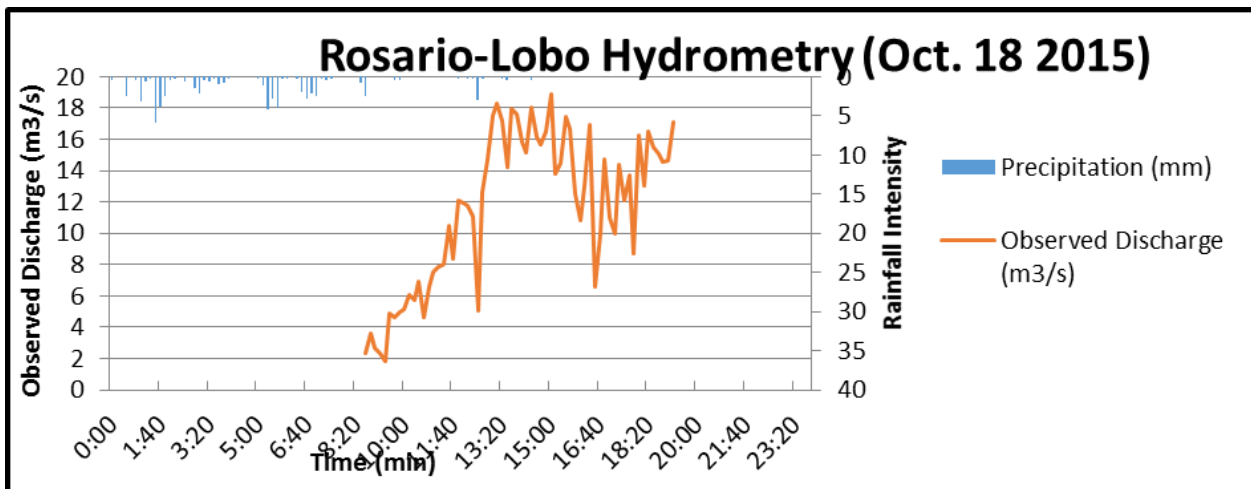


Figure 47. Rainflow and outflow data at Rosario-Lobo River used for modeling

5.2 RIDF Station

The Philippines Atmospheric Geophysical and Astronomical Services Administration (PAGASA) computed Rainfall Intensity Duration Frequency (RIDF) values for the Ambulong Gauge. This station chosen based on its proximity to the Rosario-Lobo watershed. The extreme values for this watershed were computed based on a 54-year record, as shown in Table 25.

Table 25. RIDF values for Ambulong Rain Gauge computed by PAGASA

COMPUTED EXTREME VALUES (in mm) OF PRECIPITATION									
T (yrs)	10 mins	20 mins	30 mins	1 hr	2 hrs	3 hrs	6 hrs	12 hrs	24 hrs
2	22.7	35.5	36.3	50.2	68.2	80.1	104.1	125.7	150.8
5	27.9	45.5	53.8	74.2	103.4	122.5	159.7	192.9	226.7
10	34.2	52.1	65.4	90.1	126.7	150.6	196.5	237.3	276.9
15	37.8	57.4	71.9	99	139.8	166.4	217.3	262.4	305.3
20	40.3	61	76.5	105.3	149	177.5	231.9	280	325.1
25	42.2	63.9	80	110.1	156.1	186	243.1	293.5	340.4
50	48.1	72.6	90.9	125	178	212.3	277.6	335.2	387.5
100	54	81.2	101.6	139.8	199.7	238.4	311.8	376.6	434.3

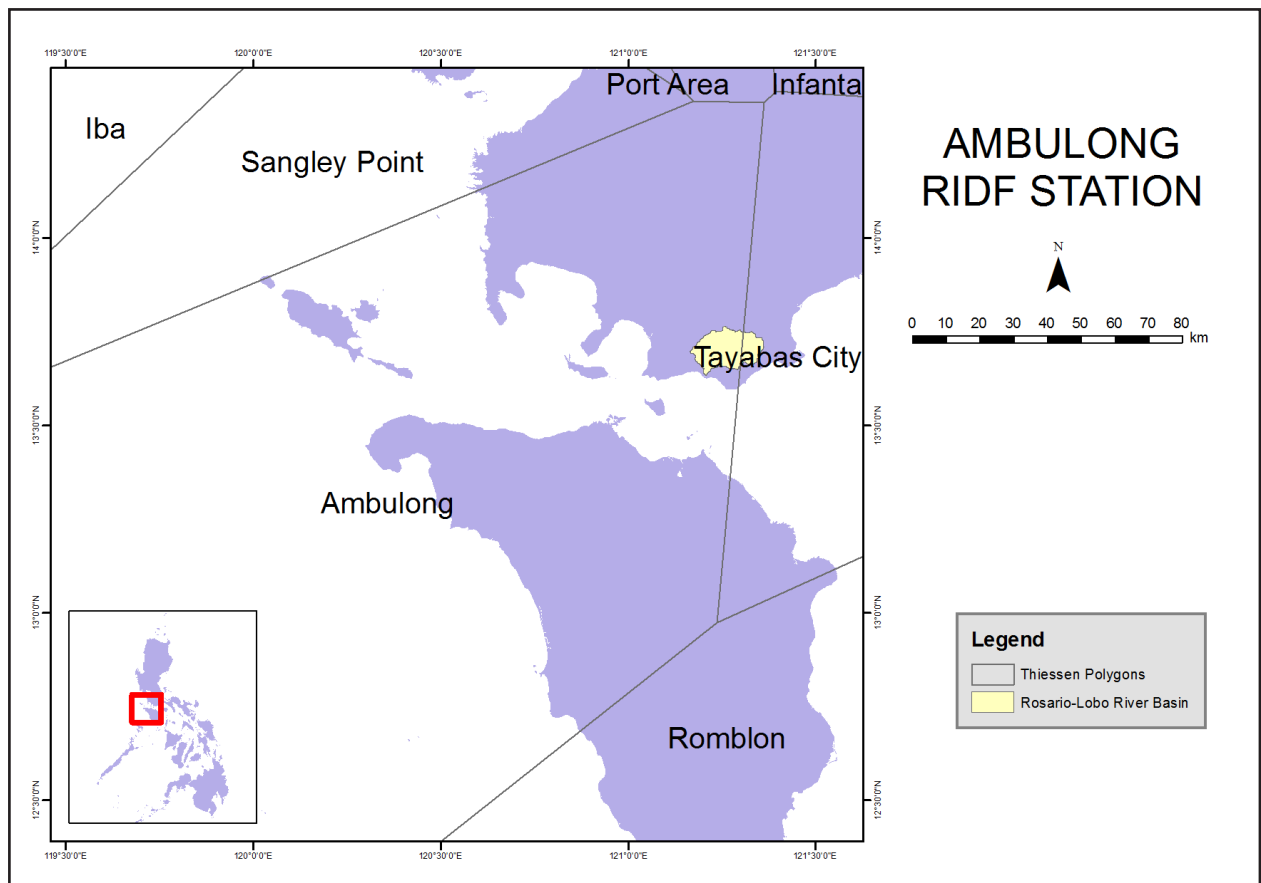


Figure 48. Ambulong RIDF location relative to Rosario-Lobo River Basin

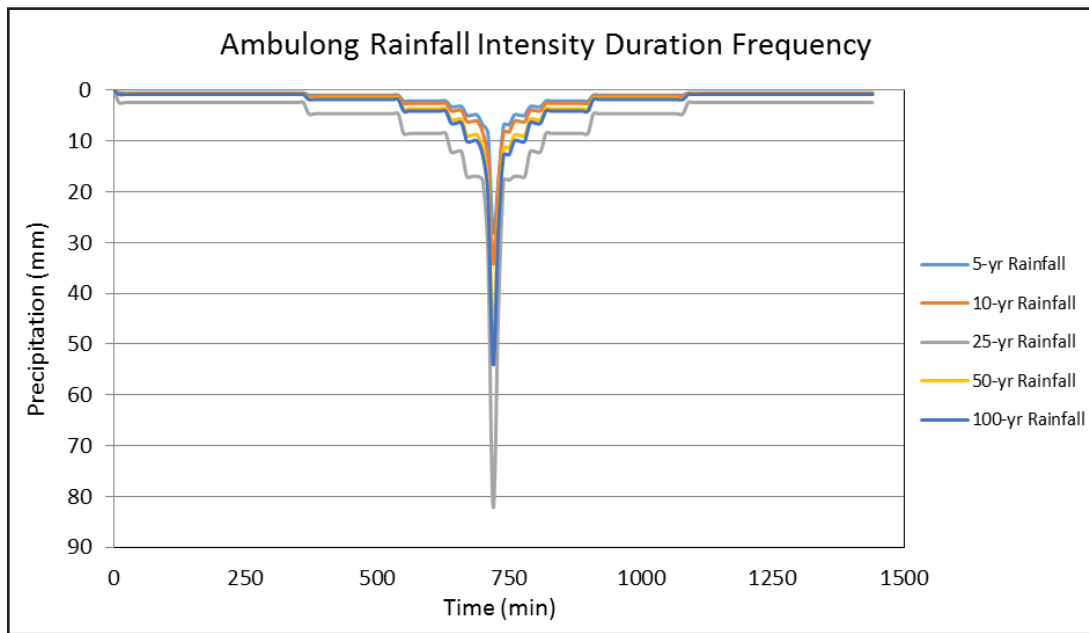


Figure 49. Synthetic storm generated for a 24-hr period rainfall for various return periods.

5.3 HMS Model

The soil dataset was generated before 2004 from the Bureau of Soil and Water Management (BSWM) under the Department of Agriculture (DA). The land cover dataset is from the National Mapping and Resource information Authority (NAMRIA). The soil and land cover of the Rosario-Lobo River Basin are shown in Figure 50 and Figure 51, respectively.

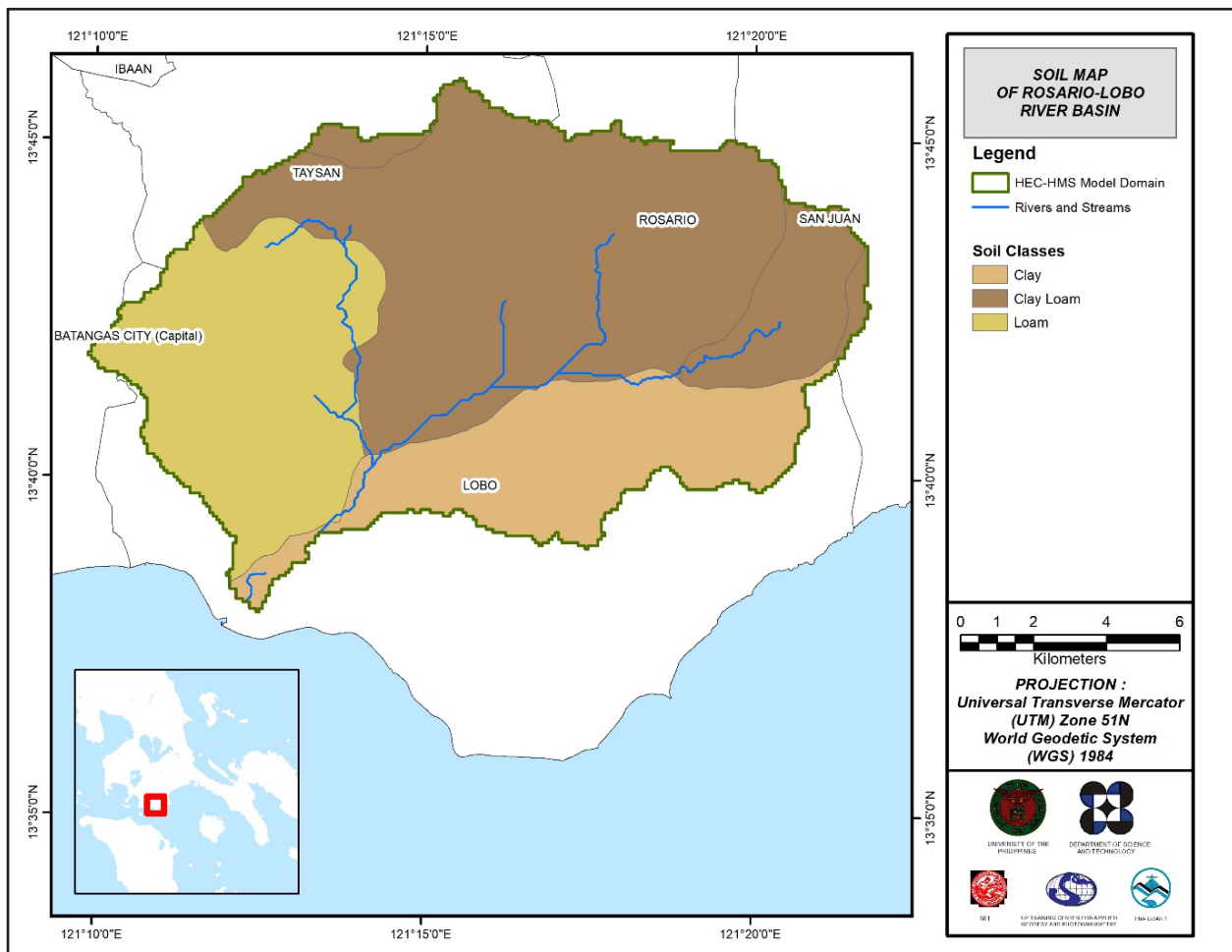


Figure 50. Soil map of the Rosario-Lobo River Basin

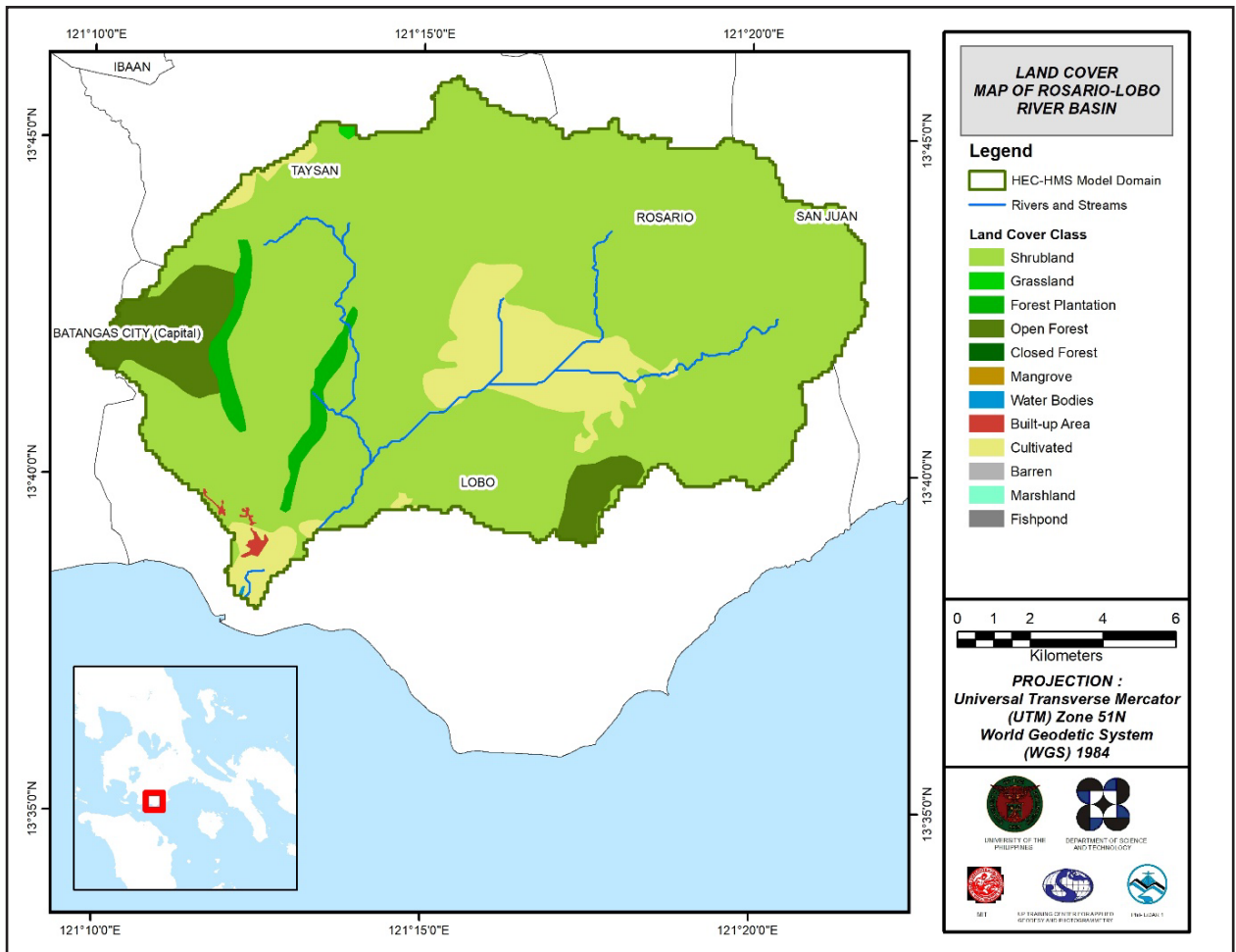


Figure 51. Land cover map of Rosario-Lobo River Basin

For the Rosario-Lobo River Basin, the three (3) soil classes identified were clay loam, clay, and loam. The seven (7) land cover types identified were open canopy forests, brushland, grassland, cultivated areas, built-up areas, inland water and tree plantations.

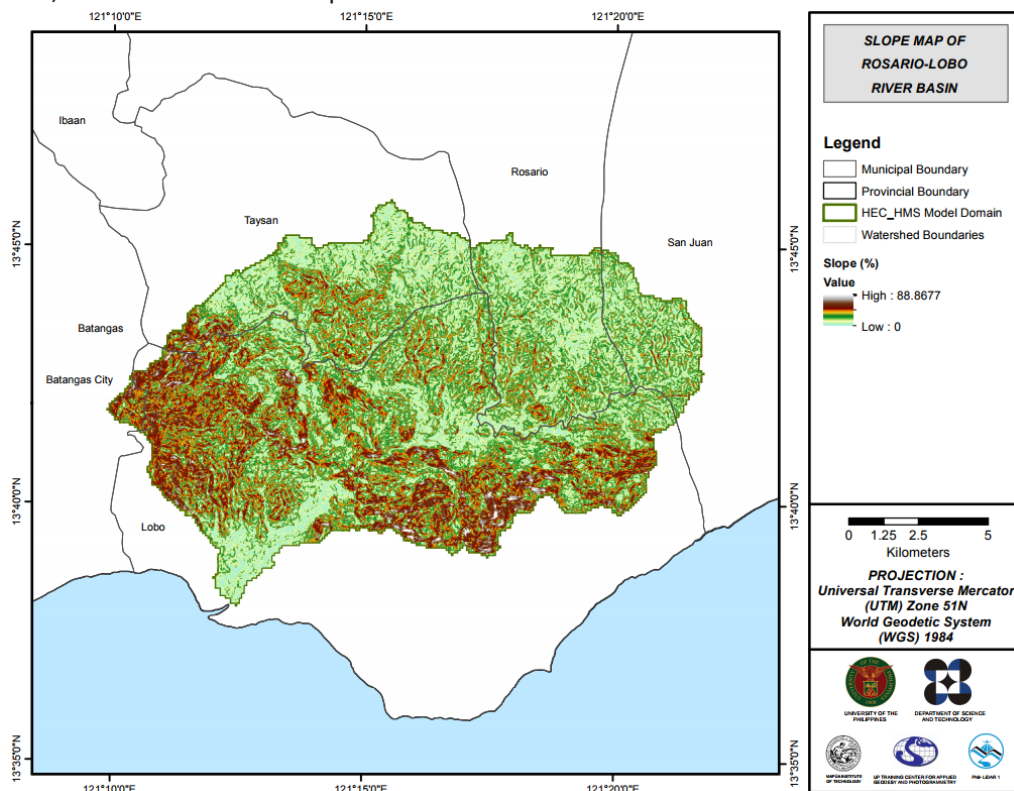


Figure 52. Slope map of Rosario-Lobo River Basin

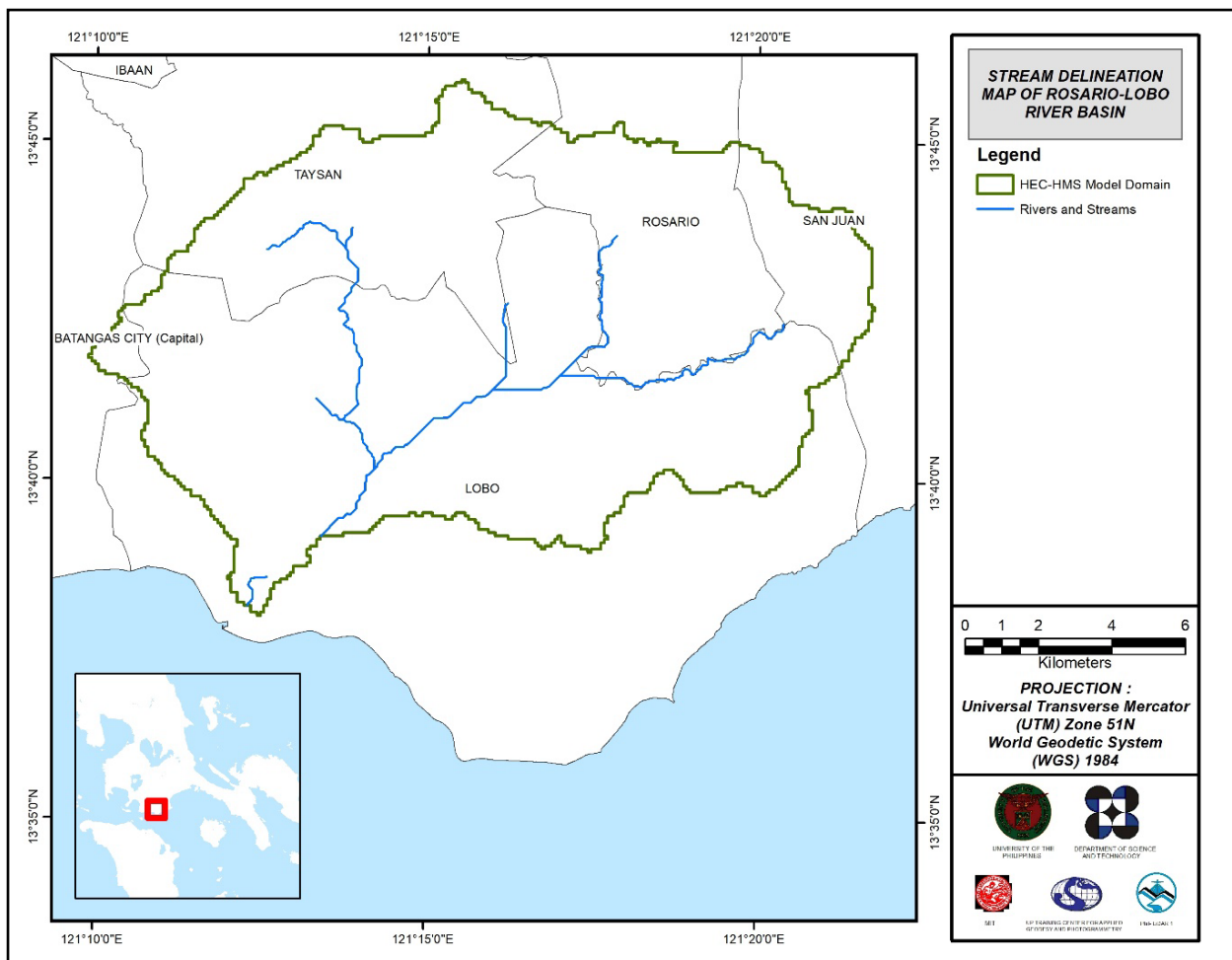


Figure 53. Stream delineation map of Rosario-Lobo River Basin

The Rosario-Lobo Basin model comprises 61 sub basins, 30 reaches, and 30 junctions. The main outlet is at the southernmost tip of the watershed. This basin model is illustrated in Figure 54. The basins were identified based on soil and land cover characteristic of the area. Precipitation was taken from an installed Rain Gauge near and inside the river basin. Finally, it was calibrated using the data from actual discharge flow gathered in the Lobo Bridge.

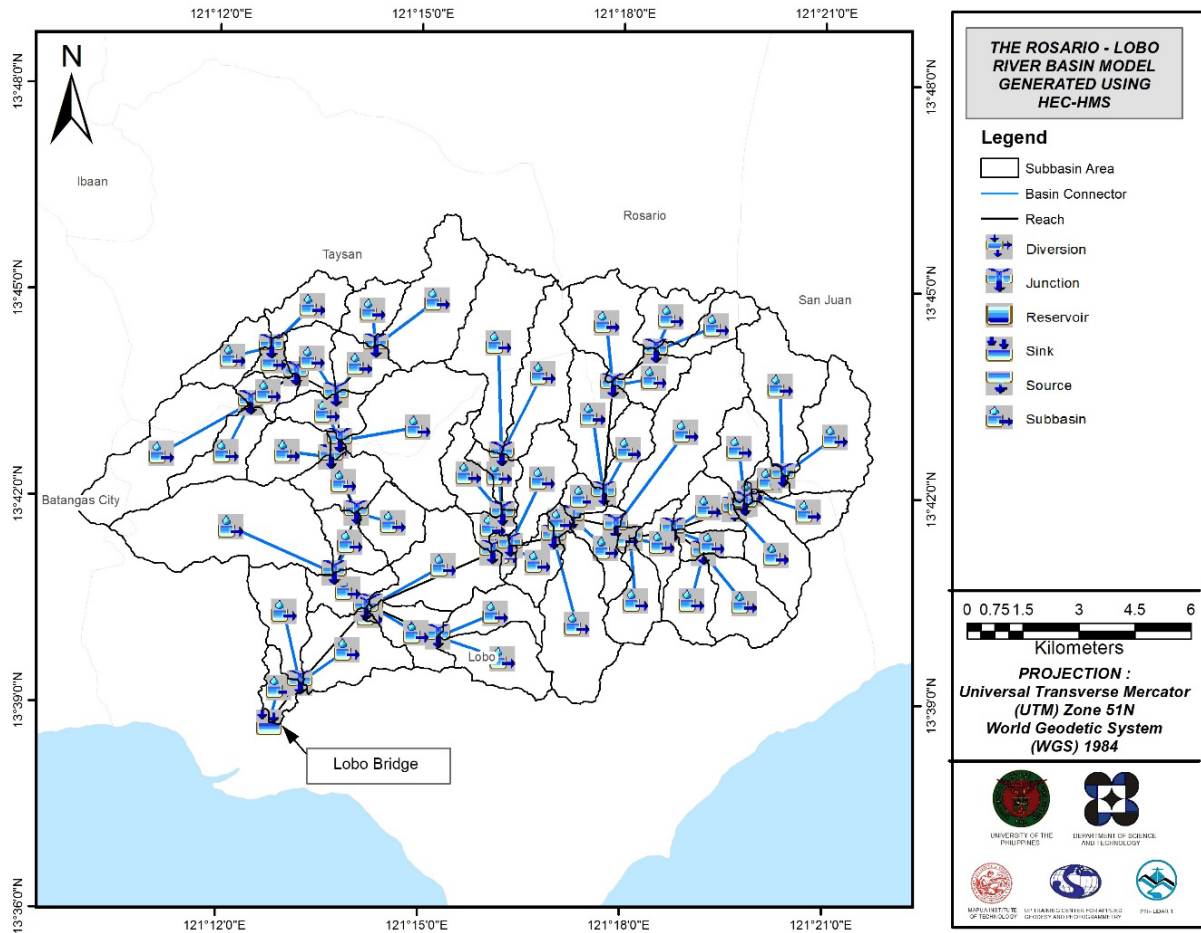


Figure 54. HEC-HMS generated Rosario-Lobo River Basin Model.

5.4 Cross-section Data

Riverbed cross-sections of the watershed are crucial in the HEC-RAS model setup. The cross-section data for the HEC-RAS model was derived using the LiDAR DEM data. It was defined using the Arc GeoRAS tool and was post-processed in ArcGIS. This is illustrated in Figure 55.

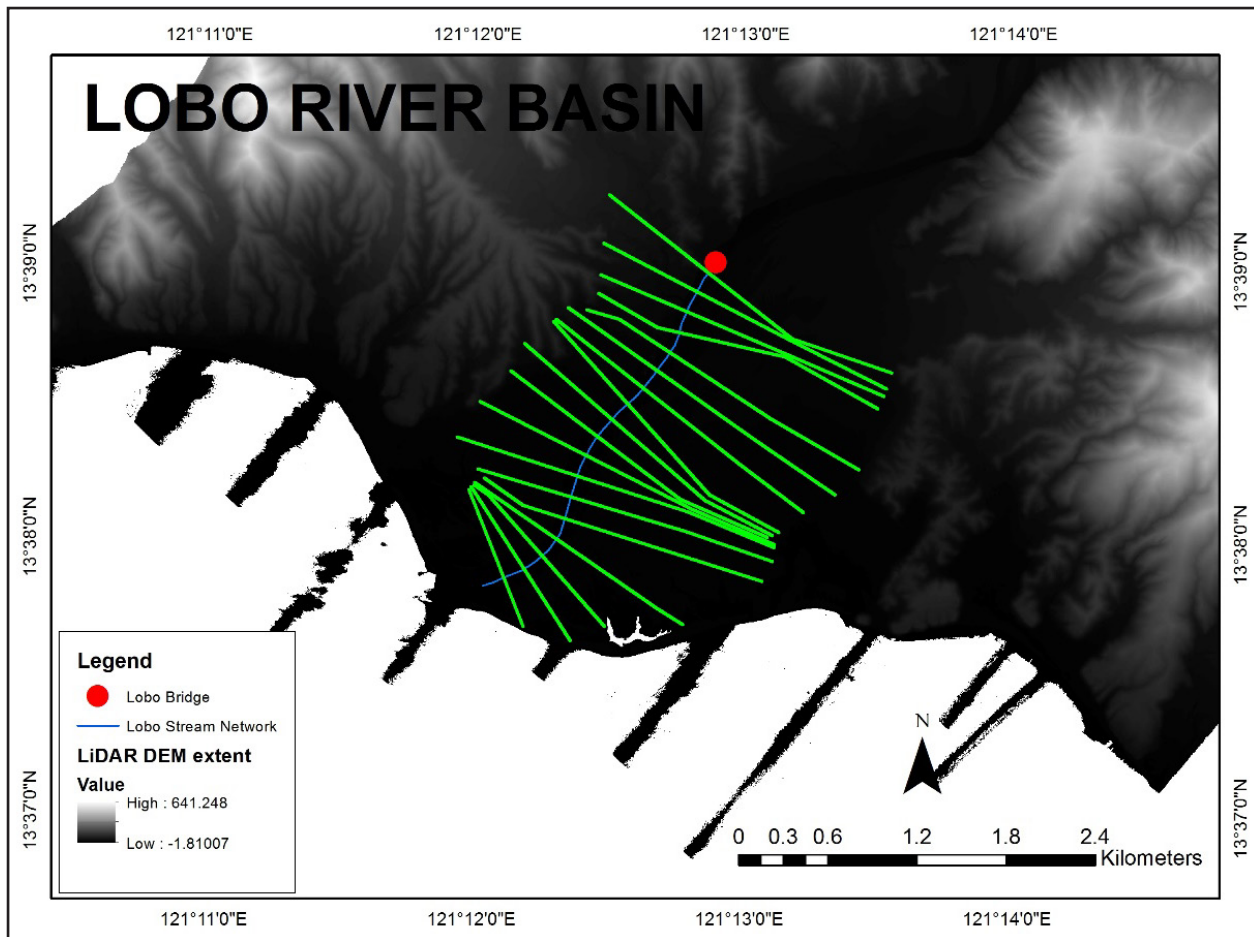


Figure 55. River cross-section of Rosario-Lobo River generated through Arcmap HEC GeoRAS tool

5.5 Flo 2D Model

The automated modelling process allows for the creation of a model with boundaries that are almost exactly coincidental with that of the catchment area. As such, they have approximately the same land area and location. The entire area is divided into square grid elements, 10 meter by 10 meter in size. Each element is assigned a unique grid element number which serves as its identifier, then attributed with the parameters required for modelling such as x-and y-coordinate of centroid, names of adjacent grid elements, Manning coefficient of roughness, infiltration, and elevation value. The elements are arranged spatially to form the model, allowing the software to simulate the flow of water across the grid elements and in eight directions (north, south, east, west, northeast, northwest, southeast, southwest).

Based on the elevation and flow direction, it is seen that the water will generally flow from the northeast of the model to the southwest, following the main channel. As such, boundary elements in those particular regions of the model are assigned as inflow and outflow elements respectively.



Figure 56. Screenshot of subcatchment with the computational area to be modeled in FLO-2D GDS Pro

The simulation is then run through FLO-2D GDS Pro. This particular model had a computer run time of 26.47314 hours. After the simulation, FLO-2D Mapper Pro is used to transform the simulation results into spatial data that shows flood hazard levels, as well as the extent and inundation of the flood. Assigning the appropriate flood depth and velocity values for Low, Medium, and High creates the following food hazard map. Most of the default values given by FLO-2D Mapper Pro are used, except for those in the Low hazard level. For this particular level, the minimum h (Maximum depth) is set at 0.2 m while the minimum vh (Product of maximum velocity (v) times maximum depth (h)) is set at 0 m²/s.

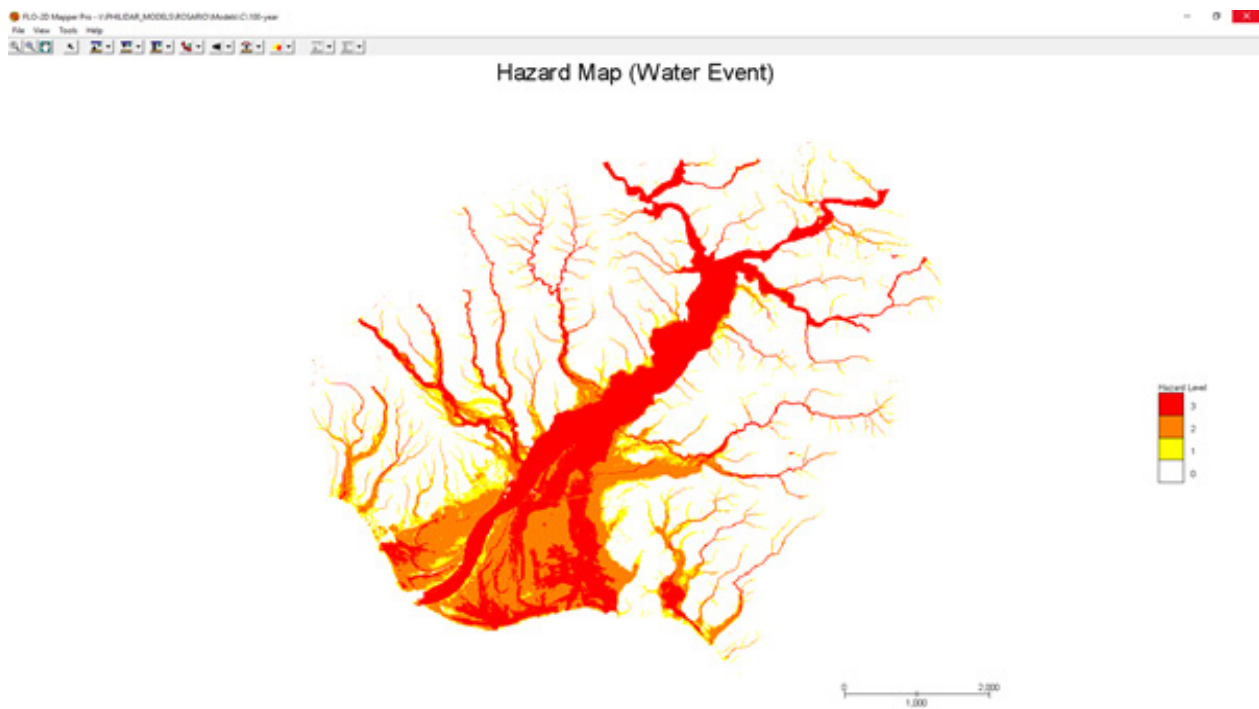


Figure 57. Generated 100-year rain return hazard map from FLO-2D Mapper

The creation of a flood hazard map from the model also automatically creates a flow depth map depicting the maximum amount of inundation for every grid element. The legend used by default in Flo-2D Mapper is not a good representation of the range of flood inundation values, so a different legend is used for the layout. In this particular model, the inundated parts cover a maximum land area of 42622200.00 m2.

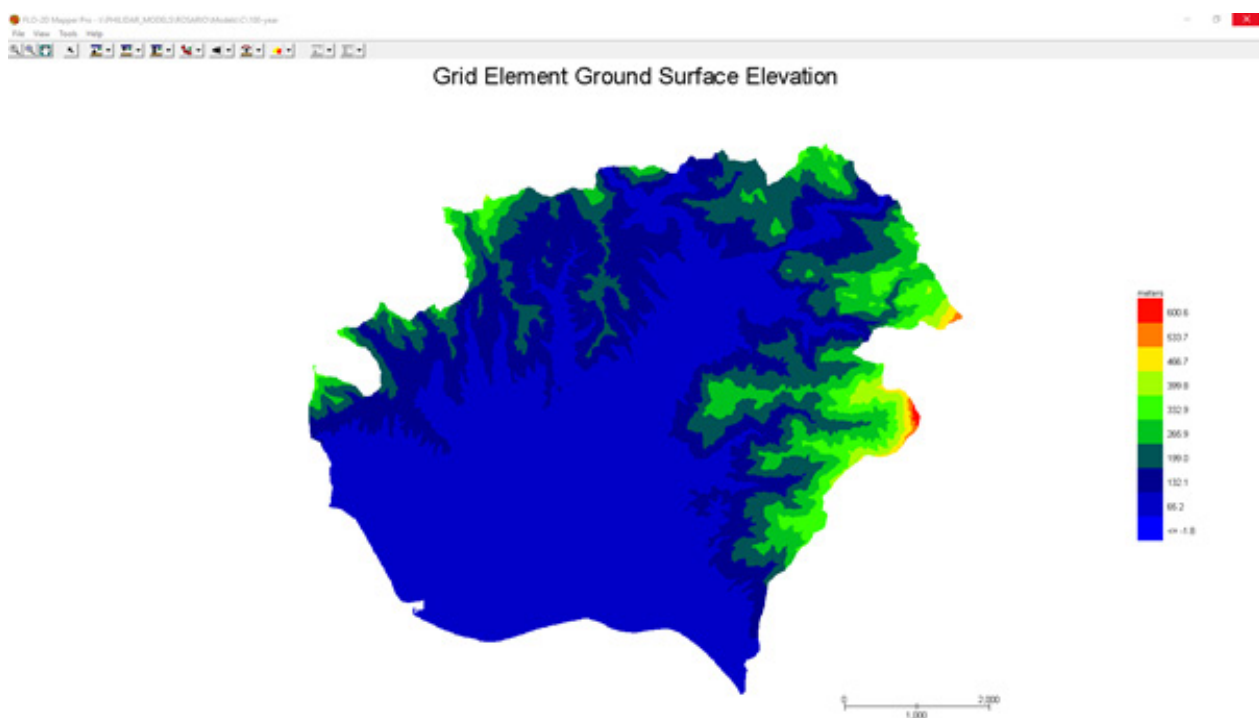


Figure 58. Generated 100-year rain return flow depth map from FLO-2D Mapper

There is a total of 72937531.21 m3 of water entering the model. Of this amount 17953371.22 m3 is due to rainfall while 54984159.99 m3 is inflow from other areas outside the model. 4437633.00 m3 of this water is lost to infiltration and interception, while 1903871.14 m3 is stored by the flood plain. The rest, amounting up to 66596049.76 m3, is outflow.

5.6 Results of HMS Calibration

After calibrating the Rosario-Lobo HEC-HMS river basin model, its accuracy was measured against the observed values. Figure 59 shows the comparison between the two discharge data.

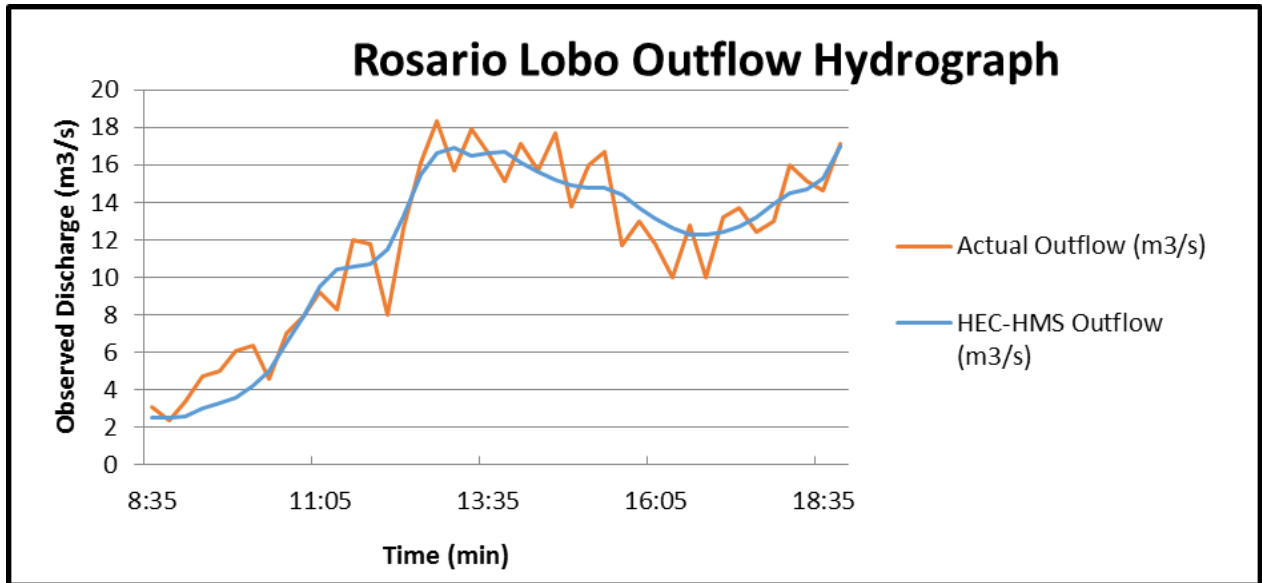


Figure 59. Outflow Hydrograph of Rosario-Lobo produced by the HEC-HMS model compared with observed outflow.

Enumerated in Table 30 are the adjusted ranges of values of the parameters used in calibrating the model.

Table 26. Range of Calibrated Values for Rosario-Lobo

Hydrologic Element	Calculation Type	Method	Parameter	Range of Calibrated Values
Basin	Loss	SCS Curve number	Initial Abstraction (mm)	0.015 – 31.133
			Curve Number	41.587 - 99
	Transform	Clark Unit Hydrograph	Time of Concentration (hr)	0.017 – 9.025
			Storage Coefficient (hr)	0.081 – 27.56
	Baseflow	Recession	Recession Constant	0.058 - 1
			Ratio to Peak	0.23 – 0.77
Reach	Routing	Muskingum-Cunge	Manning's Coefficient	0.00040 – 0.30

Initial abstraction defines the amount of precipitation that must fall before surface runoff. The magnitude of the outflow hydrograph increases as initial abstraction decreases. The range of values from 0.015mm to 31.133mm means that there is minimal to average amount of infiltration or rainfall interception by vegetation.

Curve number is the estimate of the precipitation excess of soil cover, land use, and antecedent moisture. The magnitude of the outflow hydrograph increases as curve number increases. The range of 41.587 to 99 for curve number is advisable for Philippine watersheds depending on the soil and land cover of the area (M. Horritt, personal communication, 2012). For Rosario-Lobo, the soil classes identified were clay loam, clay, and loam. The land cover types identified were open canopy forests, brushland, grassland, cultivated areas, built-up areas, inland water and tree plantations.

Time of concentration and storage coefficient are the travel time and index of temporary storage of runoff in a watershed. The range of calibrated values from 0.017 hours to 9.025 hours determines the reaction time of the model with respect to the rainfall. The peak magnitude of the hydrograph also decreases when these parameters are increased.

Recession constant is the rate at which baseflow recedes between storm events and ratio to peak is the ratio of the baseflow discharge to the peak discharge. The Recession Constant for each of the watershed's basins ranges from 0.058 to 1 and the Ratio to Peak ranges from 0.23 to 0.77. These influence the receding limb of the outflow hydrograph which in this case is not likely to quickly return to its original discharge values.

Manning's roughness coefficient ranging from 0.0004 to 0.30 corresponds to the common roughness values in Rosario-Lobo watershed's subbasins. (Brunner, 2010).

Table 27. Summary of the Efficiency Test of Rosario-Lobo HMS Model

Accuracy measure	Value
RMSE	4.713
r ²	0.7793
NSE	0.907
PBIAS	0.867
RSR	0.306

The Root Mean Square Error (RMSE) method aggregates the individual differences of these two measurements. It was identified at 4.713.

The Pearson correlation coefficient (r²) assesses the strength of the linear relationship between the observations and the model. This value being close to 1 corresponds to an almost perfect match of the observed discharge and the resulting discharge from the HEC HMS model. Here, it measured 0.7793.

The Nash-Sutcliffe (E) method was also used to assess the predictive power of the model. Here the optimal value is 1. The model attained an efficiency coefficient of 0.907.

A positive Percent Bias (PBIAS) indicates a model's propensity towards under-prediction. Negative values indicate bias towards over-prediction. Again, the optimal value is 0. In the model, the PBIAS is 0.867.

The Observation Standard Deviation Ratio, RSR, is an error index. A perfect model attains a value of 0 when the error in the units of the valuable a quantified. The model has an RSR value of 0.306.

5.7 Calculated outflow hydrographs and discharge values for different rainfall return periods

5.7.1 Hydrograph using the Rainfall Runoff Model

The summary graph (Figure 60) shows the Rosario-Lobo outflow using the Ambulong Rainfall Intensity-Duration-Frequency curves (RIDF) in 5 different return periods (5-year, 10-year, 25-year, 50-year, and 100-year rainfall time series) based on the Philippine Atmospheric Geophysical and Astronomical Services Administration (PAG-ASA) data. The simulation results reveal significant increase in outflow magnitude as the rainfall intensity increases for a range of durations and return periods.

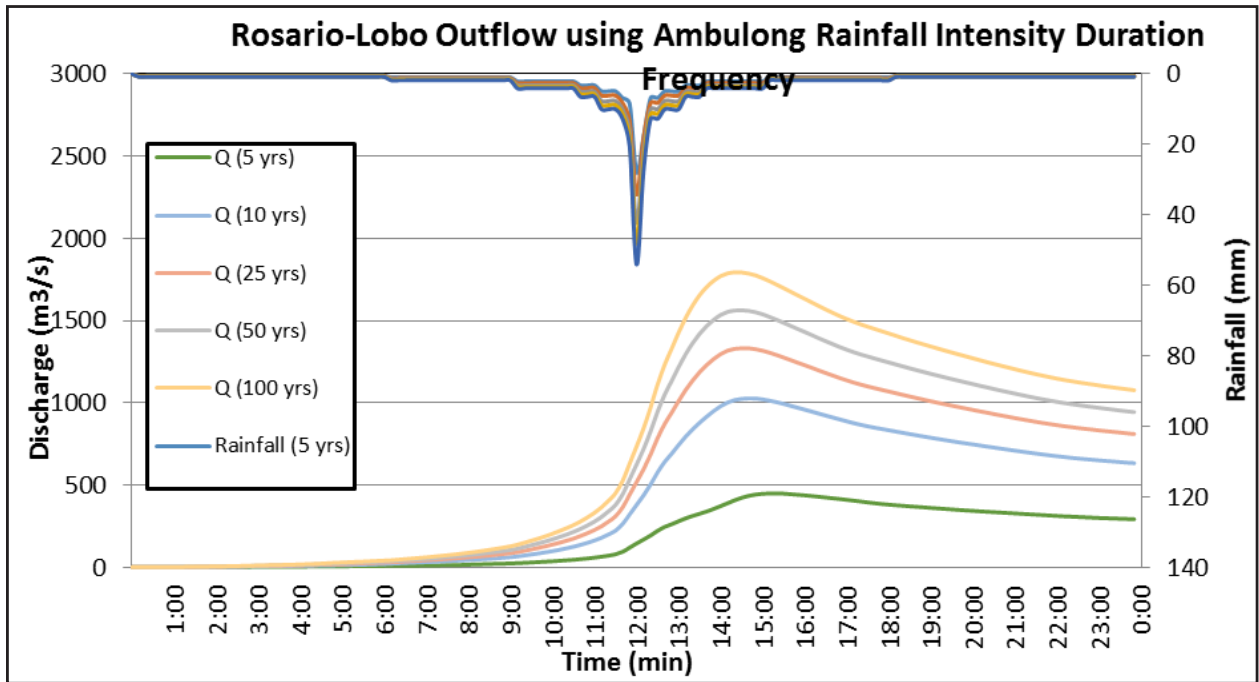


Figure 60. Outflow hydrograph at Rosario-Lobo Station generated using Ambulong RIDF simulated in HEC-HMS

A summary of the total precipitation, peak rainfall, peak outflow and time to peak of the Rosario-Lobo River discharge using the Ambulong Rainfall Intensity-Duration-Frequency curves (RIDF) in five different return periods is shown in Table 28.

Table 28. Peak values of the Rosario-Lobo HEC-HMS Model outflow using the Ambulong RIDF

RIDF Period	Total Precipitation (mm)	Peak rainfall (mm)	Peak outflow (m ³ /s)	Time to Peak
5-Year	209.4	28.3	451	15 hours, 20 minutes
10-Year	276.9	34.2	1029.1	14 hours, 40 minutes
25-Year	340.4	42.2	1333.9	14 hours, 30 minutes
50-Year	387.5	48.1	1564.4	14 hours, 30 minutes
100-Year	434.3	54	1795	14 hours, 20 minutes

5.8 River Analysis (RAS) Model Simulation

The HEC-RAS Flood Model produced a simulated water level at every cross-section for every time step for every flood simulation created. The resulting model will be used in determining the flooded areas within the model. The simulated model will be an integral part in determining real-time flood inundation extent of the river after it has been automated and uploaded on the DREAM website. For this publication, only a sample output map river was to be shown, since only the Flood Acquisition and Validation Component (MIT-FAVC) base flow was calibrated. The sample generated map of Rosario-Lobo River using the calibrated HMS base flow is shown in Figure 61.



Figure 61. Sample output of Rosario-Lobo RAS Model

5.9 Flow Depth and Flood Hazard

The resulting hazard and flow depth maps have a 10m resolution. Figure 60 to Figure 65 shows the 5-, 25-, and 100-year rain return scenarios of the Rosario-Lobo floodplain.

Table 29. Municipalities affected in Rosario-Lobo Floodplain

Municipality	Total Area	Area Flooded	% Flooded
Lobo	199.87	42.32	21.18%

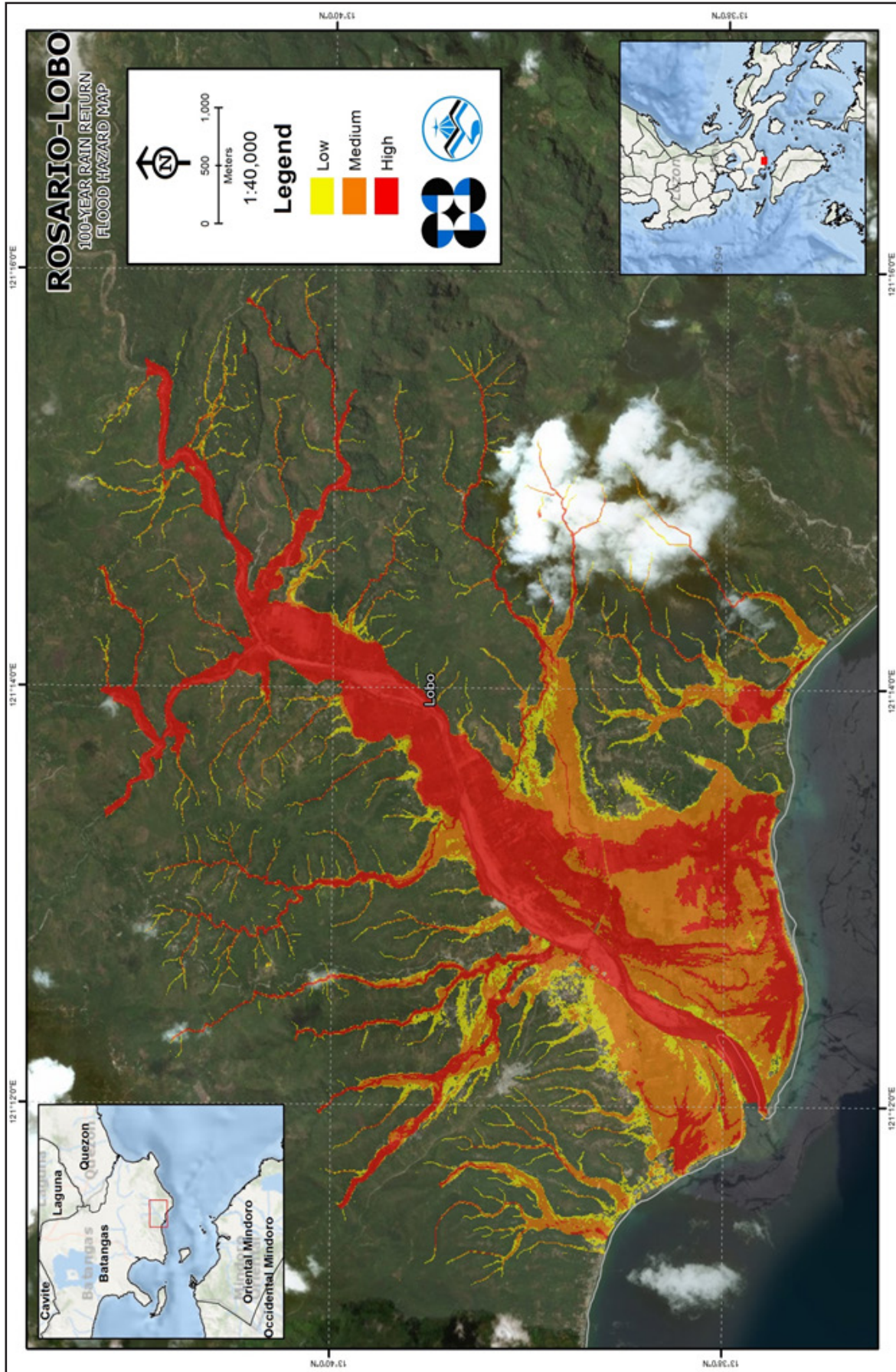


Figure 62. 100-year Flood Hazard Map for Rosario-Lobo Floodplain overlaid on Google Earth imagery

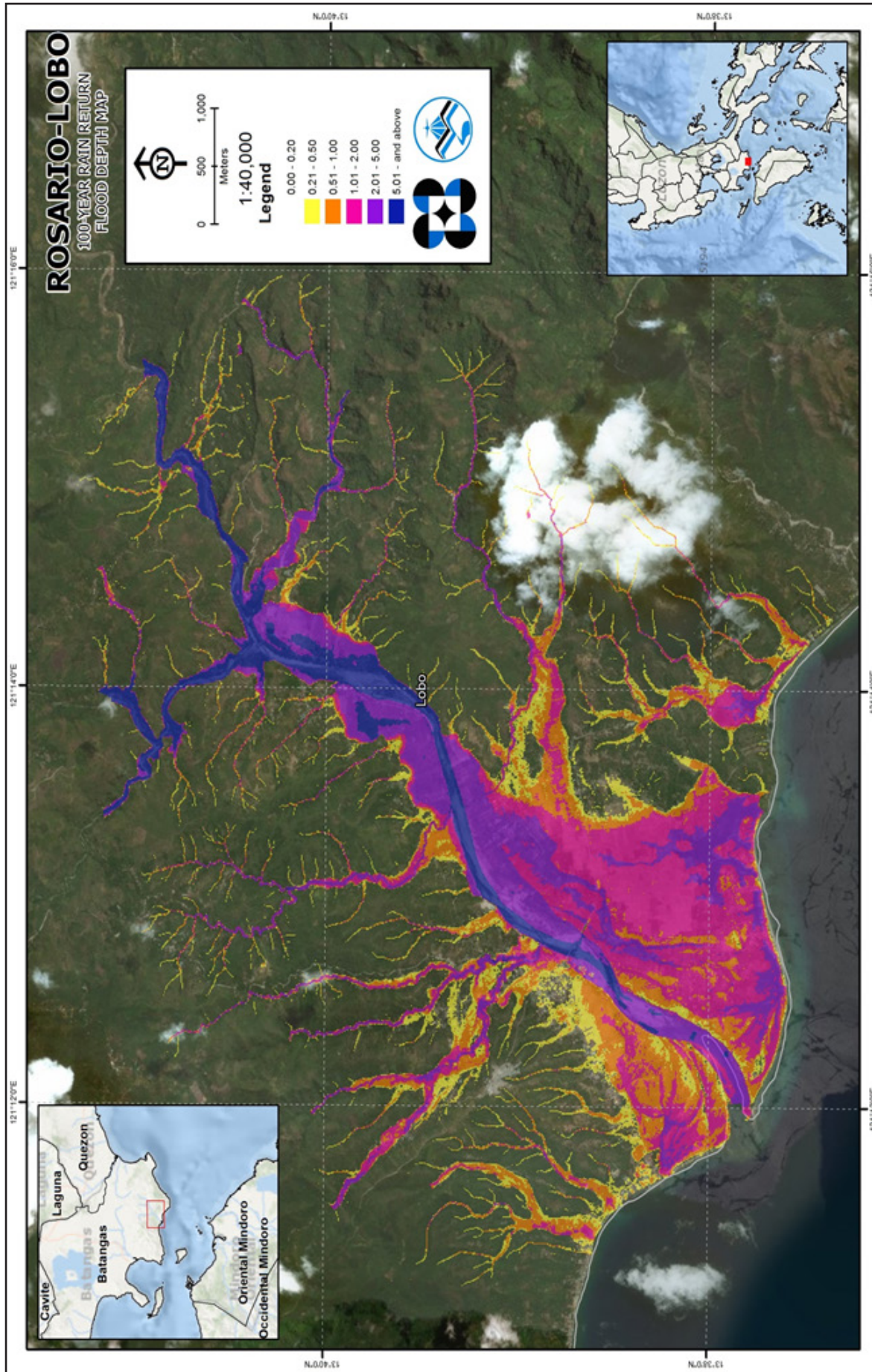


Figure 63. 100-year Flow Depth Map for Rosario-Lobo Floodplain overlaid on Google Earth imagery

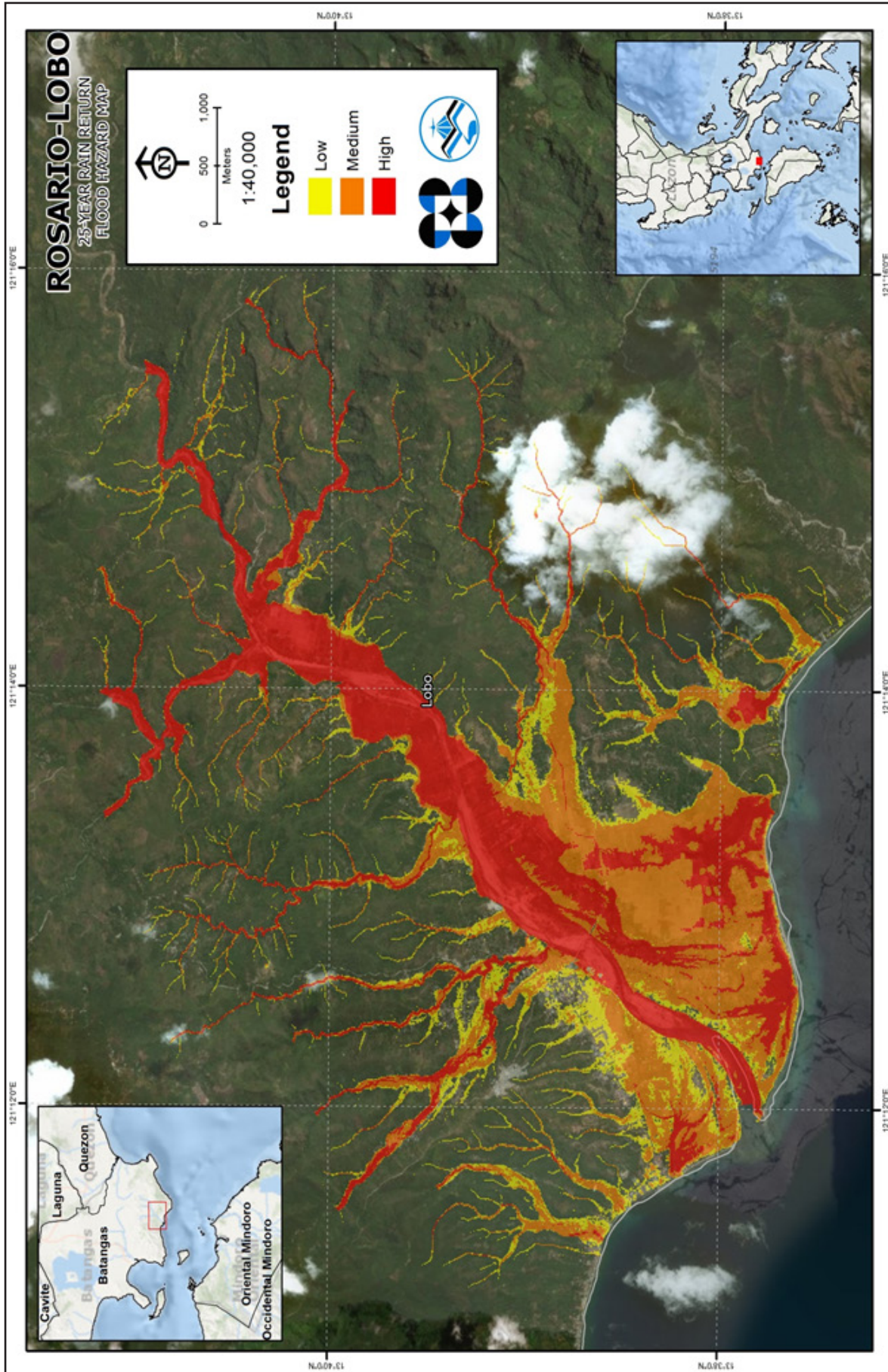


Figure 64. 25-year Flood Hazard Map for Rosario-Lobo Floodplain overlaid on Google Earth imagery

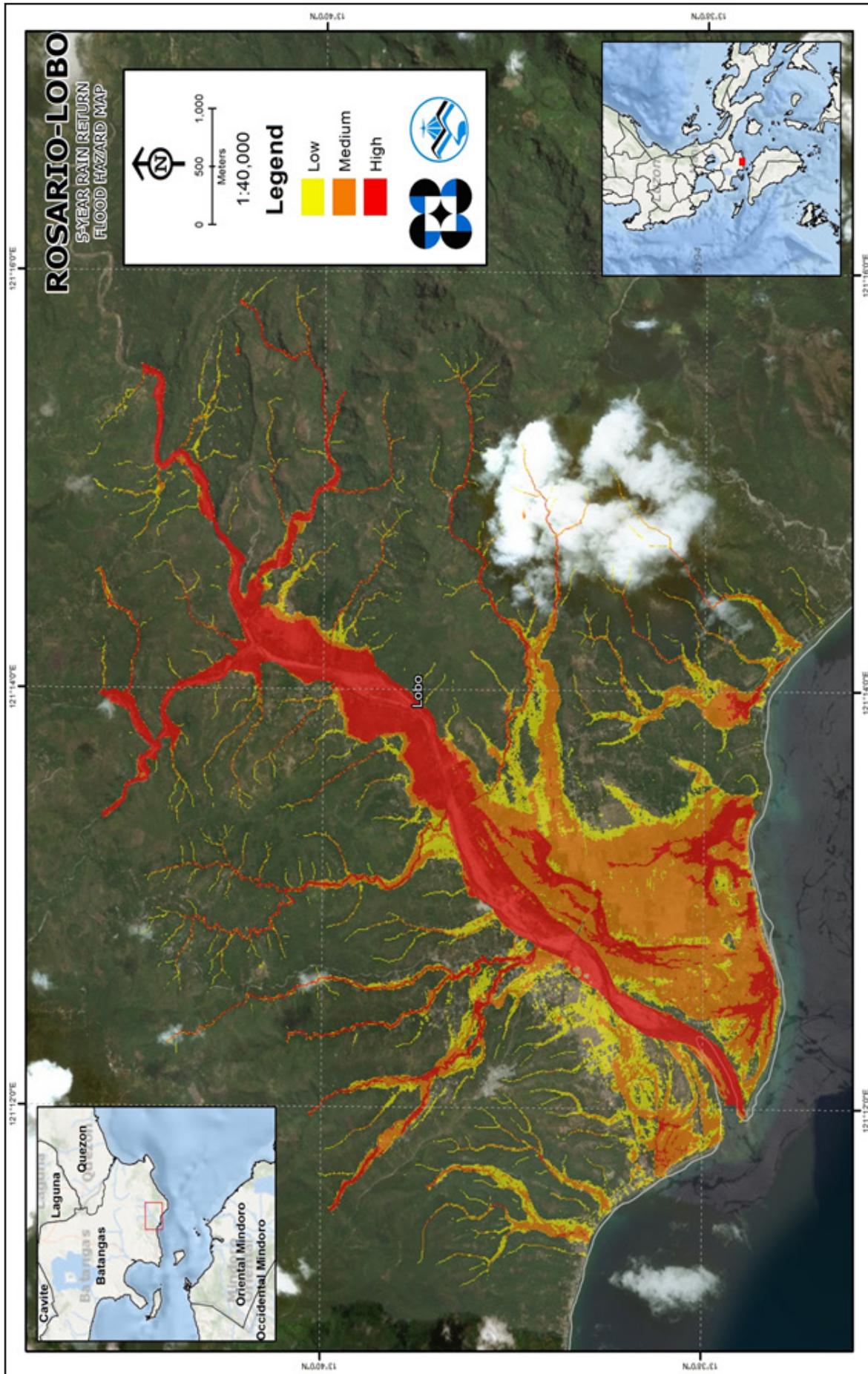


Figure 66. 5-year Flood Hazard Map for Rosario-Lobo Floodplain overlaid on Google Earth imagery

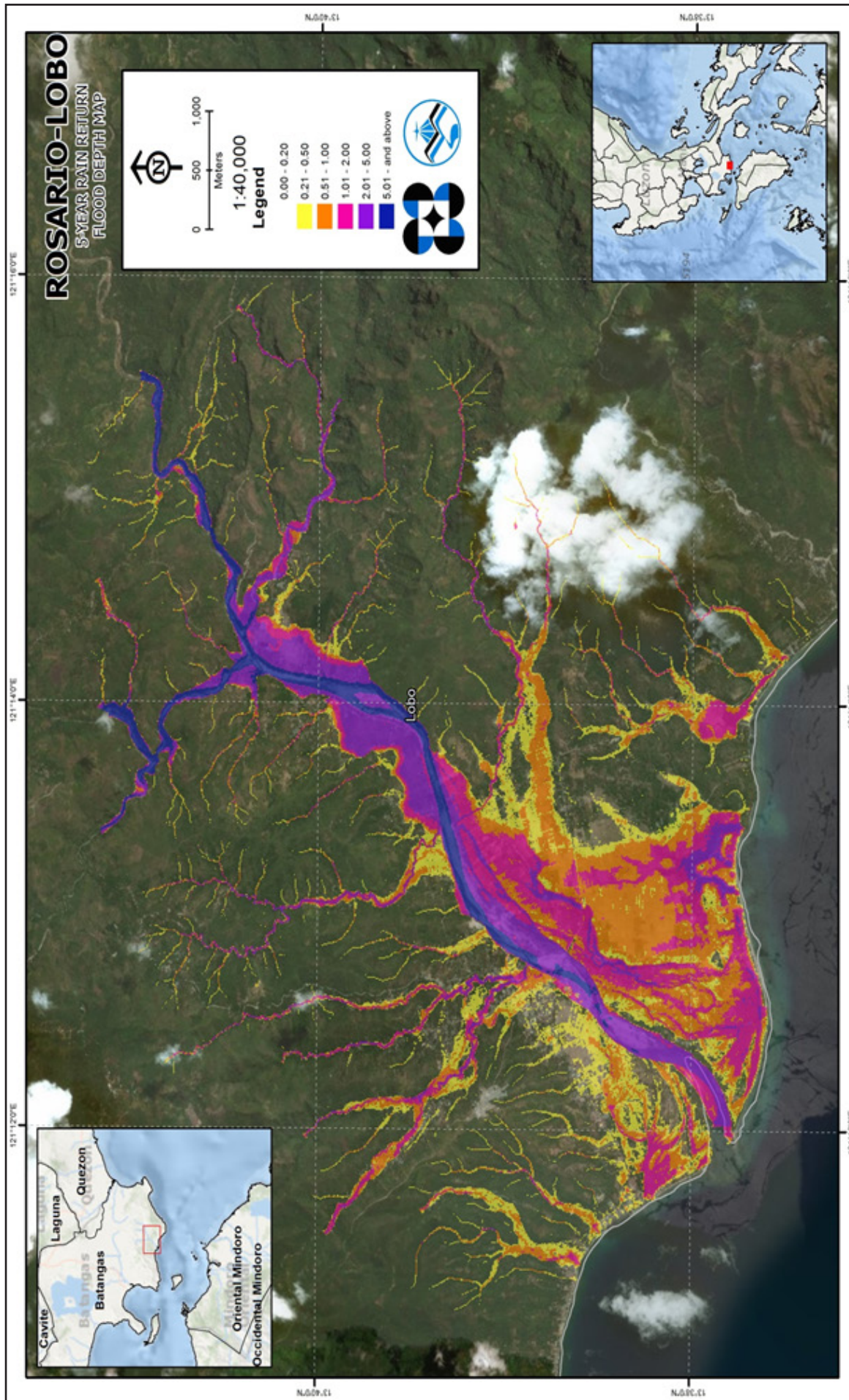


Figure 67. 5-year Flood Depth Map for Rosario-Lobo Floodplain overlaid on Google Earth imagery

5.10 Inventory of Areas Exposed to Flooding

Listed below are the barangays affected by the Rosario-Lobo River Basin, grouped accordingly by municipality. For the said basin, one (1) municipality consisting of 34 barangays are expected to experience flooding when subjected to a 5-year rainfall return period.

For the 5-year return period, 15.37% of the municipality of Lobo with an area of 199.87 sq. km. will experience flood levels of less than 0.20 meters. 1.43% of the area will experience flood levels of 0.21 to 0.50 meters while 1.61%, 1.34%, 1.00%, and 0.42% of the area will experience flood depths of 0.51 to 1 meter, 1.01 to 2 meters, 2.01 to 5 meters, and more than 5 meters, respectively. Listed in Table 30 and Table 31 are the affected areas in square kilometers by flood depth per barangay.

Table 30. Affected areas in Lobo, Batangas during a 5-Year Rainfall Return Period

Affected area (sq. km.) by flood depth (in m.)	Area of affected barangays in Lobo (in sq. km)								
	Balatbat	Banalo	Bignay	Calo	Fabrica	Lagadlarin	Mabilog Na Bundok	Malapad Na Parang	Masaguitsit
0.03-0.20	3.25	0.8	3.2	0.05	0.96	0.18	1.64	0.5	0.7
0.21-0.50	0.23	0.055	0.084	0.00036	0.4	0.24	0.25	0.0062	0.15
0.51-1.00	0.19	0.043	0.046	0	0.25	0.9	0.19	0.0064	0.084
1.01-2.00	0.16	0.003	0.06	0	0.14	0.89	0.19	0.0085	0.022
2.01-5.00	0.043	0.0006	0.22	0	0.028	0.36	0.083	0.023	0.0014
> 5.00	0	0	0.33	0	0.0014	0.028	0.075	0.049	0

Table 31. Affected areas in Lobo, Batangas during a 5-Year Rainfall Return Period

Affected area (sq. km.) by flood depth (in m.)	Area of affected barangays in Lobo (in sq. km)							
	Nagtalongtong	Nagtoctoc	Olo-Olo	Poblacion	San Miguel	Sawang	Soloc	Tayuman
0.03-0.20	2.43	4.37	1.06	0.41	2.55	6.24	0.78	1.6
0.21-0.50	0.1	0.16	0.38	0.19	0.068	0.3	0.033	0.21
0.51-1.00	0.078	0.099	0.84	0.033	0.039	0.22	0.031	0.16
1.01-2.00	0.14	0.15	0.46	0.0078	0.045	0.18	0.0078	0.21
2.01-5.00	0.43	0.27	0.13	0.038	0.035	0.016	0.0001	0.33
> 5.00	0.13	0.08	0	0.0023	0.0001	0	0	0.15

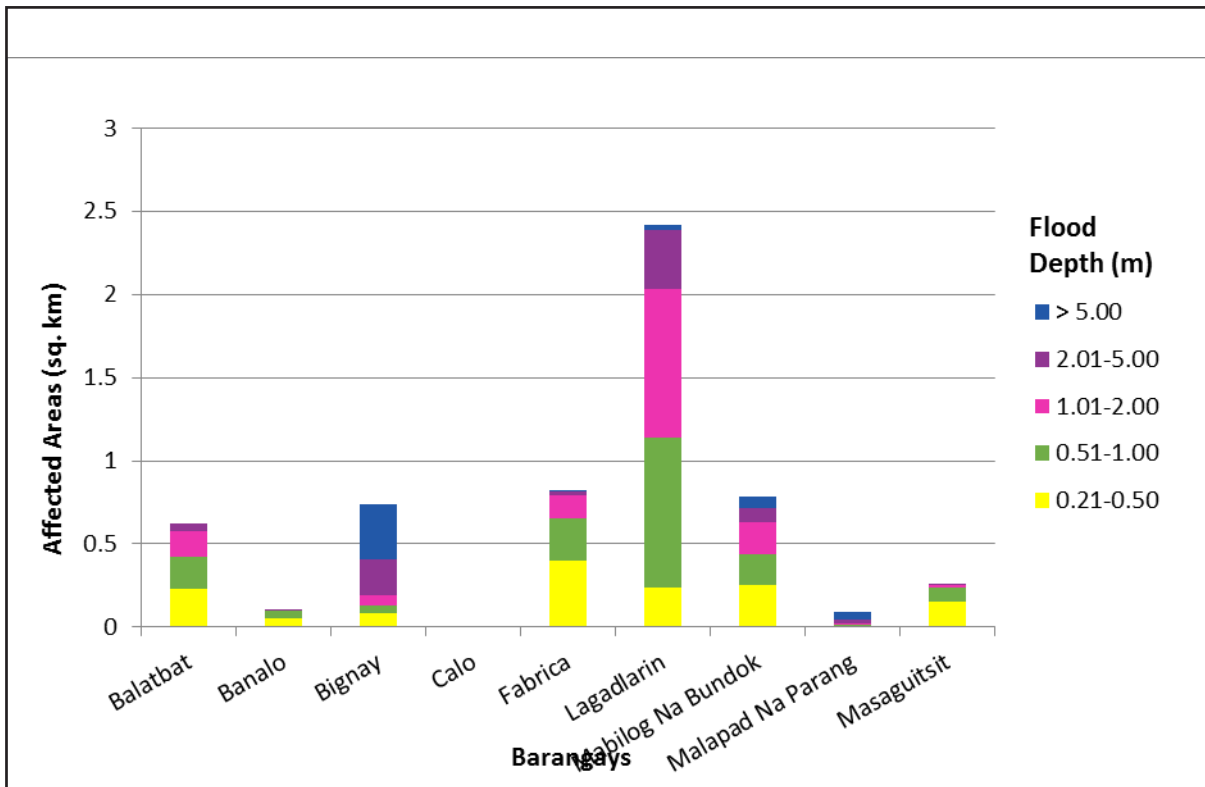


Figure 68. Affected areas in General Trias, Cavite during a 5-year rainfall return period

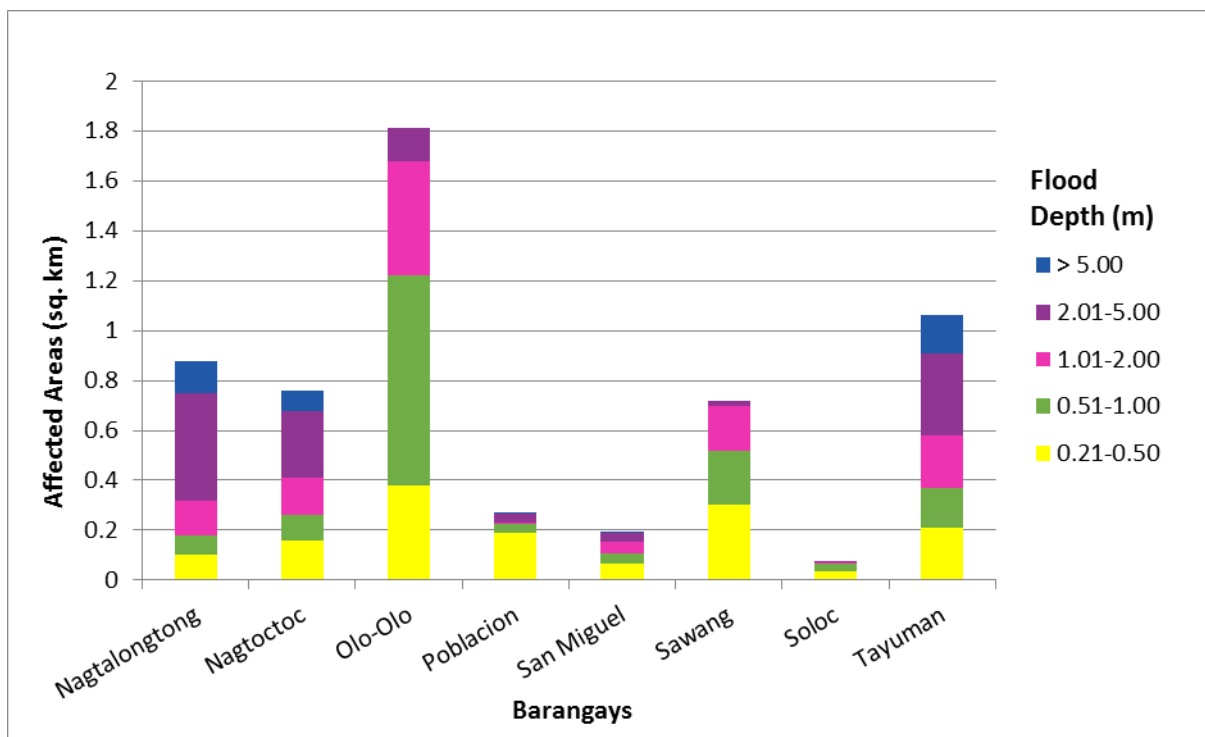


Figure 69. Affected areas in Lobo, Batangas during a 5-Year Rainfall Return Period.

For the 25-year return period, 14.67% of the municipality of Lobo with an area of 199.87 sq. km. will experience flood levels of less than 0.20 meters. 1.24% of the area will experience flood levels of 0.21 to 0.50 meters while 1.46%, 1.84%, 1.41%, and 0.56% of the area will experience flood depths of 0.51 to 1 meter, 1.01 to 2 meters, 2.01 to 5 meters, and more than 5 meters, respectively. Listed in Table 32 and Table 33 are the affected areas in square kilometers by flood depth per barangay.

Table 32. Affected Areas in Lobo, Batangas during 25-Year Rainfall Return Period

Affected area (sq. km.) by flood depth (in m.)	Area of affected barangays in Lobo (in sq. km)								
	Balatbat	Banalo	Bignay	Calo	Fabrica	Lagadlarin	Mabilog Na Bundok	Malapad Na Parang	Masaguitsit
0.03-0.20	3.11	0.78	3.12	0.05	0.71	0.068	1.56	0.49	0.66
0.21-0.50	0.26	0.053	0.093	0.00056	0.34	0.14	0.23	0.0078	0.14
0.51-1.00	0.22	0.055	0.045	0	0.45	0.52	0.18	0.0035	0.13
1.01-2.00	0.2	0.007	0.05	0	0.25	1.29	0.19	0.008	0.03
2.01-5.00	0.088	0.0013	0.19	0	0.03	0.53	0.17	0.022	0.0024
> 5.00	0	0	0.44	0	0.0045	0.049	0.11	0.062	0

Table 33. Affected Areas in Lobo, Batangas during 25-Year Rainfall Return Period

Affected area (sq. km.) by flood depth (in m.)	Area of affected barangays in Lobo (in sq. km)							
	Nagtalongtong	Nagtoctoc	Olo-Olo	Poblacion	San Miguel	Sawang	Soloc	Tayuman
0.03-0.20	2.35	4.25	0.92	0.33	2.52	6.11	0.77	1.52
0.21-0.50	0.11	0.17	0.17	0.2	0.074	0.31	0.03	0.16
0.51-1.00	0.065	0.099	0.51	0.1	0.042	0.25	0.04	0.2
1.01-2.00	0.096	0.12	0.98	0.0077	0.048	0.23	0.011	0.16
2.01-5.00	0.54	0.38	0.3	0.041	0.052	0.034	0.0005	0.43
> 5.00	0.15	0.12	0	0.0037	0.0008	0	0	0.17

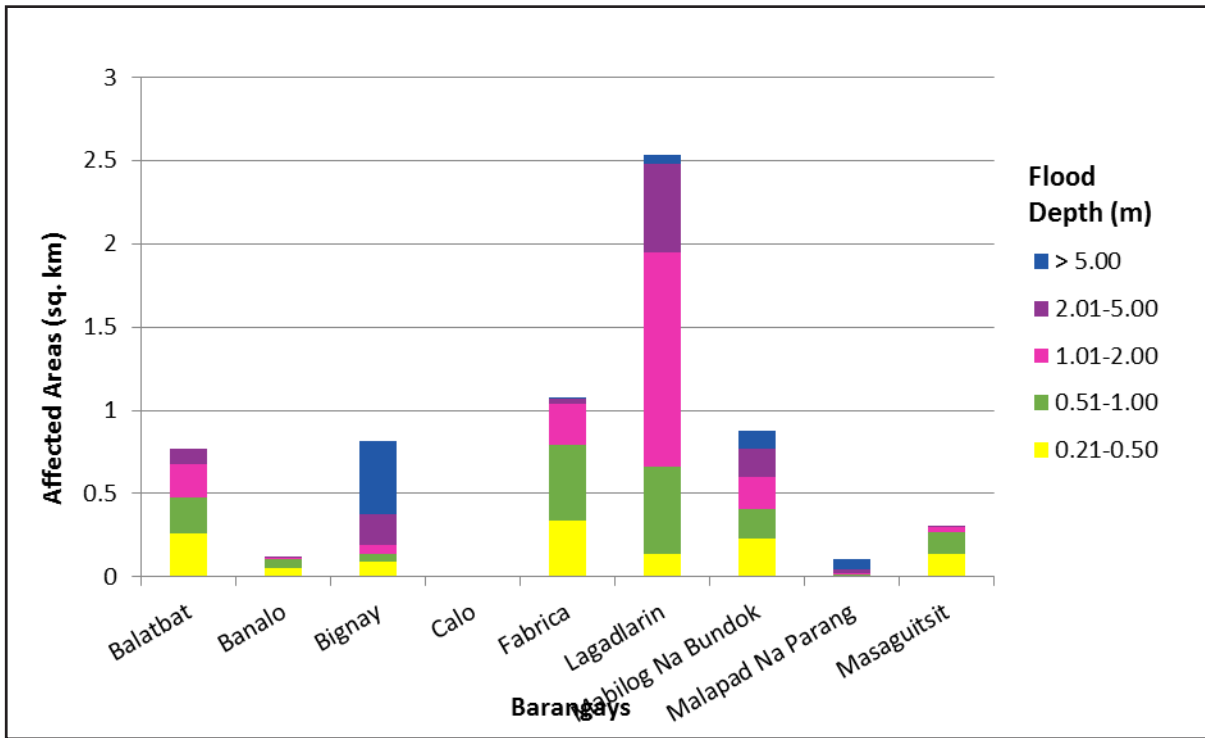


Figure 70. Affected Areas in Lobo, Batangas during 25-Year Rainfall Return Period

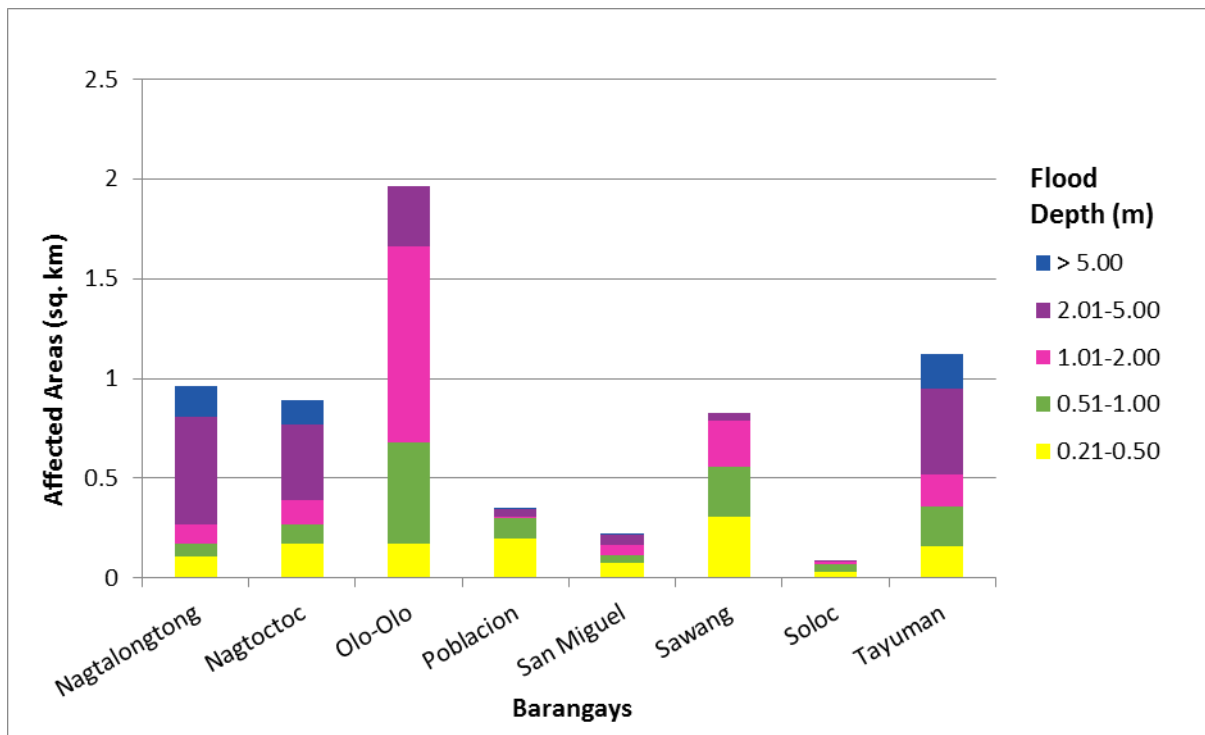


Figure 71. Affected Areas in Lobo, Batangas during 25-Year Rainfall Return Period

For the 100-year return period, 14.30% of the municipality of Lobo with an area of 199.87 sq. km. will experience flood levels of less than 0.20 meters. 1.15% of the area will experience flood levels of 0.21 to 0.50 meters while 1.38%, 2.04%, 1.59%, and 0.71% of the area will experience flood depths of 0.51 to 1 meter, 1.01 to 2 meters, 2.01 to 5 meters, and more than 5 meters, respectively. Listed in Table 34 and Table 35 are the affected areas in square kilometers by flood depth per barangay.

Table 34. Affected Areas in Lobo, Batangas during 100-Year Rainfall Return Period

Affected area (sq. km.) by flood depth (in m.)	Area of affected barangays in Lobo (in sq. km)								
	Balatbat	Banalo	Bignay	Calo	Fabrica	Lagadlarin	Mabilog Na Bundok	Malapad Na Parang	Masaguitsit
0.03-0.20	3.01	0.77	3.07	0.049	0.63	0.032	1.53	0.48	0.63
0.21-0.50	0.28	0.054	0.1	0.00096	0.21	0.086	0.2	0.0078	0.14
0.51-1.00	0.24	0.06	0.049	0	0.5	0.37	0.18	0.0045	0.15
1.01-2.00	0.22	0.012	0.047	0	0.37	1.39	0.19	0.007	0.042
2.01-5.00	0.13	0.0015	0.15	0	0.075	0.65	0.21	0.019	0.0038
> 5.00	0.0001	0	0.53	0	0.007	0.065	0.13	0.073	0

Table 35. Affected Areas in Lobo, Batangas during 100-Year Rainfall Return Period

Affected area (sq. km.) by flood depth (in m.)	Area of affected barangays in Lobo (in sq. km)							
	Nagtalongtong	Nagtoctoc	Olo-Olo	Poblacion	San Miguel	Sawang	Soloc	Tayuman
0.03-0.20	2.3	4.18	0.86	0.28	2.5	6.03	0.76	1.48
0.21-0.50	0.12	0.18	0.16	0.18	0.079	0.33	0.032	0.14
0.51-1.00	0.067	0.1	0.32	0.15	0.046	0.27	0.04	0.21
1.01-2.00	0.088	0.11	1.1	0.021	0.049	0.23	0.016	0.19
2.01-5.00	0.5	0.37	0.42	0.041	0.066	0.085	0.001	0.45
> 5.00	0.23	0.2	0	0.0049	0.0012	0.0001	0	0.18

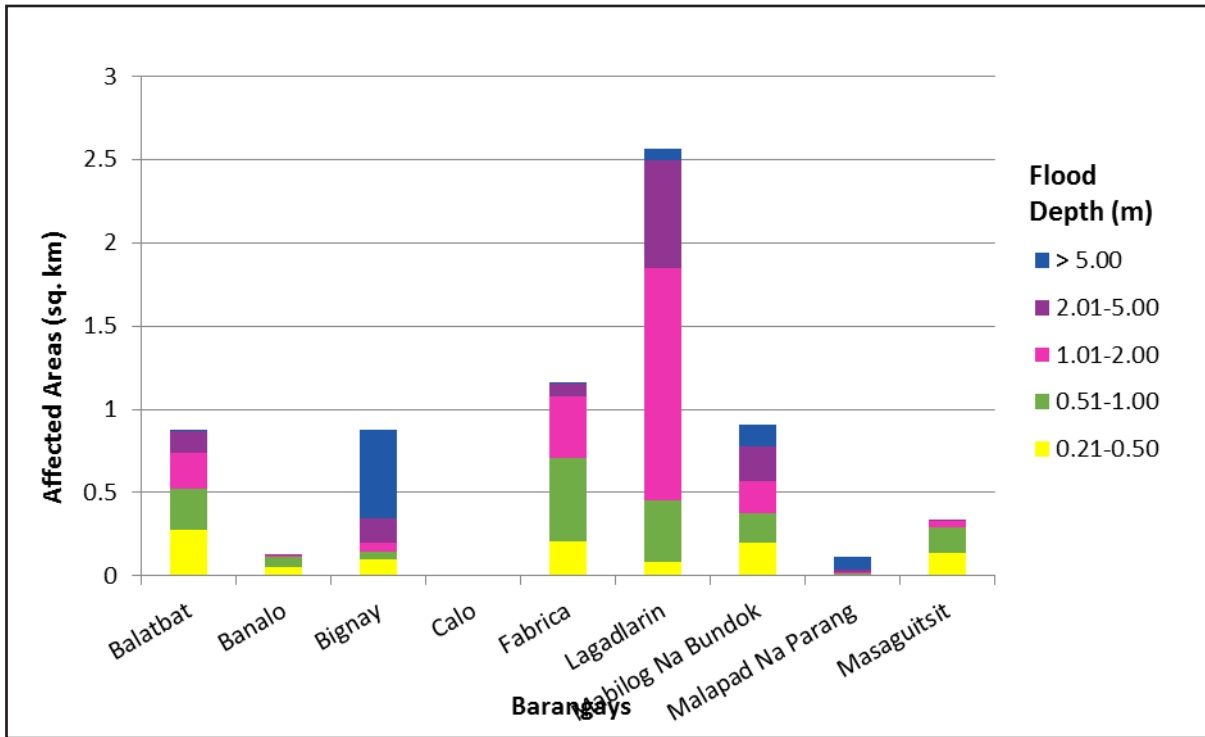


Figure 72. Affected Areas in Lobo, Batangas during 100-Year Rainfall Return Period

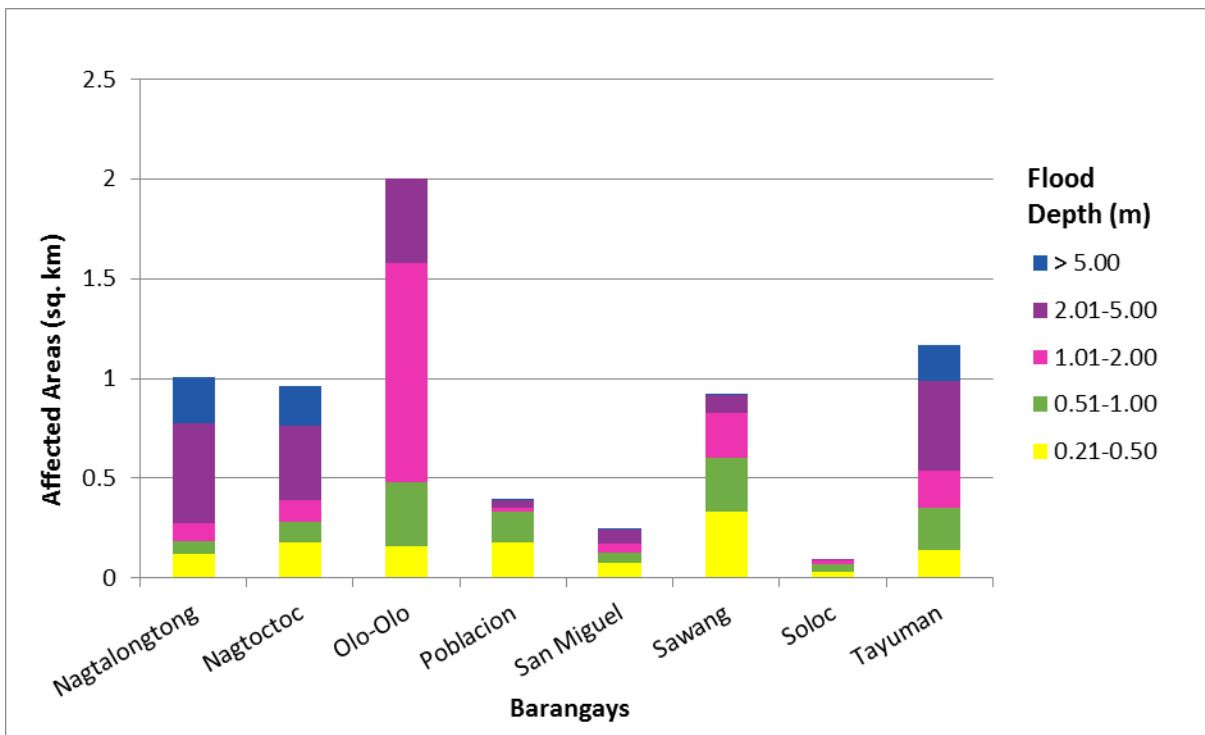


Figure 73. Affected Areas in Lobo, Batangas during 100-Year Rainfall Return Period

Moreover, the generated flood hazard maps for the Rosario-Lobo Floodplain were used to assess the vulnerability of the educational and medical institutions in the floodplain. Using the flood depth units of PAG-ASA for hazard maps (“Low”, “Medium”, and “High”), the affected institutions were given their individual assessment for each Flood Hazard Scenario (5-year, 25-year, and 10-year).

Table 36. Areas covered by each warning level with respect to the rainfall scenarios

Warning Level	Area Covered in sq. km.		
	5 year	25 year	100 year
Low	2.83	2.44	2.2
Medium	4.8	5.06	5.05
High	4.15	5.68	6.65
TOTAL	11.78	13.18	13.9

Of the 20 identified educational institutions in Rosario-Lobo Floodplain, seven (7) schools were discovered to be exposed to Low-level flooding during a 5-year scenario, while one (1) school each was found exposed to Medium- and High-level flooding in the same scenario.

In the 25-year scenario, three (3) schools were found exposed to Low-level flooding, while six (6) schools were discovered exposed to Medium-level flooding. Two (2) schools were found exposed to High-level flooding in the same scenario.

For the 100-year scenario, five (5) school was discovered exposed to Low-level flooding , while the same number of schools were exposed to Medium-level flooding. In the same scenario, three (3) schools were found exposed to High-level flooding. The educational institutions Rosario-Lobo River Basin exposed to flooding are found in Annex 12.

Apart from this, six (6) Medical Institutions were identified in the Rosario-Lobo Floodplain, of which only one (1) was found exposed to low-level flooding for the 5-year scenario.

One (1) school each was found exposed to low- and medium-level flooding for the 25-year scenario.

For the 100-year scenario, two (2) schools were found exposed to low-level flooding while one (1) was found exposed to medium-level flooding. The medical institutions in Rosario-Lobo River Basin exposed to flooding are found in Annex 13.

5.11 Flood Validation

In order to check and validate the extent of flooding in different river systems, there is a need to perform validation survey work. Field personnel gathered secondary data regarding flood occurrence in the area within the major river system in the Philippines.

From the Flood Depth Maps produced by Phil-LiDAR 1 Program, multiple points representing the different flood depths for different scenarios were identified for validation.

The validation personnel went to the specified points identified in a river basin and gathered data regarding the actual flood level in each location. Data gathering was done through a local DRRM office, obtaining maps or situation reports about the past flooding events and through interview with some residents who have knowledge of or have had experienced flooding in a particular area.

After which, the actual data from the field was compared to the simulated data to assess the accuracy of the Flood Depth Maps produced and to improve on what is needed. The points in the flood map versus its corresponding validation depths are shown in Figure 75.

The flood validation consists of 148 points randomly selected all over the Rosario-Lobo floodplain (Figure 74). Comparing it with the flood depth map of the nearest storm event, the map has an RMSE value of 2.29m. Table 37 shows a contingency matrix of the comparison.

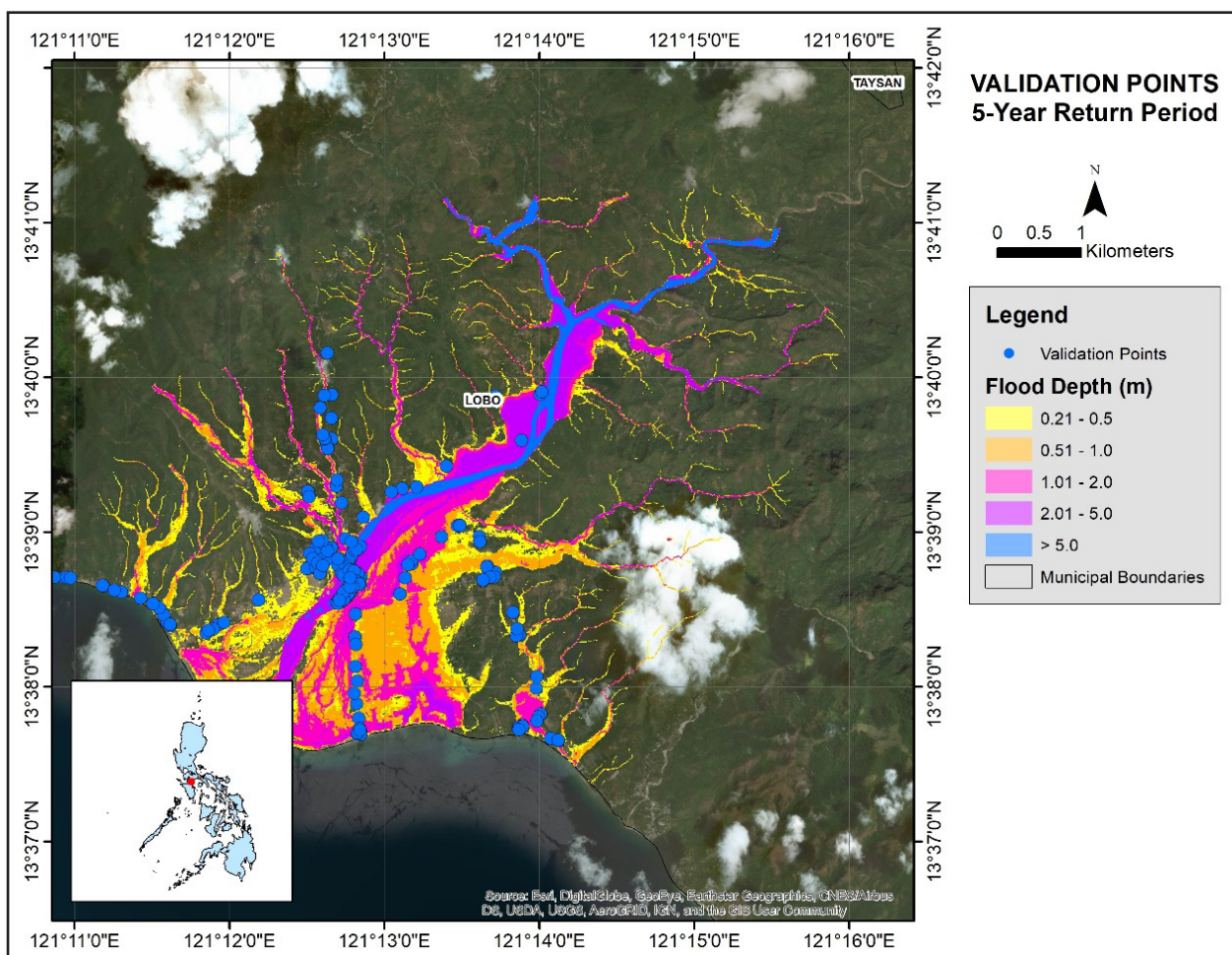


Figure 74. Rosario-Lobo Flood Validation Points

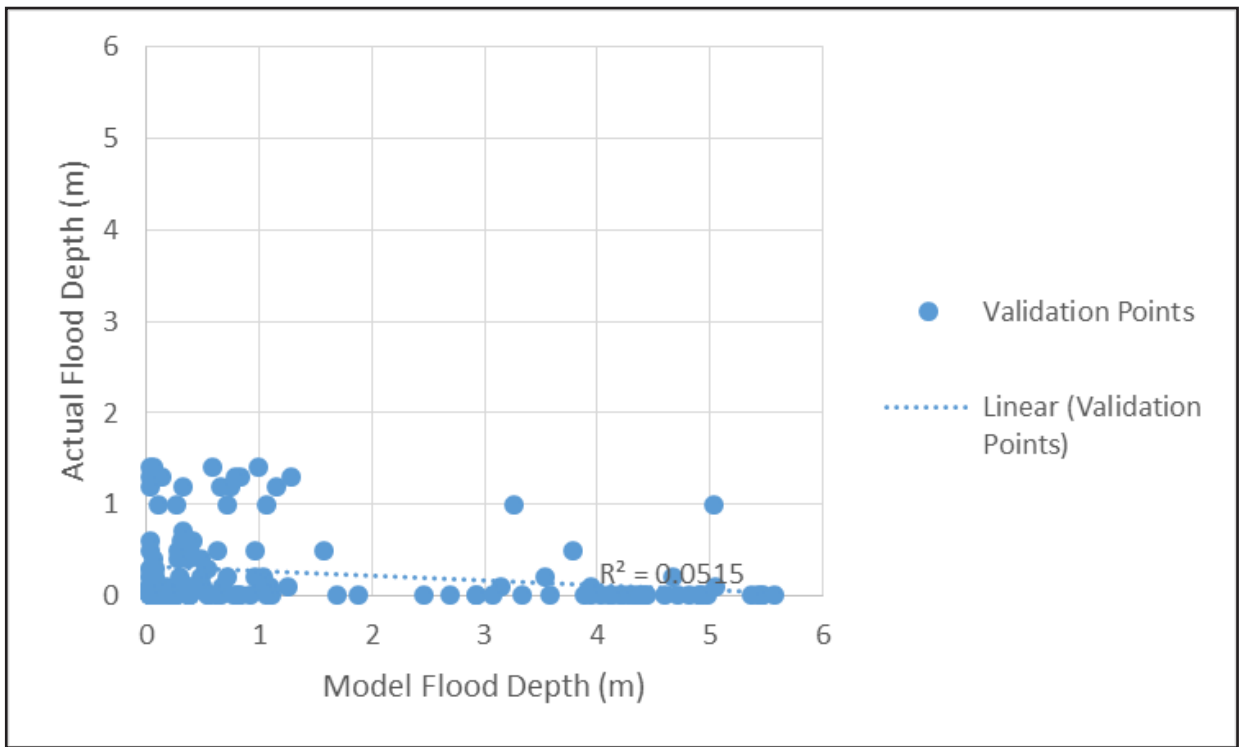


Figure 75. Flood map depth vs. actual flood depth

Table 37. Actual flood vs simulated flood depth at different levels in the Rosario-Lobo River Basin.

Actual Flood Depth (m)	Modeled Flood Depth (m)						Total
	0-0.20	0.21-0.50	0.51-1.00	1.01-2.00	2.01-5.00	> 5.00	
0-0.20	34	16	12	9	31	6	108
0.21-0.50	5	5	3	1	1	0	15
0.51-1.00	2	5	1	1	1	1	11
1.01-2.00	5	1	6	2	0	0	14
2.01-5.00	0	0	0	0	0	0	0
> 5.00	0	0	0	0	0	0	0
Total	46	27	22	13	33	7	148

The overall accuracy generated by the flood model is estimated at 28.38% with 42 points correctly matching the actual flood depths. In addition, there were 31 points estimated one level above and below the correct flood depths while there were 17 points and 53 points estimated two levels above and below, and three or more levels above and below the correct flood. A total of 4 points were overestimated while a total of 24 points were underestimated in the modelled flood depths of Rosario Lobo. Table 38 depicts the summary of the Accuracy Assessment in the Rosario-Lobo River Basin Survey.

Table 38. Summary of the Accuracy Assessment in the Rosario-Lobo River Basin Survey

	No. of Points	%
Correct	57	42
Overestimated	15	82
Underestimated	112	24
Total	184	148

REFERENCES

- Ang M.C., Paringit E.C., et al. 2014. DREAM Data Processing Component Manual. Quezon City, Philippines: UP Training Center for Applied Geodesy and Photogrammetry
- Balicanta L.P, Paringit E.C., et al. 2014. DREAM Data Validation Component Manual. Quezon City, Philippines: UP Training Center for Applied Geodesy and Photogrammetry
- Brunner, G. H. 2010a. HEC-RAS River Analysis System Hydraulic Reference Manual. Davis, CA: U.S. Army Corps of Engineers, Institute for Water Resources, Hydrologic Engineering Center.
- Lagmay A.F., Paringit E.C., et al. 2014. DREAM Flood Modeling Component Manual. Quezon City, Philippines: UP Training Center for Applied Geodesy and Photogrammetry
- Paringit, E.C., Balicanta, L.P., Ang, M.C., Lagmay, A.F., Sarmiento, C. 2017, Flood Mapping of Rivers in the Philippines Using Airborne LiDAR: Methods. Quezon City, Philippines: UP Training Center for Applied Geodesy and Photogrammetry
- Sarmiento C.J.S., Paringit E.C., et al. 2014. DREAM Data Aquisition Component Manual. Quezon City, Philippines: UP Training Center for Applied Geodesy and Photogrammetry
- UP TCAGP 2016. Acceptance and Evaluation of Synthetic Aperture Radar Digital Surface Model (SAR DSM) and Ground Control Points (GCP). Quezon City, Philippines: UP Training Center for Applied Geodesy and Photogrammetry

ANNEXES

Annex 1. Optech Technical Specification of the Pegasus Sensor

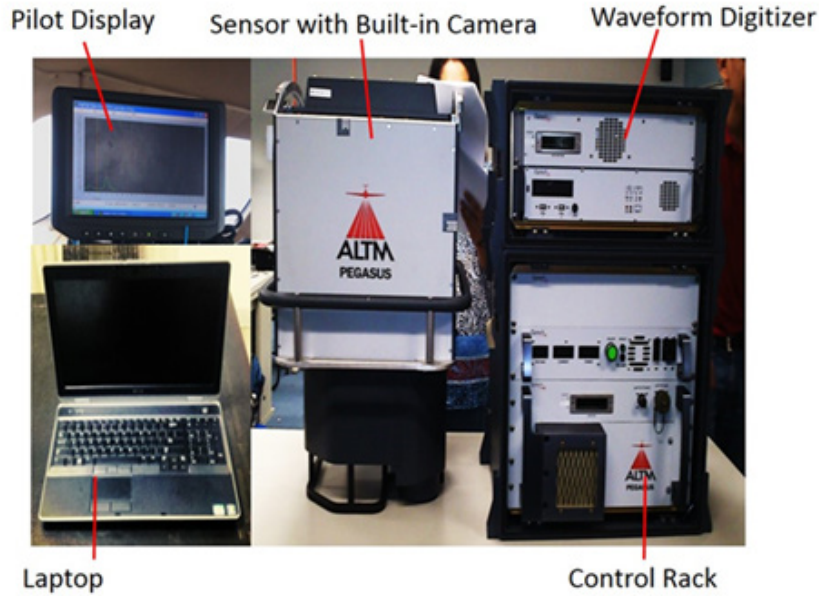


Figure A-1.1 Pegasus Sensor

Table A-1.1 Pegasus Sensor Parameters and Specification

Parameter	Specification
Operational envelope (1,2,3,4)	150-5000 m AGL, nominal
Laser wavelength	1064 nm
Horizontal accuracy (2)	1/5,500 x altitude, 1 σ
Elevation accuracy (2)	< 5-20 cm, 1 σ
Effective laser repetition rate	Programmable, 100-500 kHz
Position and orientation system	POS AV TM AP50 (OEM)
Scan width (FOV)	Programmable, 0-75 °
Scan frequency (5)	Programmable, 0-140 Hz (effective)
Sensor scan product	800 maximum
Beam divergence	0.25 mrad (1/e)
Roll compensation	Programmable, $\pm 37^\circ$ (FOV dependent)
Vertical target separation distance	<0.7 m
Range capture	Up to 4 range measurements, including 1st, 2nd, 3rd, and last returns
Intensity capture	Up to 4 intensity returns for each pulse, including last (12 bit)
Image capture	5 MP interline camera (standard); 60 MP full frame (optional)
Full waveform capture	12-bit Optech IWD-2 Intelligent Waveform Digitizer
Data storage	Removable solid state disk SSD (SATA II)
Power requirements	28 V, 800 W, 30 A
Dimensions and weight	Sensor: 630 x 540 x 450 mm; 65 kg;
	Control rack: 650 x 590 x 490 mm; 46 kg
Operating Temperature	-10°C to +35°C
Relative humidity	0-95% non-condensing

Annex 2. NAMRIA Certification of Reference Points Used in the LIDAR Survey

1. BTG-30



Republic of the Philippines
 Department of Environment and Natural Resources
NATIONAL MAPPING AND RESOURCE INFORMATION AUTHORITY

February 19, 2014

CERTIFICATION

To whom it may concern:

This is to certify that according to the records on file in this office, the requested survey information is as follows -

Province: BATANGAS	Station Name: BTG-30	Barangay: PALLOCAN
Island: LUZON	Order: 2nd	
Municipality: BATANGAS CITY (CAPITAL)	PRS92 Coordinates	
Latitude: 13° 45' 23.09641"	Longitude: 121° 3' 43.87174"	Ellipsoidal Hgt: 7.82000 m.
	WGS84 Coordinates	
Latitude: 13° 45' 17.88182"	Longitude: 121° 3' 48.83762"	Ellipsoidal Hgt: 53.87200 m.
	PTM Coordinates	
Northing: 1521226.725 m.	Easting: 506725.034 m.	Zone: 3
	UTM Coordinates	
Northing: 1,521,536.18	Easting: 290,477.09	Zone: 51

Location Description

BTG-30

Is in the vicinity of Brgy. Pallocan, Batangas City along the E side dike of Calumpang River, on the N side of Calumpang Bridge. It is about 0.67 m. WNW of the E edge of the dike, 1.3 m. ENE of the center of the concrete balluster and 50 m. NNE of the N side of the said bridge. Mark is the head of a 4" copper nail centered and embedded on top of a 30 cm. x 30 cm. cement putty set flushed to the pavement with inscriptions, "BTG-30 2004 NAMRIA".

Requesting Party: **UP DREAM**
 Purpose: **Reference**
 OR Number: **8795394 A**
 T.N.: **2014-354**

RUEL M. BELEN, MNSA
 Director, Mapping And Geodesy Branch



NAMRIA OFFICES:
 Main : Lawton Avenue, Fort Bonifacio, 1634 Taguig City, Philippines Tel. No.: (632) 810-4831 to 41
 Branch : 421 Barraco St. San Nicolas, 1010 Manila, Philippines, Tel. No. (632) 241-3494 to 98
www.namria.gov.ph

Figure A-2.1 BTG-30

Annex 3. Baseline Processing Reports of Control Points used in the LIDAR Survey

1. BTG-30A

Baseline Processing Report

Processing Summary

Observation	From	To	Solution Type	H. Prec. (Meter)	V. Prec. (Meter)	Geodetic Az.	Ellipsoid Dist. (Meter)	ΔHeight (Meter)
BTG-30 -- BTG-30A (B2)	BTG-30	BTG-30A	Fixed	0.004	0.005	190°01'30"	4.793	0.078

Acceptance Summary

Processed	Passed	Flag	Fail
1	1	0	0

Vector Components (Mark to Mark)

From: BTG-30					
Grid		Local		Global	
Easting	290477.094 m	Latitude	N13°45'23.09641"	Latitude	N13°45'17.88182"
Northing	1521536.181 m	Longitude	E121°03'43.87174"	Longitude	E121°03'48.83762"
Elevation	8.942 m	Height	7.820 m	Height	53.872 m

To: BTG-30A					
Grid		Local		Global	
Easting	290476.221 m	Latitude	N13°45'22.94284"	Latitude	N13°45'17.72826"
Northing	1521531.468 m	Longitude	E121°03'43.84397"	Longitude	E121°03'48.80985"
Elevation	9.020 m	Height	7.898 m	Height	53.950 m

Vector					
ΔEasting	-0.872 m	NS Fwd Azimuth	190°01'30"	ΔX	0.096 m
ΔNorthing	-4.713 m	Ellipsoid Dist.	4.793 m	ΔY	1.457 m
ΔElevation	0.078 m	ΔHeight	0.078 m	ΔZ	-4.566 m

Standard Errors

Vector errors:					
σ ΔEasting	0.002 m	σ NS fwd Azimuth	0°01'04"	σ ΔX	0.002 m
σ ΔNorthing	0.001 m	σ Ellipsoid Dist.	0.001 m	σ ΔY	0.002 m
σ ΔElevation	0.002 m	σ ΔHeight	0.002 m	σ ΔZ	0.001 m

Figure A-3.1. BTG-30A

Annex 4. The LIDAR Survey Team Composition

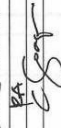
Data Acquisition Component Sub-Team	Designation	Name	Agency/ Affiliation
PHIL-LIDAR 1	Program Leader	ENRICO C. PARINGIT, D.ENG	UP-TCAGP
Data Acquisition Component Leader	Data Component Project Leader - I	ENGR. CZAR JAKIRI SARMIENTO	UP-TCAGP
Survey Supervisor	Data Component Project Leader – I	ENGR. LOUIE P. BALICANTA	UP-TCAGP
	Chief Science Research Specialist (CSRS)	ENGR. CHRISTOPHER CRUZ	UP-TCAGP
		LOVELY GRACIA ACUÑA	UP-TCAGP
	Supervising Science Research Specialist (Supervising SRS)	LOVELYN ASUNCION	UP-TCAGP
FIELD TEAM			
LiDAR Operation	Senior Science Research Specialist (SSRS)	JASMINE ALVIAR	UP-TCAGP
	Research Associate (RA)	ENGR. IRO ROXAS	UP-TCAGP
	RA	MA. REMEDIOS VILLANUEVA	UP-TCAGP
Ground Survey, Data Download and Transfer	RA	ENGR. CHRISTOPHER JOAQUIN	UP-TCAGP
		JERIEL PAUL ALAMBAN	
LiDAR Operation	Airborne Security	SSG LEEJAY PUNZALAN	PHILIPPINE AIR FORCE (PAF)
	Pilot	CAPT. MARK LAWRENCE TANGONAN	ASIAN AEROSPACE CORPORATION (AAC)
		CAPT. JEROME MOONEY	AAC
		CAPT. FRANK PEPITO	AAC

Annex 5. Data Transfer Sheet for Rosario-Lobo Floodplain

DATA TRANSFER SHEET
CALIBRACION 9/7/2015

DATE	FLIGHT NO.	MISSION NAME	SENSOR	RAW LAS		LOGS(MB)	POS	RAW IMAGES/CASI	MISSION LOG FILE/CASI LOGS	RANGE	DIGITIZER	BASE STATION(S)		OPERATOR LOGS (OP LOG)	FLIGHT PLAN		SERVER LOCATION
				Output LAS	KML (svwidth)							BASE STATION(S)	Base Info (lat)		Actual	KML	
15-Aug	3299P	IBLK18KS227A	PEGASUS	535	614	5.45	143	na	na	10.4	na	3.73	1KB	1KB	222	NA	Z:\DACRAW DATA
26-Aug	3341P	IBLK18ANS238A	PEGASUS	* 1.49	NA	10.1	240	na	na	16.1	*na	7.02	1KB	1KB	69	NA	Z:\DACRAW DATA
26-Aug	3343P	IBLK18AGS238B	PEGASUS	1.84	NA	9.44	214	na	na	17.9	na	5.96	1KB	1KB	59	NA	Z:\DACRAW DATA
27-Aug	3345P	IBLK18TS239A	PEGASUS	2.5	NA	7.11	177	na	na	22.5	na	5.99	1KB	1KB	NA	NA	Z:\DACRAW DATA
27-Aug	3347P	IBLK18TS239B	PEGASUS	0.99	NA	6.27	152	na	na	9.85	na	4.13	1KB	1KB	NA	NA	Z:\DACRAW DATA
29-Aug	3353P	IBLK18QRS241A	PEGASUS	1.91	NA	10.3	246	na	na	18.8	na	7.19	1KB	1KB	87.1	NA	Z:\DACRAW DATA
1-Sep	3365P	IBLK18BCS244A	PEGASUS	1.92	NA	8.57	192	na	na	18.2	na	6.61	1KB	1KB	41	NA	Z:\DACRAW DATA
2-Sep	3369P	IBLK18CS245A	PEGASUS	1.34	NA	7.43	154	na	na	13.5	na	35	1KB	1KB	54	NA	Z:\DACRAW DATA

Received from

Name: C. JORDAN
Position: BA
Signature: 

Received by

Name: JOIDA F. PRIETO
Position: SIA
Signature:  7/7/15

1c-2

Figure A-5.1 Data Transfer Sheet for Rosario-Lobo Floodplain - A

DATA TRANSFER SHEET
Calabarzon 9/10/15

DATE	FLIGHT NO.	MISSION NAME	SENSOR	RAW LAS		LOGS(MB)	POS	RAW IMAGES/CASI	MISSION LOG FILE/CASI LOGS	RANGE	DIGITIZER	BASE STATION(S)		OPERATOR LOGS (OPLOG)	FLIGHT PLAN		SERVER LOCATION
				Output LAS	KML (width)							BASE STATION(S)	Base Info (tot)		Actual	KML	
17-Aug	3307P	1BLK18JS229B	Pegasus	972	756	6.66	171	na	na	9.59	na	18.4	1KB	1KB	1/42	na	Z:\DACIRAW DATA
18-Aug	3309P	1BLK18AsS230A	Pegasus	1.17	757	7.85	202	na	na	11.9	na	18.4	1KB	1KB	88	na	Z:\DACIRAW DATA
3-Sep	3373P	1BLK18OS246A	Pegasus	1.81	2.06	9.59	212	na	na	18.2	na	7.67	1KB	1KB	1	na	Z:\DACIRAW DATA
4-Sep	3377P	1BLK18JS247A	Pegasus	1.29	777	8.1	196	na	na	13.4	na	6.43	1KB	1KB	61.6	na	Z:\DACIRAW DATA
5-Sep	3381P	1BLK18OS248A	Pegasus	2.12	1.64	10.3	256	na	na	20.6	na	9.05	1KB	1KB	59/69	na	Z:\DACIRAW DATA

Received from

Name C. J. J. J.
Position RS
Signature [Signature]

Received by

Name K. B. B.
Position SR
Signature [Signature]
Date 9/11/15

Figure A-5.2 Data Transfer Sheet for Rosario-Lobo Floodplain - B

Annex 6. Flight logs for the flight missions

1. Flight Log for 1BLK18QRS241A Mission

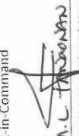
Data Acquisition Flight Log				Flight Log No.: 3353 P
1 LIDAR Operator: MR VILLANUEVA	2 ALTM Model: 060605	3 Mission Name: 1BLK18QRS241A	4 Type: VFR	5 Aircraft Type: Cessna T206H
7 Pilot: M. Tansman	8 Co-Pilot: J. Plomay	9 Route: NAVA - NAVA	12 Airport of Arrival (Airport, City/Province): NAVA	6 Aircraft Identification: 702 Z
10 Date: AUG - 29, 2015	11 Airport of Departure (Airport, City/Province): NAVA	15 Total Engine Time: 3:55	16 Take off: 0636 A	17 Landing: 1021 H
13 Engine On: 0631 H	14 Engine Off: 1026 H	18 Total Flight Time: 3:40		
19 Weather: Partly cloudy				
20 Flight Classification				
20.a Billable		20.b Non Billable		
<input checked="" type="checkbox"/> Acquisition Flight <input type="checkbox"/> Ferry Flight <input type="checkbox"/> System Test Flight <input type="checkbox"/> Calibration Flight		<input type="checkbox"/> LIDAR System Maintenance <input type="checkbox"/> Aircraft Maintenance <input type="checkbox"/> Phil-LIDAR Admin Activities		
21 Remarks: Successful				
22 Problems and Solutions				
<input type="checkbox"/> Weather Problem <input type="checkbox"/> System Problem <input type="checkbox"/> Aircraft Problem <input type="checkbox"/> Pilot Problem <input type="checkbox"/> Others:				
Acquisition Flight Approved by  Signature over Printed Name (End User Representative)		Acquisition Flight Certified by  Signature over Printed Name (PAF Representative)		Lidar Operator  Signature over Printed Name
		Pilot-in-Command  Signature over Printed Name		Aircraft Mechanic/ Technician  Signature over Printed Name

Figure A-6.1 Flight log for 1BLK18QRS241A Mission

2. Flight Log for 1BLK180S248A Mission

Flight Log No.: 53819

10 Acquisition Flight Log		2 ALTM Model: RCASUS		3 Mission Name: IBLK180S248A		4 Type: VFR		5 Aircraft Type: Cessna T200H		6 Aircraft Identification: 9022	
11 LIDAR Operator: 1. Roxas		8 Co Pilot: F. Papito		9 Route: NAIA - NAIA		12 Airport of Arrival (Airport, City/Province): NAIA					
13 Date: SEPT. 5, 2015		14 Engine Off: 1053H		15 Total Engine Time: 4405		16 Take off: 0653H		17 Landing: 1048H		18 Total Flight Time: 3455	
19 Weather		21 Remarks: <i>Aircraft</i>									
20 Flight Classification											
20.a Billable		20.b Non Billable				20.c Others					
<input checked="" type="checkbox"/> Acquisition Flight <input type="checkbox"/> Ferry Flight <input type="checkbox"/> System Test Flight <input type="checkbox"/> Calibration Flight		<input type="checkbox"/> Aircraft Test Flight <input type="checkbox"/> AAC Admins Flight <input type="checkbox"/> Others: _____		<input type="checkbox"/> LIDAR System Maintenance <input type="checkbox"/> Aircraft Maintenance <input type="checkbox"/> Phil LIDAR Admin Activities							
22 Problems and Solutions											
<input type="checkbox"/> Weather Problem <input type="checkbox"/> System Problem <input type="checkbox"/> Aircrafts Problem <input type="checkbox"/> Pilot Problems <input type="checkbox"/> Others: _____											

Acquisition Flight Performed by  Signature over Printed Name (PAB Representative)	Acquisition Flight Certified by  Signature over Printed Name (PAB Representative)	Pilot in Command  Signature over Printed Name	Lidar Operator  Signature over Printed Name	Aircraft Mechanic / Technician  Signature over Printed Name
---	---	--	--	--

Figure A-6.2 Flight log for 1BLK180S248AMission

Annex 7. Flight status reports

CALABARZON
August 29, 2016 and Sept 5, 2016

Table A-7.1. Flight Status Reports

FLIGHT NO	AREA	MISSION	OPERATOR	DATE FLOWN	REMARKS
3353P	QRS	1BLK18QRS241A	MR. VILLANUEVA	August 29,2015	Mission Completed Without Digitizer and Camera
3381P	BLK 18OS	1BLK18OS248A	I. ROXAS	September 5, 2015	Line cut due to heavy cloud buildup Without Digitizer and Camera

SWATH PER FLIGHT MISSION

LAS BOUNDARIES PER FLIGHT

Flight No. : 23244P
Parameters: PRF 200 SF 30 FOV 50

LAS/SWATH



Figure A-7.1 Swath for Flight No. 23244P

Flight No. : 23250P
Parameters: PRF 200 SF 30 FOV 50

LAS/SWATH

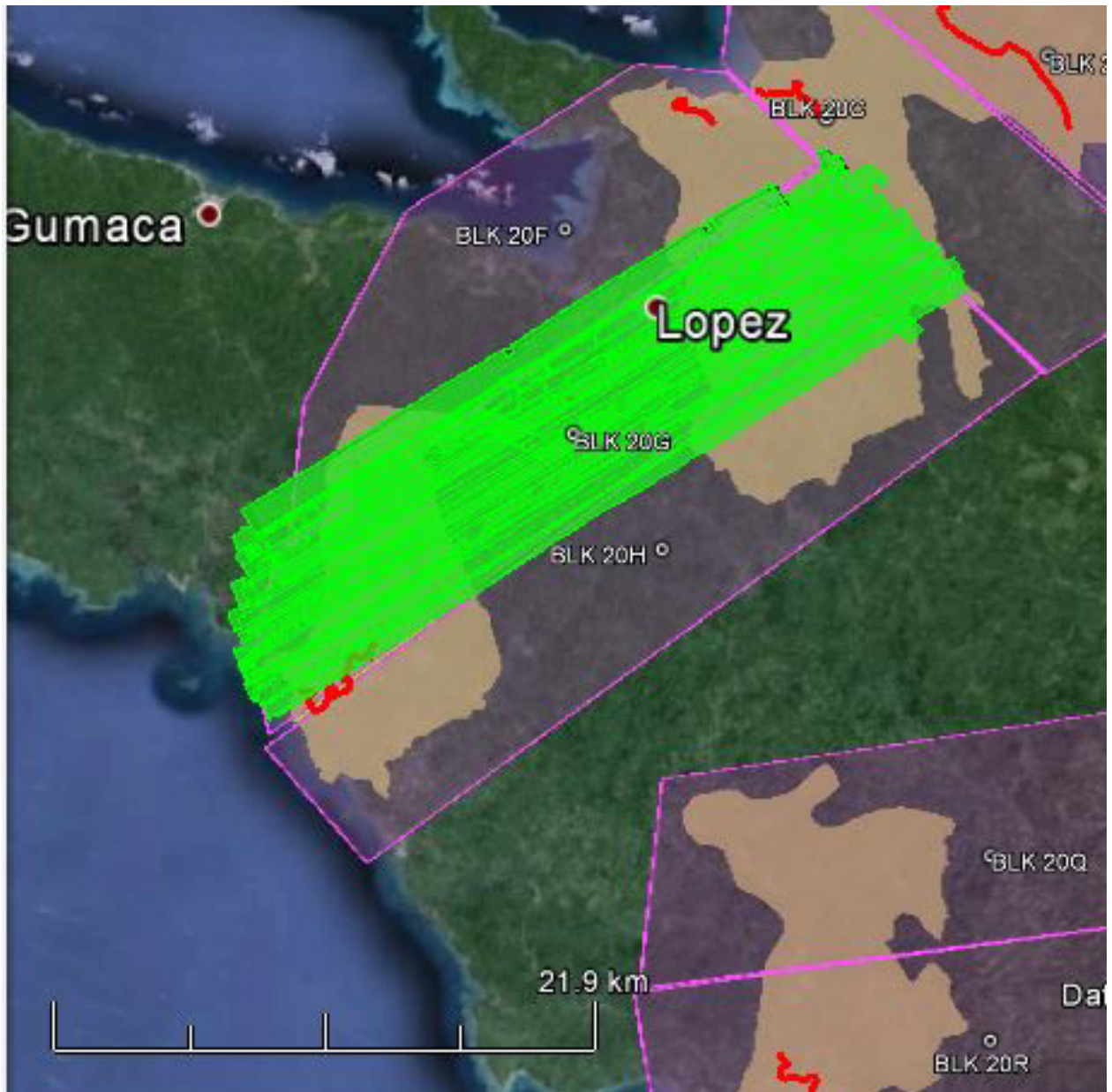


Figure A-7.2 Swath for Flight No. 23250P

Flight No. : 23254P
Parameters: PRF 200 SF 30 FOV 50

LAS/SWATH

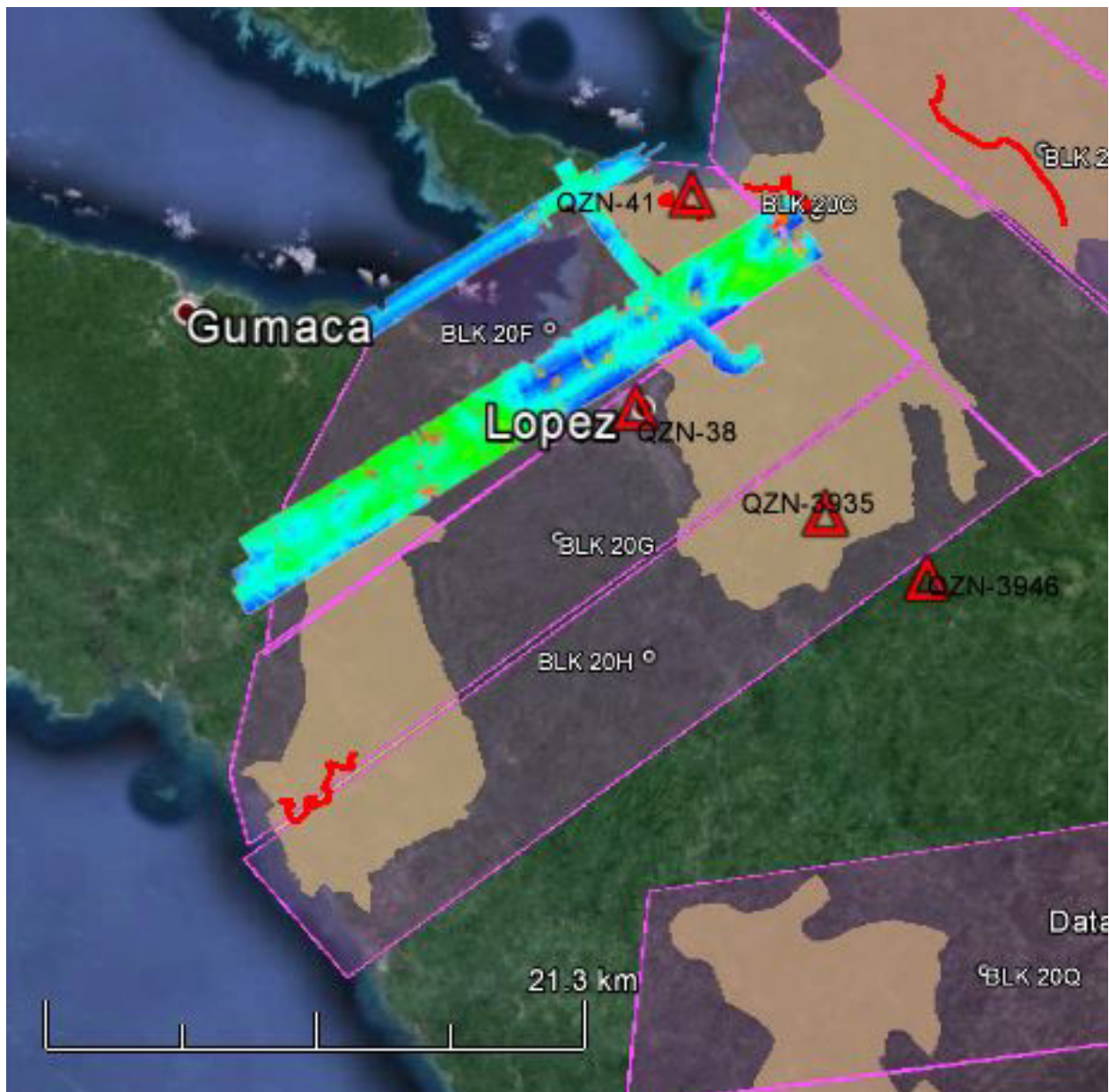


Figure A-7.3 Swath for Flight No. 23254P

Annex 8. Mission Summary Reports

Table A-8.1 Mission Summary Report of Mission Blk18U_supplement

Flight Area	CALABARZON
Mission Name	Blk18U_supplement
Inclusive Flights	3381P
Range data size	20.6 GB
POS	256 MB
Base data size	9.05 MB
Image	N/A
Transfer date	09/11/2015
Solution Status	
Number of Satellites (>6)	Yes
PDOP (<3)	Yes
Baseline Length (<30km)	No
Processing Mode (<=1)	No
Smoothed Performance Metrics (in cm)	
RMSE for North Position (<4.0 cm)	1.1
RMSE for East Position (<4.0 cm)	2.0
RMSE for Down Position (<8.0 cm)	3.3
Boresight correction stdev (<0.001deg)	0.000232
IMU attitude correction stdev (<0.001deg)	0.000478
GPS position stdev (<0.01m)	0.0073
Minimum % overlap (>25)	33.91%
Ave point cloud density per sq.m. (>2.0)	3.00
Elevation difference between strips (<0.20 m)	Yes
Number of 1km x 1km blocks	248
Maximum Height	1142.15 m
Minimum Height	33.16 m
Classification (# of points)	
Ground	116,430,535
Low vegetation	71,532,461
Medium vegetation	215,467,664
High vegetation	328,004,432
Building	10,242,231
Orthophoto	No
Processed by	Engr. Jennifer Saguran, Engr. Melanie Hingpit, Jovy Narisma

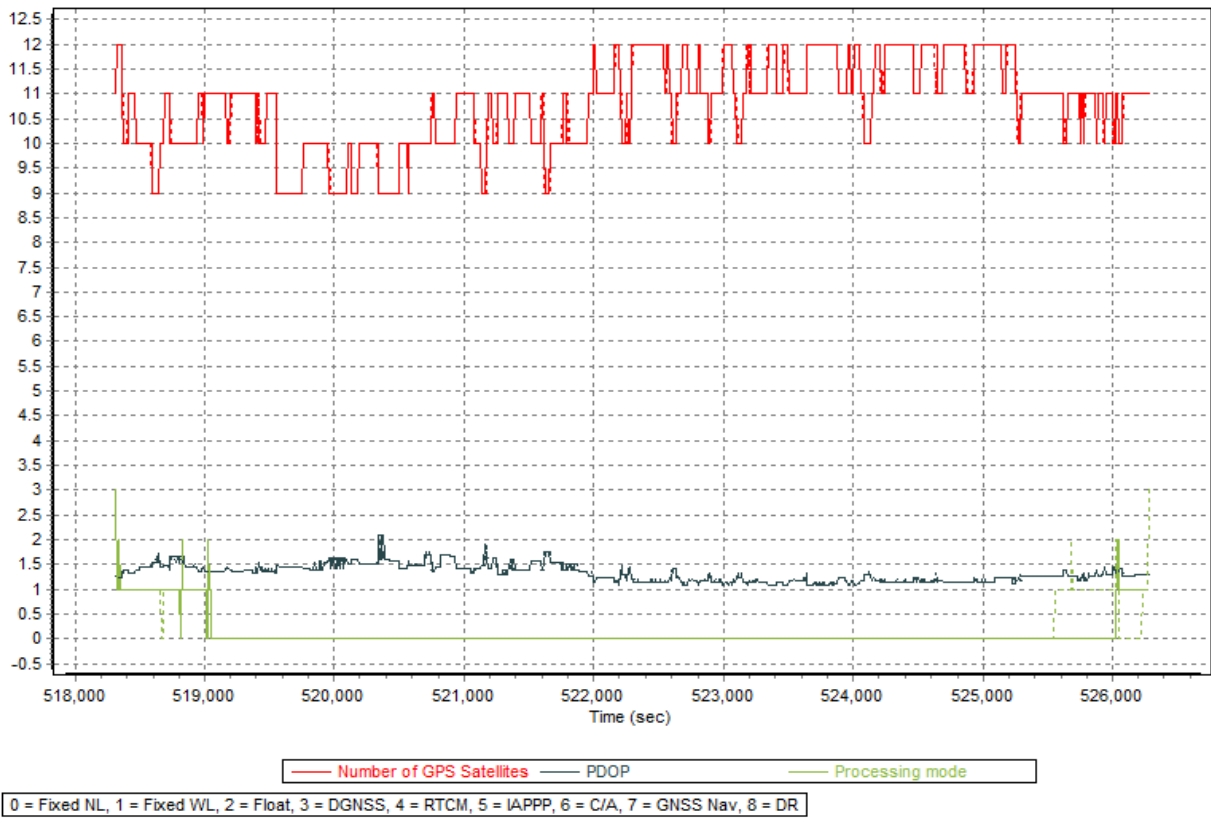


Figure A-8.1 Solution Status

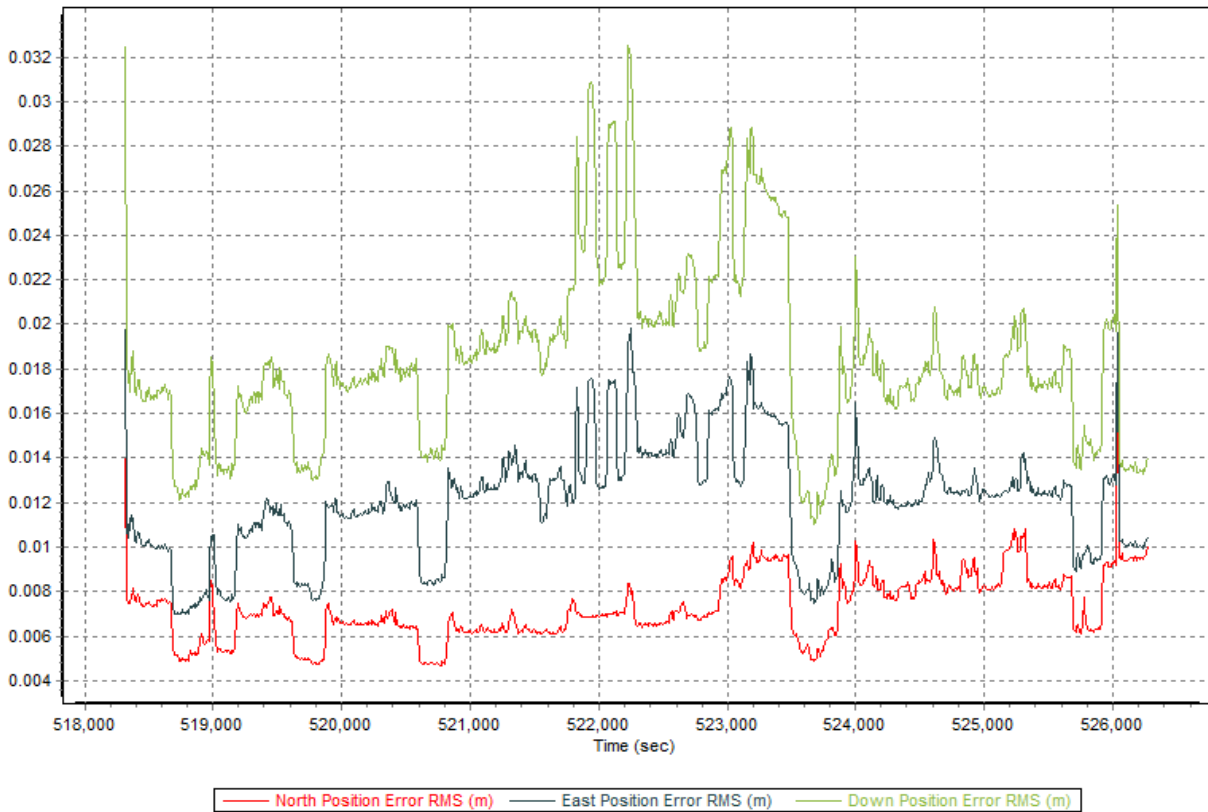


Figure A-8.2. Smoothed Performance Metrics Parameters

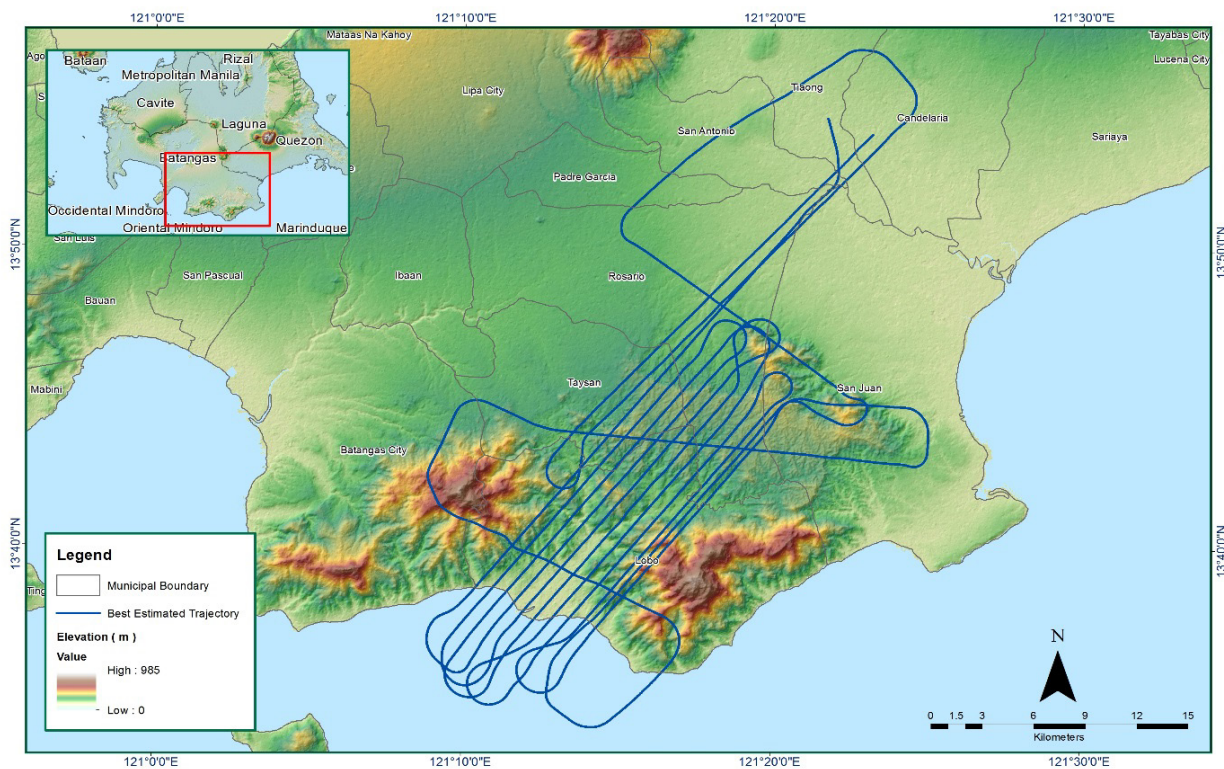


Figure A-8.3. Best Estimated Trajectory

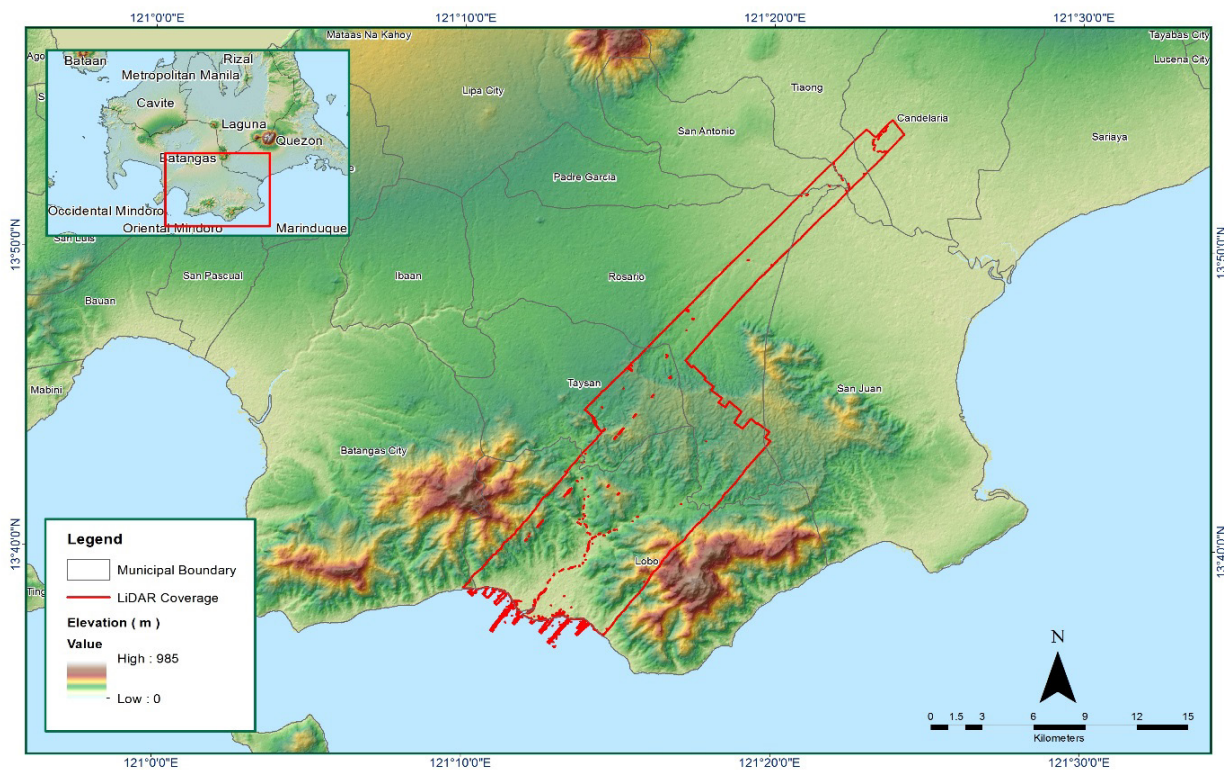


Figure A-8.4. Coverage of LiDAR data

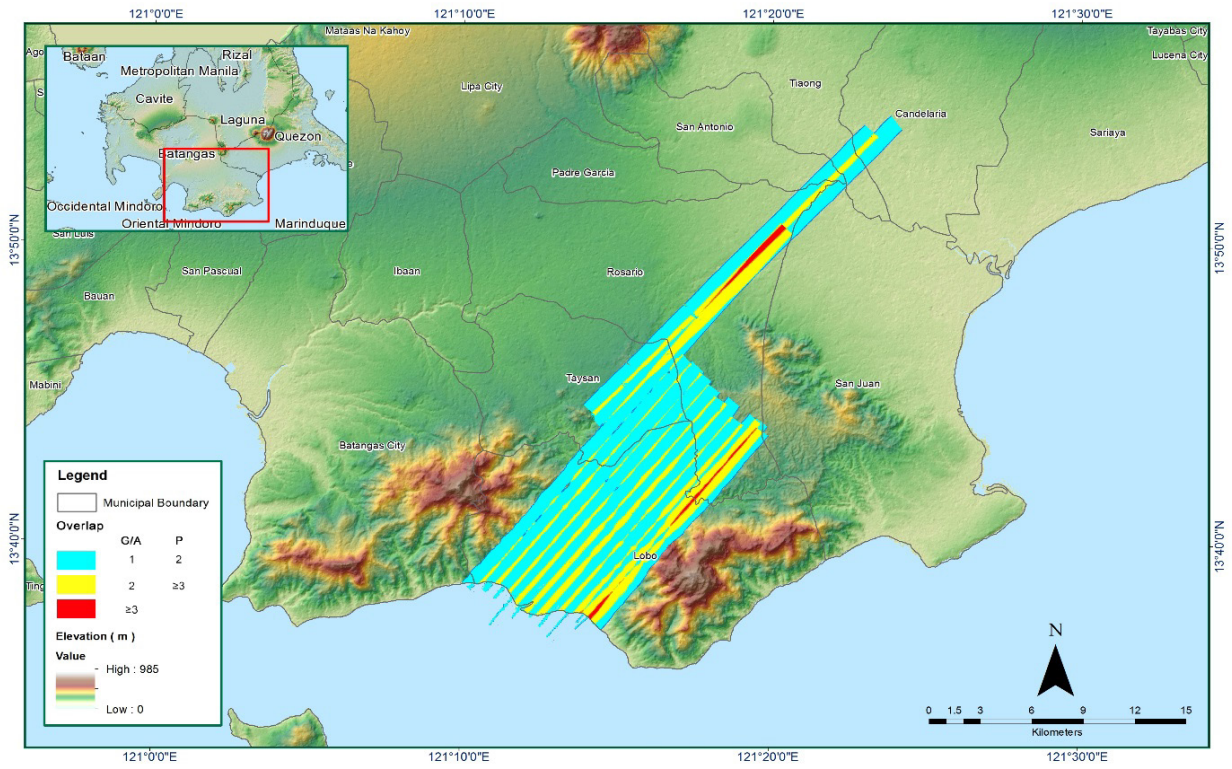


Figure A-8.5. Image of data overlap

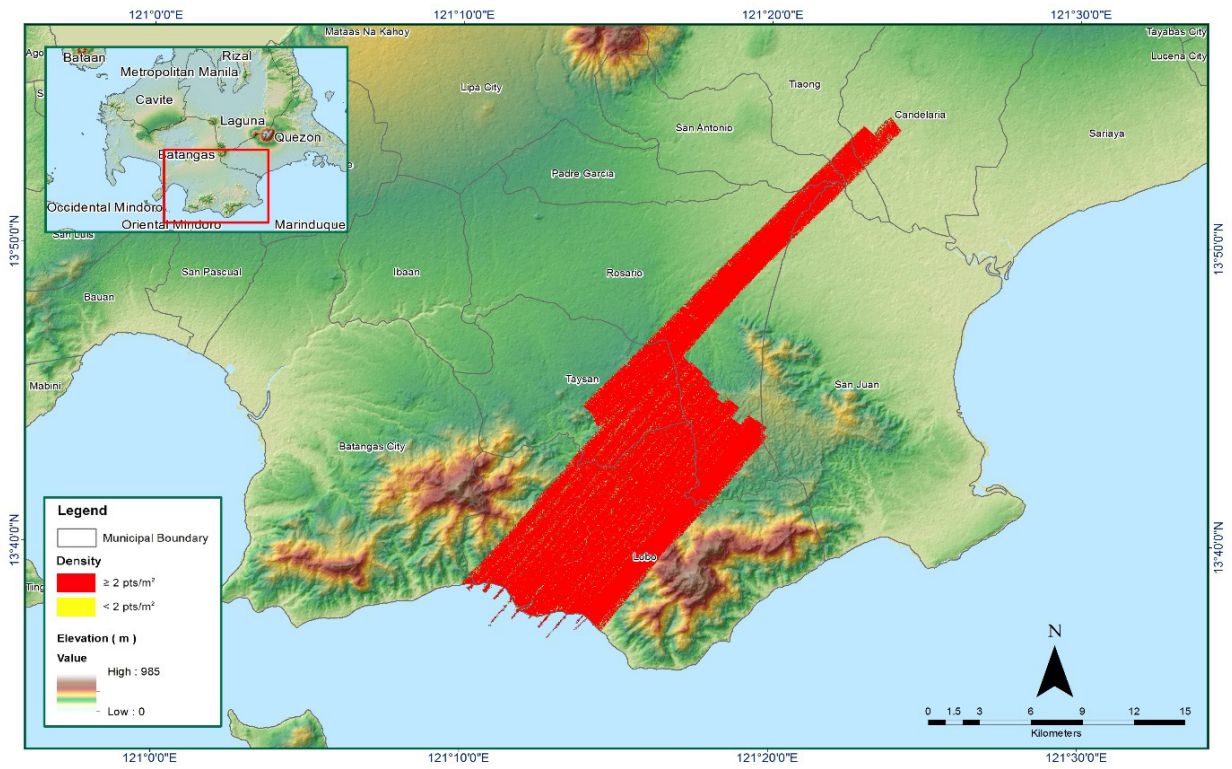


Figure A-8.6. Density map of merged LiDAR data

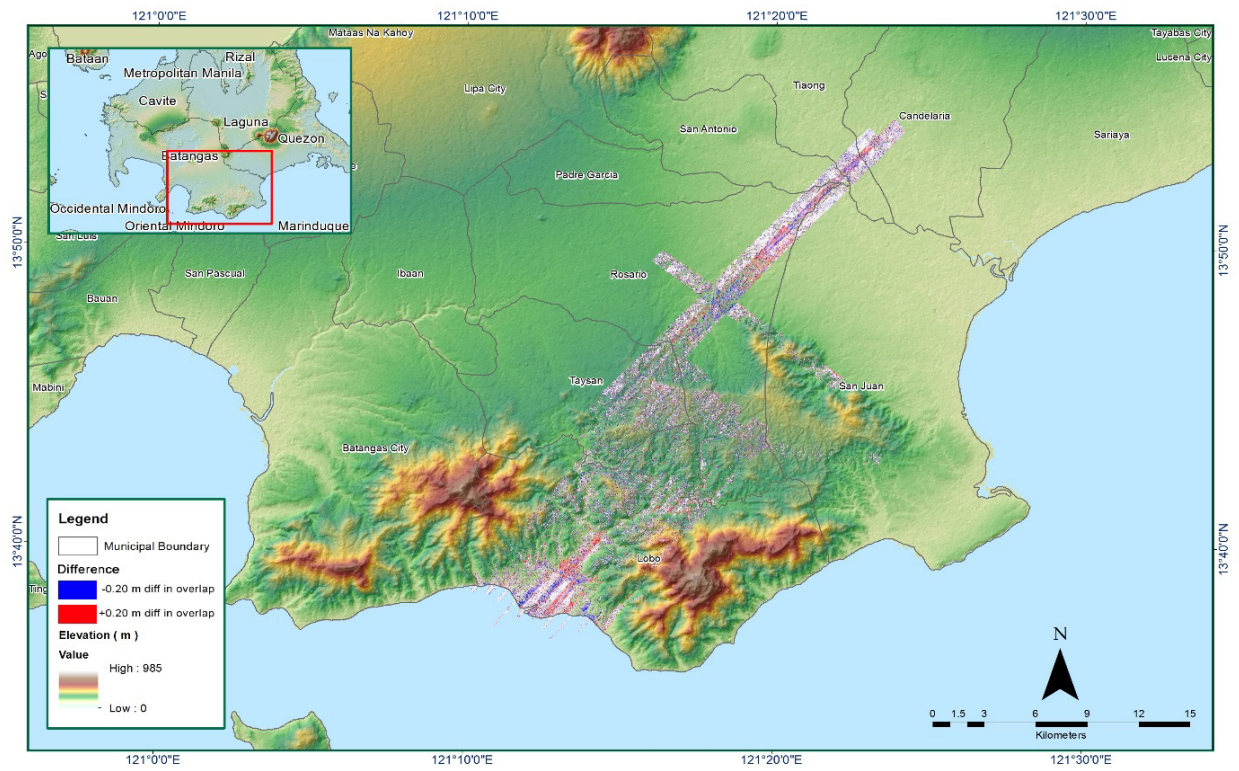


Figure A-8.7. Elevation difference between flight lines

Table A-8.2 Mission Summary Report for Mission Blk18U_additional

Flight Area	CALABARZON
Mission Name	Blk18U_additional
Inclusive Flights	3353P
Range data size	18.8 GB
POS	246 MB
Base data size	7.19 MB
Image	N/A
Transfer date	09/08/2015
Solution Status	
Number of Satellites (>6)	Yes
PDOP (<3)	Yes
Baseline Length (<30km)	No
Processing Mode (<=1)	No
Smoothed Performance Metrics (in cm)	
RMSE for North Position (<4.0 cm)	1.2
RMSE for East Position (<4.0 cm)	1.6
RMSE for Down Position (<8.0 cm)	3.4
Boresight correction stdev (<0.001deg)	0.000181
IMU attitude correction stdev (<0.001deg)	0.000961
GPS position stdev (<0.01m)	0.0026
Minimum % overlap (>25)	34.18%
Ave point cloud density per sq.m. (>2.0)	3.13
Elevation difference between strips (<0.20 m)	Yes
Number of 1km x 1km blocks	192
Maximum Height	749.60 m
Minimum Height	48.73 m
Classification (# of points)	
Ground	79,218,508
Low vegetation	47,266,805
Medium vegetation	163,471,309
High vegetation	423,404,180
Building	12,745,086
Orthophoto	No
Processed by	Engr. Abigail Joy Ching, Aljon Rie Araneta, Engr. Melissa Fernandez

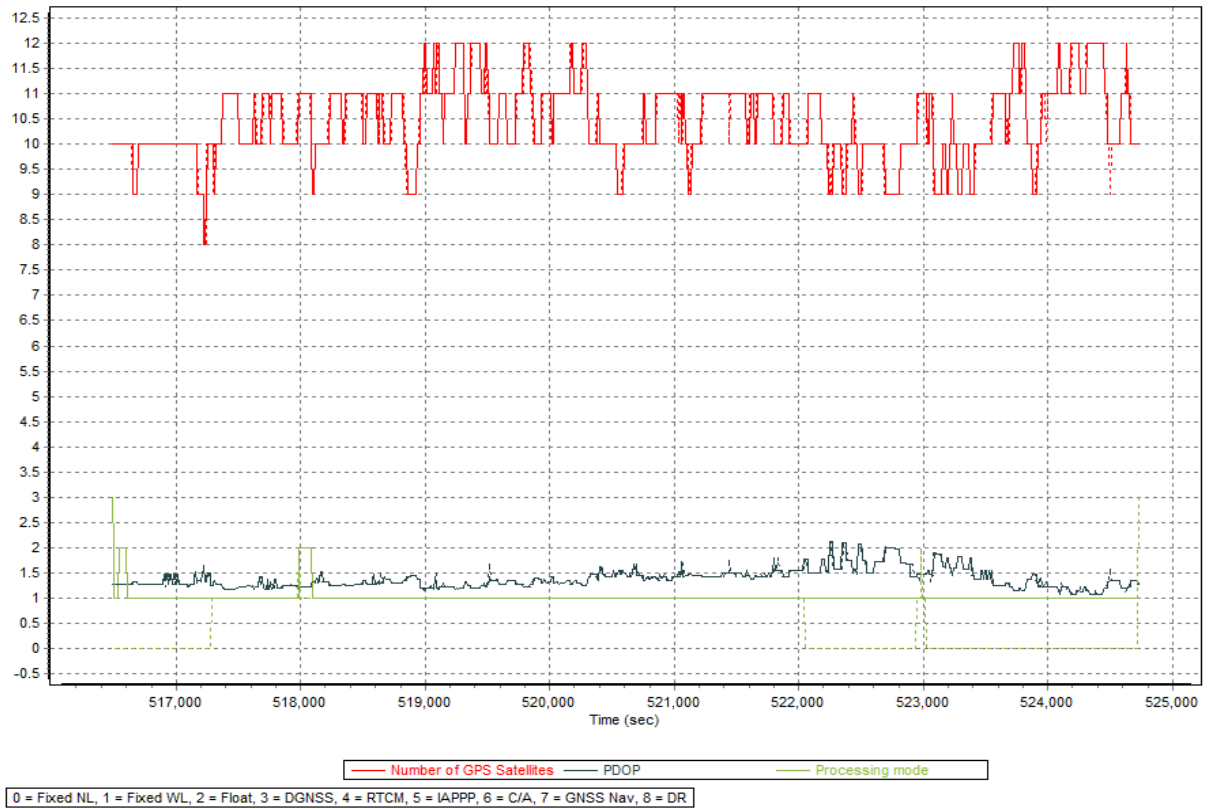


Figure A-8.8. Solution Stat

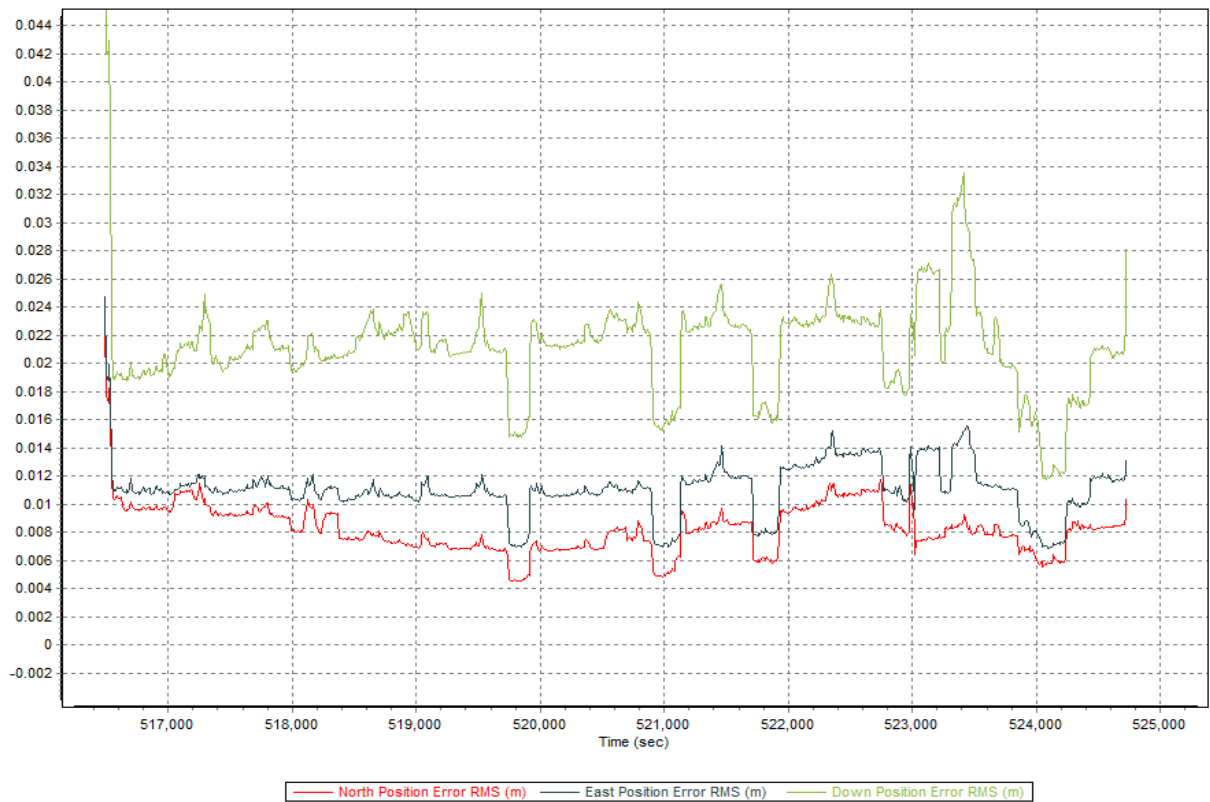


Figure A-8.9. Smoothed Performance Metrics Parameters

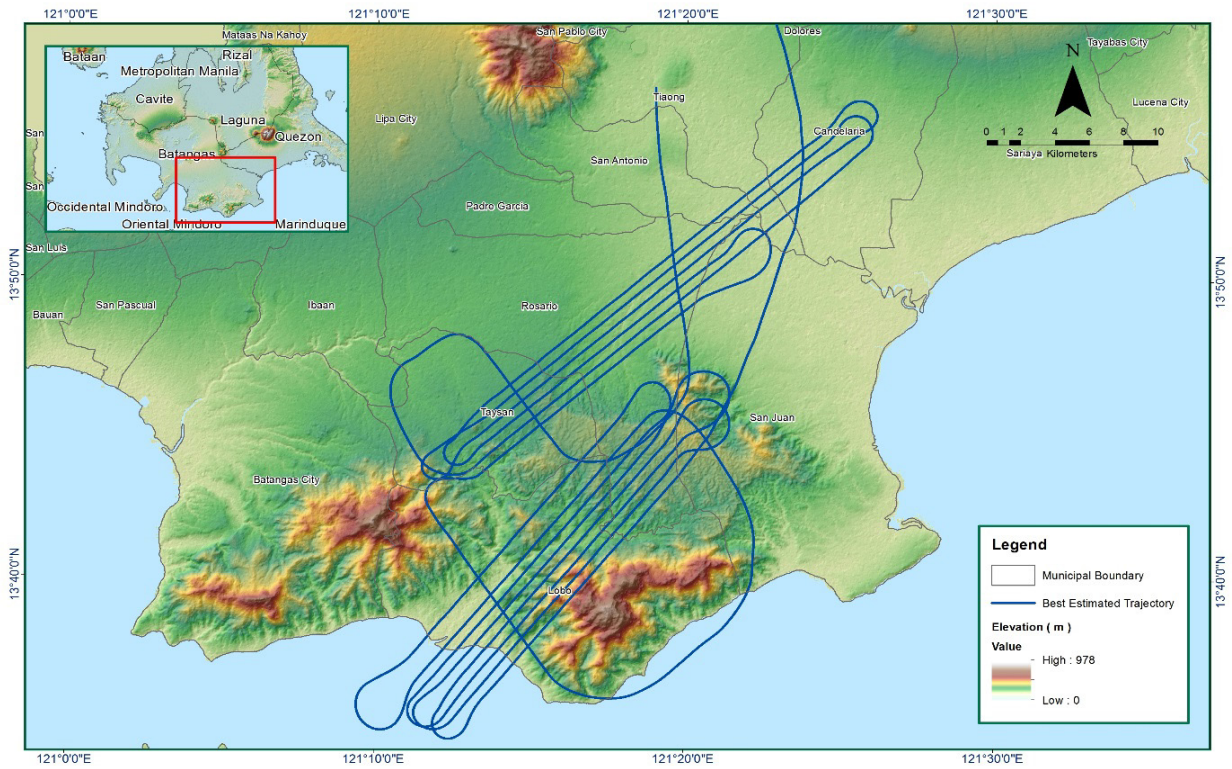


Figure A-8.10. Best Estimated Trajectory

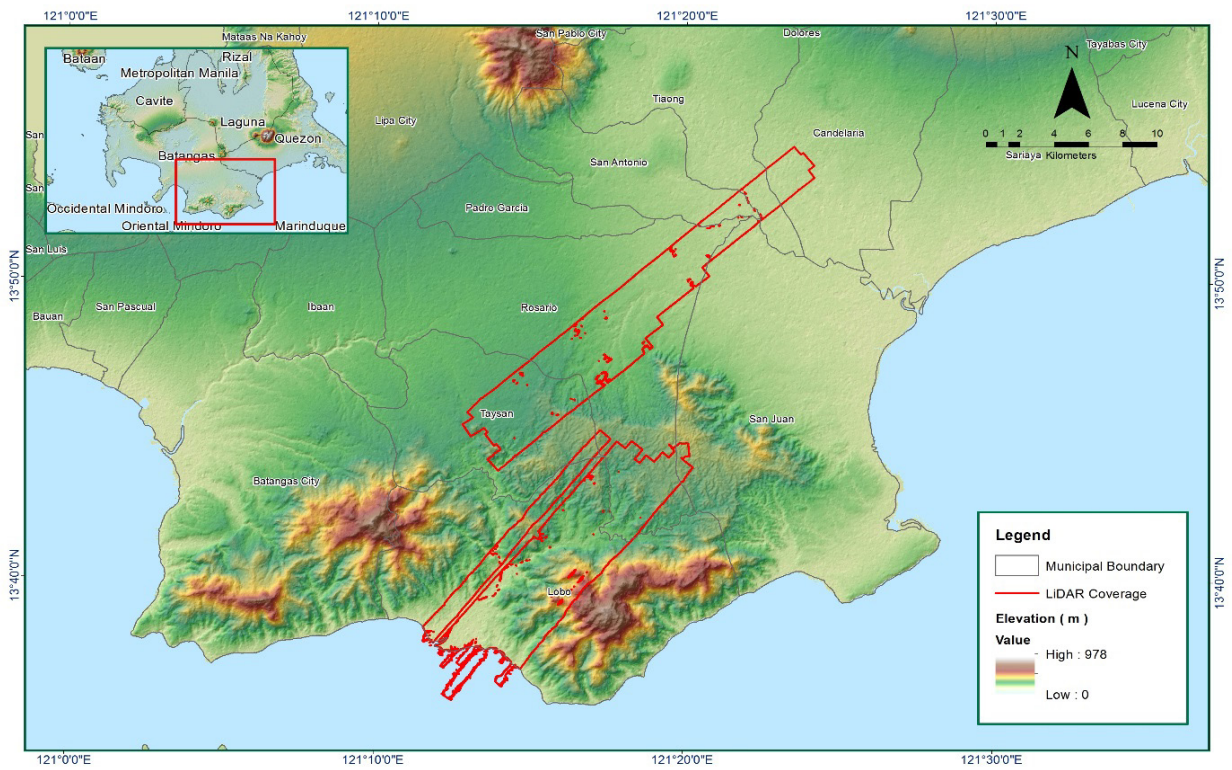


Figure A-8.11. Coverage of LiDAR data

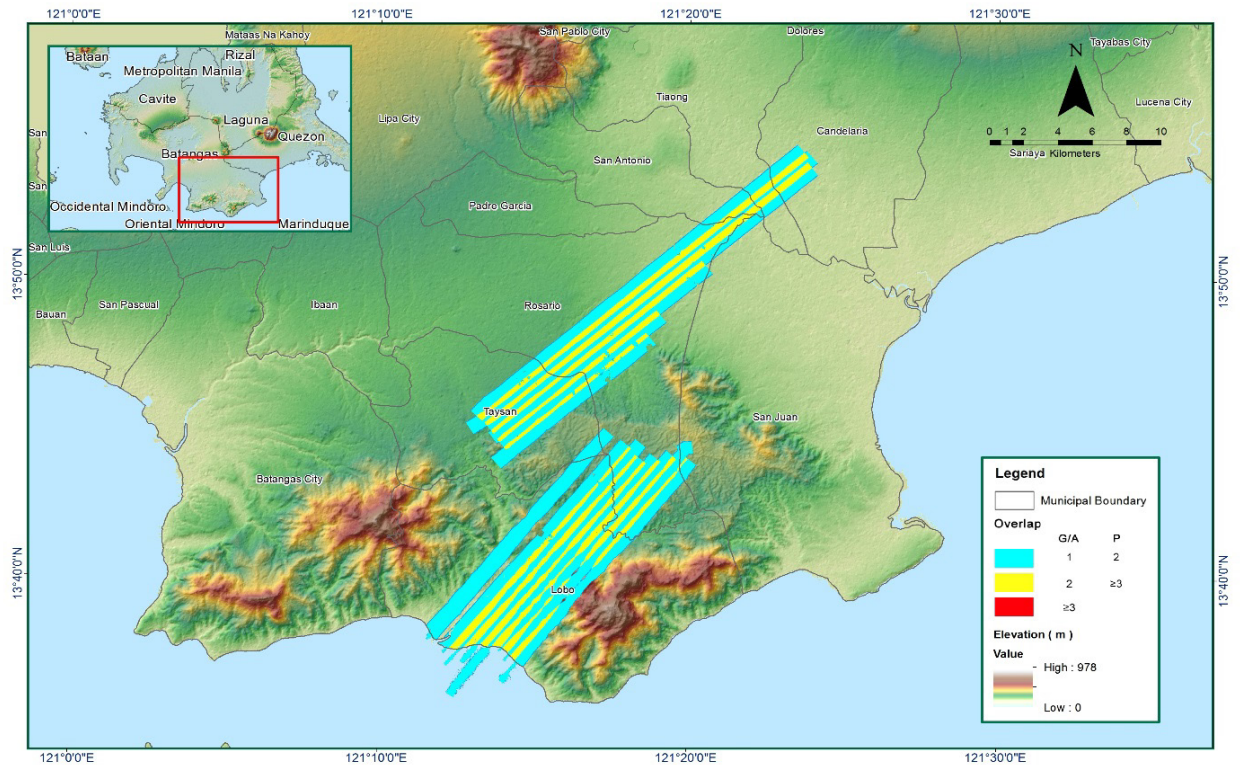


Figure A-8.12. Image of data overlap

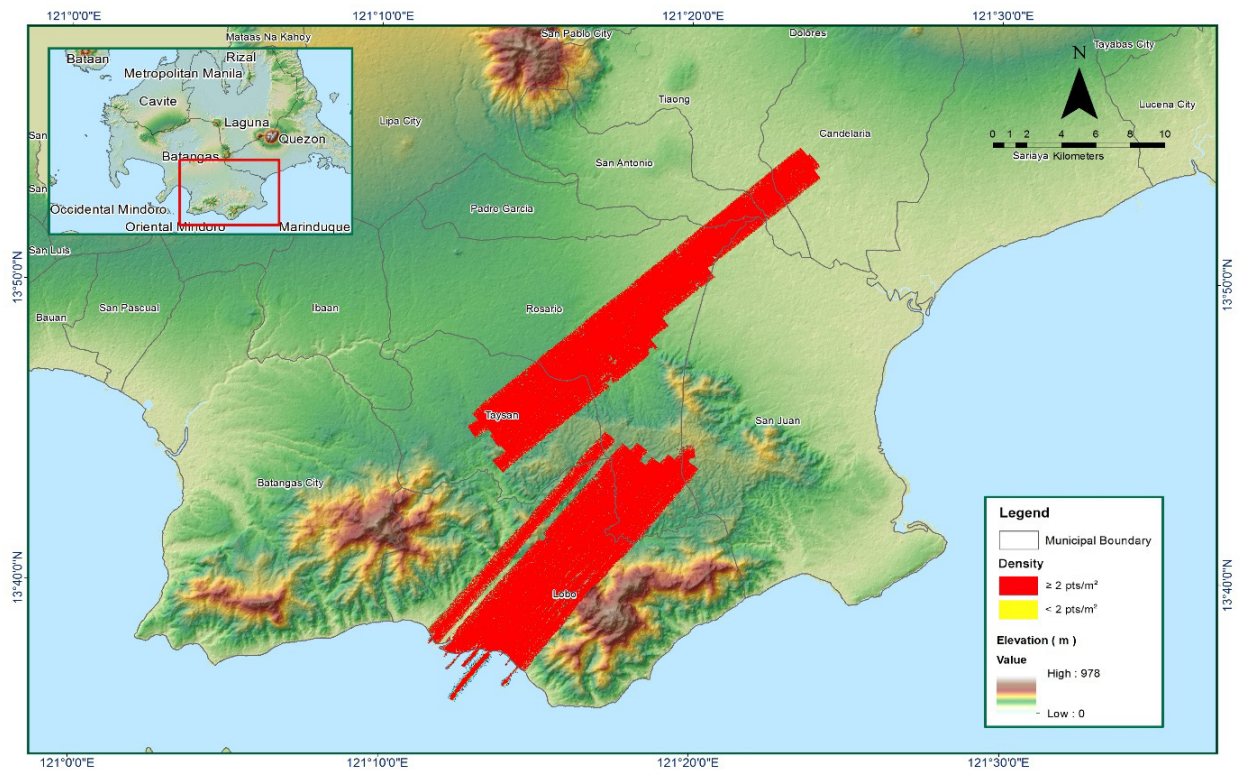


Figure A-8.13. Density map of merged LiDAR data

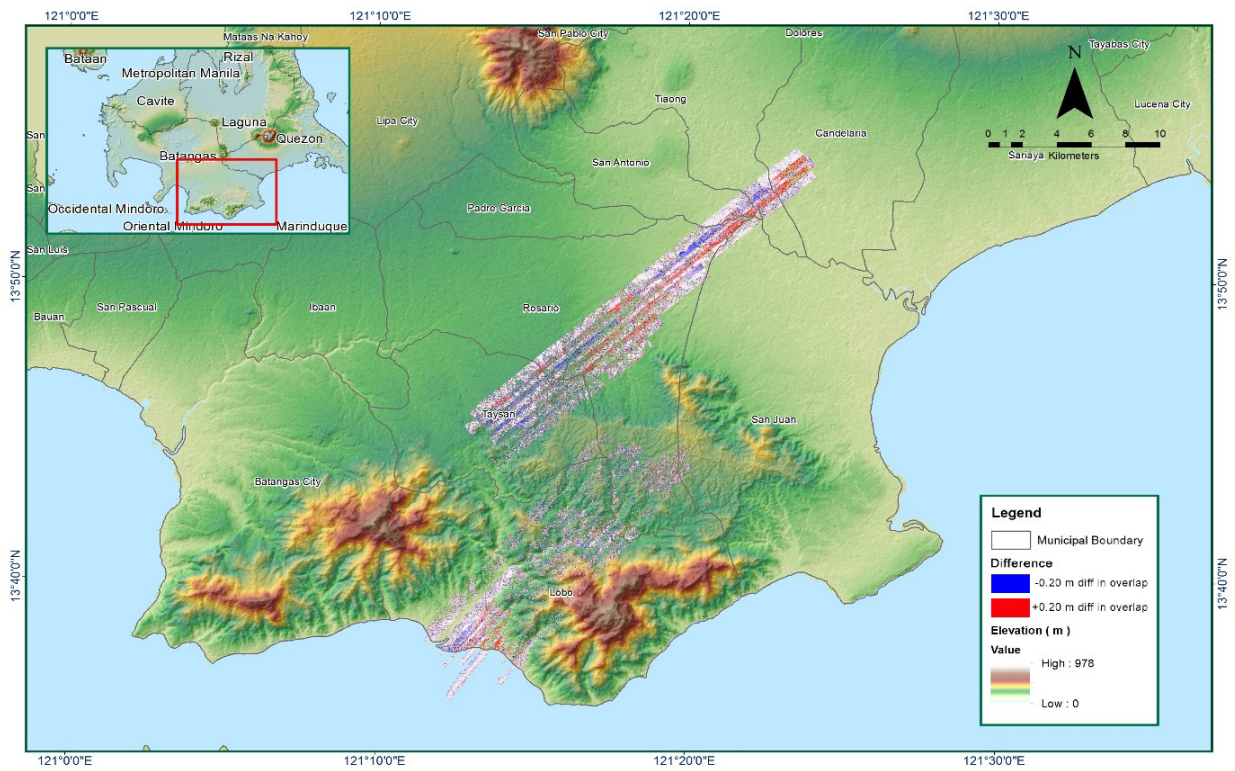


Figure A-8.14. Elevation difference between flight lines

Annex 9. Rosario-Lobo Model Basin Parameters

Table A-9.1 Rosario-Lobo Model Basin Parameters

Basin Number	SCS Curve Number Loss			Clark Unit Hydrograph Transform			Recession Baseflow				
	Initial Abstraction (mm)	Curve Number	Impervious (%)	Time of Concentration (HR)	Storage Coefficient (HR)	Initial Type	Initial Discharge (M3/S)	Recession Constant	Threshold Type	Ratio to Peak	
W1000	3.7937	99	0	0.18549	1.9762	Discharge	0.0330357	0.67343	Ratio to Peak	0.49442	
W1010	7.6127	99	0	1.2843	1.0696	Discharge	0.0262776	1	Ratio to Peak	0.49299	
W1020	0.0250409	93.383	0	0.0166667	1.5241	Discharge	0.0107316	0.9895	Ratio to Peak	0.49722	
W1030	0.31692	98.891	0	0.9277	1.8383	Discharge	0.0051864	0.52373	Ratio to Peak	0.44062	
W1040	0.3729	99	0	0.42105	2.0311	Discharge	0.0268351	0.83898	Ratio to Peak	0.50935	
W1050	3.5628	99	0	0.90623	0.64498	Discharge	0.0035353	0.0576299	Ratio to Peak	0.45973	
W1060	18.703	83.284	0	1.5708	5.9063	Discharge	0.0224537	0.0576391	Ratio to Peak	0.46118	
W1070	4.6938	70.591	0	2.0663	11.957	Discharge	0.0163801	0.0864594	Ratio to Peak	0.5	
W1080	4.8188	53.319	0	0.50329	0.62792	Discharge	0.0852096	0.23842	Ratio to Peak	0.45436	
W1090	1.2736	99	0	1.2855	2.0215	Discharge	0.0261359	1	Ratio to Peak	0.49414	
W1100	9.1838	50.792	0	0.14091	7.0097	Discharge	0.0345346	0.17508	Ratio to Peak	0.49115	
W1110	0.18324	99	0	0.15882	0.34989	Discharge	0.0067197	0.64622	Ratio to Peak	0.50724	
W1120	0.27035	83.052	0	0.62123	2.0312	Discharge	0.0749639	0.65259	Ratio to Peak	0.4482	
W1130	9.559	68.953	0	1.2269	0.87111	Discharge	0.0337547	0.19064	Ratio to Peak	0.49253	
W1140	6.0738	79.325	0	1.2678	2.9106	Discharge	0.0477806	0.28024	Ratio to Peak	0.5	
W1150	0.0184552	66.947	0	0.98373	0.37424	Discharge	0.0277076	0.6529	Ratio to Peak	0.50493	
W1160	0.0152976	99	0	0.15339	0.0805956	Discharge	0.0010871	0.19063	Ratio to Peak	0.77007	
W1170	17.267	81.484	0	4.004	6.9458	Discharge	0.0577668	0.60557	Ratio to Peak	0.5	
W1180	23.287	71.046	0	0.36801	0.8652	Discharge	0.0327404	0.41196	Ratio to Peak	0.5	
W1190	0.74277	99	0	0.29935	0.52543	Discharge	0.0328768	0.65275	Ratio to Peak	0.45447	
W1200	17.209	99	0	0.0166667	0.17462	Discharge	0.0455694	0.60557	Ratio to Peak	0.23333	
W1130	12.658	41.587	0	1.7343	0.64058	Discharge	0.0491961	0.28024	Ratio to Peak	0.5	

W1140	0.27272	86.194	0	0.15351	0.13317	Discharge	0.0174235	0.6054	Ratio to Peak	0.49115
W1150	2.936	76.599	0	9.0247	0.70117	Discharge	0.0848296	0.42151	Ratio to Peak	0.5
W1160	3.4403	53.839	0	1.7968	5.5641	Discharge	0.0312760	0.64973	Ratio to Peak	0.5
W1170	9.0847	45.748	0	2.7258	3.3658	Discharge	0.0937817	0.41196	Ratio to Peak	0.5
W1180	4.0277	79.649	0	1.2876	1.4796	Discharge	0.0569829	0.64789	Ratio to Peak	0.48511
W1190	2.8266	68.3	0	1.77	3.9646	Discharge	0.0304233	0.64973	Ratio to Peak	0.5
W1200	3.9337	80.001	0	0.87244	1.4099	Discharge	0.0270284	0.58196	Ratio to Peak	0.575
W1210	7.2744	84.77	0	1.3712	6.6942	Discharge	0.0268311	0.19064	Ratio to Peak	0.5
W1220	4.893	77.359	0	0.49293	6.8501	Discharge	0.0321406	0.65291	Ratio to Peak	0.5
W620	1.9015	85.453	0	1.5756	2.4793	Discharge	0.0271767	0.65288	Ratio to Peak	0.48511
W630	5.1933	56.761	0	0.64637	2.7844	Discharge	0.0244583	0.65283	Ratio to Peak	0.5
W640	10.548	59.021	0	1.3456	1.172	Discharge	0.0279658	0.19065	Ratio to Peak	0.5
W650	5.0381	90.455	0	0.84817	1.1151	Discharge	0.0101358	0.28024	Ratio to Peak	0.49
W660	31.133	75.67	0	0.26481	0.14495	Discharge	0.0174765	0.41054	Ratio to Peak	0.5
W670	2.9237	50.55	0	2.6239	13.053	Discharge	0.0652386	0.19064	Ratio to Peak	0.5
W680	7.3708	66.95	0	5.0427	19.35	Discharge	0.0518548	0.28024	Ratio to Peak	0.5
W690	13.029	61.191	0	1.3673	0.27796	Discharge	0.0271780	0.41831	Ratio to Peak	0.58931
W700	6.3623	42.282	0	6.0265	27.557	Discharge	0.0767249	0.64974	Ratio to Peak	0.5
W710	8.1849	46.239	0	8.04	23.664	Discharge	0.10368	0.61492	Ratio to Peak	0.5
W720	21.157	91.148	0	3.393	0.50078	Discharge	0.0965781	0.81942	Ratio to Peak	0.5
W730	9.5586	64.582	0	0.4237	3.1447	Discharge	0.0346418	0.64972	Ratio to Peak	0.5
W740	12.125	72.108	0	1.1944	7.0876	Discharge	0.11285	0.61492	Ratio to Peak	0.5
W750	13.14	84.605	0	1.6194	1.4348	Discharge	0.0369947	0.63641	Ratio to Peak	0.5
W760	13.859	88.154	0	0.74495	1.8316	Discharge	0.0028613	0.43312	Ratio to Peak	0.5
W770	4.7347	48.062	0	3.2182	9.5155	Discharge	0.0699748	0.64974	Ratio to Peak	0.5
W780	1.1153	99	0	0.43472	1.5399	Discharge	0.0168012	0.65273	Ratio to Peak	0.4858
W790	11.21	51.135	0	5.6598	14.559	Discharge	0.0379255	0.62079	Ratio to Peak	0.5
W800	5.9187	99	0	1.2311	2.6985	Discharge	0.0104019	0.65299	Ratio to Peak	0.59512

W810	19.712	66.772	0	4.7764	7.0393	Discharge	0.0297056	0.41196	Ratio to Peak	0.5
W820	4.9683	76.333	0	1.534	15.112	Discharge	0.0357580	0.19064	Ratio to Peak	0.5
W830	3.1229	79.669	0	0.17227	10.661	Discharge	0.0134169	0.41196	Ratio to Peak	0.5
W840	4.8192	98.01	0	0.40698	7.8669	Discharge	0.0016617	0.19064	Ratio to Peak	0.5
W850	2.6144	86.196	0	2.8534	0.35892	Discharge	0.0310456	0.6207	Ratio to Peak	0.49709
W860	3.0535	85.158	0	0.86197	1.4721	Discharge	0.0454052	0.72831	Ratio to Peak	0.58762
W870	4.9749	83.63	0	1.1542	4.3548	Discharge	0.0010447	0.19065	Ratio to Peak	0.5
W880	4.4163	90.417	0	1.2303	3.2231	Discharge	0.0286080	0.97466	Ratio to Peak	0.45
W890	4.3983	78.129	0	2.5453	2.8068	Discharge	0.0442665	0.19064	Ratio to Peak	0.4975
W900	15.822	82.334	0	4.4107	2.8398	Discharge	0.0280426	0.28025	Ratio to Peak	0.5
W910	16.933	76.046	0	4.6973	3.7731	Discharge	0.14130	0.60553	Ratio to Peak	0.5
W920	3.7937	99	0	0.18549	1.9762	Discharge	0.0330357	0.67343	Ratio to Peak	0.49442
W930	7.6127	99	0	1.2843	1.0696	Discharge	0.0262776	1	Ratio to Peak	0.49299
W940	0.0250409	93.383	0	0.0166667	1.5241	Discharge	0.0107316	0.9895	Ratio to Peak	0.49722
W950	0.31692	98.891	0	0.9277	1.8383	Discharge	0.0051864	0.52373	Ratio to Peak	0.44062
W960	0.3729	99	0	0.42105	2.0311	Discharge	0.0268351	0.83898	Ratio to Peak	0.50935
W970	3.5628	99	0	0.90623	0.64498	Discharge	0.0035353	0.0576299	Ratio to Peak	0.45973
W980	18.703	83.284	0	1.5708	5.9063	Discharge	0.0224537	0.0576391	Ratio to Peak	0.46118
W990	4.6938	70.591	0	2.0663	11.957	Discharge	0.0163801	0.0864594	Ratio to Peak	0.5

Annex 10. Rosario-Lobo Model Reach Parameters

Table A-10.1 Rosario-Lobo Model Reach Parameters

Reach Number	Muskingum Cunge Channel Routing							Side Slope
	Time Step Method	Length (m)	Slope	Manning's n	Shape	Width		
R100	Automatic Fixed Interval	1475.4	0.0134532	0.0454922	Trapezoid	50	45	
R110	Automatic Fixed Interval	2069.2	0.0259734	0.0200719	Trapezoid	50	45	
R120	Automatic Fixed Interval	1687.2	0.0130403	0.21443	Trapezoid	50	45	
R140	Automatic Fixed Interval	1704.4	0.0081977	0.11795	Trapezoid	50	45	
R190	Automatic Fixed Interval	556.98	0.0033294	0.13638	Trapezoid	50	45	
R230	Automatic Fixed Interval	3589.8	0.0140228	0.13625	Trapezoid	50	45	
R250	Automatic Fixed Interval	1385.4	0.0063823	0.12248	Trapezoid	50	45	
R270	Automatic Fixed Interval	344.56	0.0164253	0.30002	Trapezoid	50	45	
R290	Automatic Fixed Interval	337.99	0.0174861	0.1345	Trapezoid	50	45	
R300	Automatic Fixed Interval	2569.7	0.0093003	0.0695308	Trapezoid	50	45	
R330	Automatic Fixed Interval	1942.0	0.0133701	0.16562	Trapezoid	50	45	
R340	Automatic Fixed Interval	1425.4	0.0093912	0.0695262	Trapezoid	50	45	
R360	Automatic Fixed Interval	2350.7	0.0128619	0.0568927	Trapezoid	50	45	
R370	Automatic Fixed Interval	1491.0	0.0073209	0.0995814	Trapezoid	50	45	
R380	Automatic Fixed Interval	823.97	0.0052045	0.13132	Trapezoid	50	45	
R390	Automatic Fixed Interval	563.55	0.0042550	0.0872329	Trapezoid	50	45	
R410	Automatic Fixed Interval	1352.5	0.0145475	0.07976	Trapezoid	50	45	
R440	Automatic Fixed Interval	1268.1	0.0061834	0.0818315	Trapezoid	50	45	
R450	Automatic Fixed Interval	587.99	0.0012012	0.0148231	Trapezoid	50	45	
R460	Automatic Fixed Interval	1182.3	0.0107549	0.12821	Trapezoid	50	45	
R470	Automatic Fixed Interval	1451.7	0.0077532	0.0219029	Trapezoid	50	45	
R500	Automatic Fixed Interval	2166.8	0.0055008	0.0506519	Trapezoid	50	45	
R520	Automatic Fixed Interval	4475.5	0.0111129	0.022681	Trapezoid	50	45	

R530	Automatic Fixed Interval	1499.2	0.0058561	0.0376477	Trapezoid	50	45
R540	Automatic Fixed Interval	158.99	0.0192522	.000401448	Trapezoid	50	45
R560	Automatic Fixed Interval	2503.8	0.0232141	0.0653373	Trapezoid	50	45
R600	Automatic Fixed Interval	3207.6	0.0050251	0.0109072	Trapezoid	50	45
R610	Automatic Fixed Interval	1443.6	0.005	0.0364003	Trapezoid	50	45
R70	Automatic Fixed Interval	1283.7	0.0137682	0.2678	Trapezoid	50	45
R90	Automatic Fixed Interval	1774.4	0.0184216	0.0207768	Trapezoid	50	45

Annex 11. Rosario-Lobo Flood Validation Data

Table A-11.1 Rosario-Lobo Flood Validation Data

Point Number	Validation Coordinates (in WGS84)		Model Var (m)	Validation Points (m)	Error	Event/Date	Rain Return / Scenario
	Lat	Long					
1	13.627606	121.24	1	0.1	-0.9	Glenda/ July 19, 2014	5-Year
2	13.627789	121.23	0.74	0.1	-0.64	Glenda/ July 19, 2014	5-Year
3	13.628183	121.21	1	1.4	0.4	Glenda/ July 19, 2014	5-Year
4	13.628278	121.21	1.15	1	-0.15	Glenda/ July 19, 2014	5-Year
5	13.628383	121.21	1.29	1.2	-0.09	Glenda/ July 19, 2014	5-Year
6	13.6284	121.21	1.48	1	-0.48	Glenda/ July 19, 2014	5-Year
7	13.628579	121.21	1.09	1.3	0.21	Glenda/ July 19, 2014	5-Year
8	13.628667	121.21	1.26	1.4	0.14	Glenda/ July 19, 2014	5-Year
9	13.628703	121.21	0.03	1.4	1.37	Glenda/ July 19, 2014	5-Year
10	13.628835	121.21	0.16	1.3	1.14	Glenda/ July 19, 2014	5-Year
11	13.628943	121.23	0.03	0.1	0.07	Glenda/ July 19, 2014	5-Year
12	13.628958	121.23	0.45	0.1	-0.35	Glenda/ July 19, 2014	5-Year
13	13.629049	121.23	1.11	0.1	-1.01	Glenda/ July 19, 2014	5-Year
14	13.6291	121.23	1.05	0	-1.05	Glenda/ July 19, 2014	5-Year
15	13.629194	121.21	0.24	1.2	0.96	Glenda/ July 19, 2014	5-Year
16	13.629195	121.23	0.55	0	-0.55	Glenda/ July 19, 2014	5-Year
17	13.629648	121.23	1.04	0.2	-0.84	Glenda/ July 19, 2014	5-Year
18	13.629971	121.21	0.8	0.5	-0.3	Glenda/ July 19, 2014	5-Year
19	13.630084	121.23	1.42	0.1	-1.32	Glenda/ July 19, 2014	5-Year
20	13.6304	121.23	0.28	0	-0.28	Glenda/ July 19, 2014	5-Year
21	13.631501	121.21	0.35	1	0.65	Glenda/ July 19, 2014	5-Year
22	13.632622	121.21	0.32	1.2	0.88	Glenda/ July 19, 2014	5-Year

23	13.633005	121.23	0.18	0	-0.18	Glenda/ July 19, 2014	5-Year
24	13.633205	121.23	0.54	0.3	-0.24	Glenda/ July 19, 2014	5-Year
25	13.633977	121.21	0.59	1.4	0.81	Glenda/ July 19, 2014	5-Year
26	13.634442	121.23	0.56	0	-0.56	Glenda/ July 19, 2014	5-Year
27	13.635535	121.21	0.73	1.3	0.57	Glenda/ July 19, 2014	5-Year
28	13.637884	121.21	0.55	1.2	0.65	Glenda/ July 19, 2014	5-Year
29	13.638712	121.21	0.92	1.3	0.38	Glenda/ July 19, 2014	5-Year
30	13.638845	121.23	0.37	0.1	-0.27	Glenda/ July 19, 2014	5-Year
31	13.638898	121.23	0.06	0.5	0.44	Glenda/ July 19, 2014	5-Year
32	13.639146	121.2	0.22	0.7	0.48	Glenda/ July 19, 2014	5-Year
33	13.639426	121.2	0.26	1	0.74	Glenda/ July 19, 2014	5-Year
34	13.63957	121.2	0.14	0.5	0.36	Glenda/ July 19, 2014	5-Year
35	13.639575	121.23	0.17	0.6	0.43	Glenda/ July 19, 2014	5-Year
36	13.639957	121.19	0.18	0.1	-0.08	Glenda/ July 19, 2014	5-Year
37	13.639998	121.2	0.16	0.6	0.44	Glenda/ July 19, 2014	5-Year
38	13.640074	121.19	1.88	0	-1.88	Glenda/ July 19, 2014	5-Year
39	13.640273	121.2	0.03	0.6	0.57	Glenda/ July 19, 2014	5-Year
40	13.640298	121.19	1.03	0.4	-0.63	Glenda/ July 19, 2014	5-Year
41	13.641085	121.19	1.21	0.1	-1.11	Glenda/ July 19, 2014	5-Year
42	13.64115	121.21	4.9000001	1	-3.9000001	Glenda/ July 19, 2014	5-Year
43	13.641598	121.19	0.66	0	-0.66	Glenda/ July 19, 2014	5-Year
44	13.641849	121.19	4.2199998	0.5	-3.7199998	Glenda/ July 19, 2014	5-Year
45	13.642124	121.21	3.8800001	0	-3.8800001	Glenda/ July 19, 2014	5-Year
46	13.642336	121.21	4	0	-4	Glenda/ July 19, 2014	5-Year
47	13.642353	121.21	4.98	0	-4.98	Glenda/ July 19, 2014	5-Year

48	13.642618	121.21	4.3600001	0	-4.3600001	Glenda/ July 19, 2014	5-Year
49	13.642641	121.21	0.49	0	-0.49	Glenda/ July 19, 2014	5-Year
50	13.642676	121.21	4	0	-4	Glenda/ July 19, 2014	5-Year
51	13.6427	121.2	4.2199998	0.2	-4.0199998	Glenda/ July 19, 2014	5-Year
52	13.642759	121.21	0.1	0	-0.1	Glenda/ July 19, 2014	5-Year
53	13.642762	121.21	0.96	0	-0.96	Glenda/ July 19, 2014	5-Year
54	13.642891	121.19	4	0	-4	Glenda/ July 19, 2014	5-Year
55	13.642951	121.21	0.12	0	-0.12	Glenda/ July 19, 2014	5-Year
56	13.643021	121.21	0.36	0	-0.36	Glenda/ July 19, 2014	5-Year
57	13.643492	121.21	4.0300002	0	-4.0300002	Glenda/ July 19, 2014	5-Year
58	13.643513	121.21	0.93	0	-0.93	Glenda/ July 19, 2014	5-Year
59	13.643515	121.19	4.2800002	0	-4.2800002	Glenda/ July 19, 2014	5-Year
60	13.643569	121.21	4.7399998	0	-4.7399998	Glenda/ July 19, 2014	5-Year
61	13.643607	121.2	0.09	0	-0.09	Glenda/ July 19, 2014	5-Year
62	13.644166	121.21	5.1300001	0	-5.1300001	Glenda/ July 19, 2014	5-Year
63	13.644181	121.19	0.04	0.4	0.36	Glenda/ July 19, 2014	5-Year
64	13.644224	121.21	0.21	0	-0.21	Glenda/ July 19, 2014	5-Year
65	13.64426	121.21	0.19	0	-0.19	Glenda/ July 19, 2014	5-Year
66	13.644263	121.19	0.03	0.3	0.27	Glenda/ July 19, 2014	5-Year
67	13.644422	121.21	0.88	0	-0.88	Glenda/ July 19, 2014	5-Year
68	13.644477	121.21	4.8499999	0	-4.8499999	Glenda/ July 19, 2014	5-Year
69	13.644536	121.21	0.05	0	-0.05	Glenda/ July 19, 2014	5-Year
70	13.644768	121.23	0.84	0.2	-0.64	Glenda/ July 19, 2014	5-Year
71	13.64488	121.23	0.39	0.1	-0.29	Glenda/ July 19, 2014	5-Year
72	13.645056	121.22	0.04	1.4	1.36	Glenda/ July 19, 2014	5-Year

73	13.645069	121.18	0.2	0	-0.2	Glenda/ July 19, 2014	5-Year
74	13.645069	121.21	0.66	0	-0.66	Glenda/ July 19, 2014	5-Year
75	13.645104	121.18	5.46	0	-5.46	Glenda/ July 19, 2014	5-Year
76	13.645114	121.23	0.4	0	-0.4	Glenda/ July 19, 2014	5-Year
77	13.645123	121.18	0.37	0	-0.37	Glenda/ July 19, 2014	5-Year
78	13.645151	121.18	0.22	0	-0.22	Glenda/ July 19, 2014	5-Year
79	13.645155	121.23	0.61	0.2	-0.41	Glenda/ July 19, 2014	5-Year
80	13.645188	121.23	1.5700001	0.5	-1.0700001	Glenda/ July 19, 2014	5-Year
81	13.645244	121.21	0.62	0	-0.62	Glenda/ July 19, 2014	5-Year
82	13.645353	121.21	0.06	0	-0.06	Glenda/ July 19, 2014	5-Year
83	13.645554	121.21	0.29	0	-0.29	Glenda/ July 19, 2014	5-Year
84	13.645676	121.23	0.5	0.1	-0.4	Glenda/ July 19, 2014	5-Year
85	13.645918	121.21	0.29	0.2	-0.09	Glenda/ July 19, 2014	5-Year
86	13.64601	121.21	0.36	0	-0.36	Glenda/ July 19, 2014	5-Year
87	13.646075	121.21	0.06	0	-0.06	Glenda/ July 19, 2014	5-Year
88	13.646198	121.21	0.03	0	-0.03	Glenda/ July 19, 2014	5-Year
89	13.646226	121.23	0.04	0.2	0.16	Glenda/ July 19, 2014	5-Year
90	13.646233	121.21	0.03	0.1	0.07	Glenda/ July 19, 2014	5-Year
91	13.646367	121.23	0.03	0.1	0.07	Glenda/ July 19, 2014	5-Year
92	13.6464	121.21	0.03	0	-0.03	Glenda/ July 19, 2014	5-Year
93	13.646418	121.21	0.05	0.5	0.45	Glenda/ July 19, 2014	5-Year
94	13.646422	121.21	0.39	0.1	-0.29	Glenda/ July 19, 2014	5-Year
95	13.646481	121.22	0.11	0	-0.11	Glenda/ July 19, 2014	5-Year
96	13.646588	121.22	0.03	0.2	0.17	Glenda/ July 19, 2014	5-Year
97	13.6466	121.21	0.1	0.1	0	Glenda/ July 19, 2014	5-Year

98	13.646698	121.21	0.03	0	-0.03	Glenda/ July 19, 2014	5-Year
99	13.646775	121.21	0.5	0.1	-0.4	Glenda/ July 19, 2014	5-Year
100	13.646778	121.21	0.28	0.6	0.32	Glenda/ July 19, 2014	5-Year
101	13.646881	121.22	0.05	0	-0.05	Glenda/ July 19, 2014	5-Year
102	13.646948	121.21	0.03	0.1	0.07	Glenda/ July 19, 2014	5-Year
103	13.647085	121.21	0.16	0.4	0.24	Glenda/ July 19, 2014	5-Year
104	13.647106	121.21	0.03	1	0.97	Glenda/ July 19, 2014	5-Year
105	13.647116	121.21	0.03	0.3	0.27	Glenda/ July 19, 2014	5-Year
106	13.647155	121.21	0.18	0	-0.18	Glenda/ July 19, 2014	5-Year
107	13.647381	121.21	0.1	0	-0.1	Glenda/ July 19, 2014	5-Year
108	13.647543	121.21	0.03	0	-0.03	Glenda/ July 19, 2014	5-Year
109	13.64764	121.22	0.13	1.3	1.17	Glenda/ July 19, 2014	5-Year
110	13.647656	121.21	0.84	0	-0.84	Glenda/ July 19, 2014	5-Year
111	13.647689	121.21	0.03	0	-0.03	Glenda/ July 19, 2014	5-Year
112	13.647966	121.21	0.03	0.1	0.07	Glenda/ July 19, 2014	5-Year
113	13.648124	121.21	0.27	0	-0.27	Glenda/ July 19, 2014	5-Year
114	13.648229	121.21	0.03	0	-0.03	Glenda/ July 19, 2014	5-Year
115	13.64831	121.21	0.04	0	-0.04	Glenda/ July 19, 2014	5-Year
116	13.648319	121.21	0.03	0.2	0.17	Glenda/ July 19, 2014	5-Year
117	13.648397	121.21	0.03	0	-0.03	Glenda/ July 19, 2014	5-Year
118	13.648413	121.22	0.03	1.2	1.17	Glenda/ July 19, 2014	5-Year
119	13.648664	121.21	0.04	0	-0.04	Glenda/ July 19, 2014	5-Year
120	13.64248	121.21	0	3.8800001	-3.88	Rosing/ October 30, 1995	5-Year
121	13.642828	121.21	0	4.3600001	-4.36	Rosing/ October 30, 1995	5-Year
122	13.642943	121.21	0	4.7199998	-4.72	Rosing/ October 30, 1995	5-Year

123	13.643202	121.21	0	4.7399998	-4.74	Rosing/ October 30, 1995	5-Year
124	13.643288	121.21	0	3.5999999	-3.6	Rosing/ October 30, 1995	5-Year
125	13.643493	121.21	0	3.25	-3.25	Rosing/ October 30, 1995	5-Year
126	13.643635	121.21	0	4	-4	Rosing/ October 30, 1995	5-Year
127	13.643697	121.21	0	4.1300001	-4.13	Rosing/ October 30, 1995	5-Year
128	13.643913	121.21	0	3.6700001	-3.67	Rosing/ October 30, 1995	5-Year
129	13.643918	121.21	0	3.3299999	-3.33	Rosing/ October 30, 1995	5-Year
130	13.643925	121.21	0	3.1500001	-3.15	Rosing/ October 30, 1995	5-Year
131	13.644098	121.21	0	4.0300002	-4.03	Rosing/ October 30, 1995	5-Year
132	13.644296	121.21	0	4.1999998	-4.2	Rosing/ October 30, 1995	5-Year
133	13.644495	121.21	0	3.9400001	-3.94	Rosing/ October 30, 1995	5-Year
134	13.64456	121.21	0	4.6700001	-4.67	Rosing/ October 30, 1995	5-Year
135	13.644583	121.21	0	3.26	-3.26	Rosing/ October 30, 1995	5-Year
136	13.6448	121.21	0	4.4099998	-4.41	Rosing/ October 30, 1995	5-Year
137	13.644894	121.21	0	4.75	-4.75	Rosing/ October 30, 1995	5-Year
138	13.644901	121.21	0	3.5699999	-3.57	Rosing/ October 30, 1995	5-Year
139	13.645666	121.21	0	3.26	-3.26	Rosing/ October 30, 1995	5-Year
140	13.647819	121.21	0	5.3200002	-5.32	Rosing/ October 30, 1995	5-Year
141	13.647991	121.21	0	5.46	-5.46	Rosing/ October 30, 1995	5-Year
142	13.648137	121.21	0	5.5700002	-5.57	Rosing/ October 30, 1995	5-Year
143	13.648441	121.21	0	5.6599998	-5.66	Rosing/ October 30, 1995	5-Year
144	13.657122	121.22	0.1	0.23	-0.13	Rosing/ October 30, 1995	5-Year
145	13.659882	121.23	3	2.6900001	0.31	Rosing/ October 30, 1995	5-Year
146	13.666824	121.23	0.2	0.04	0.16	Rosing/ October 30, 1995	5-Year
147	13.627535	121.24	0.1	0.29	-0.19	Yolanda/ November 9, 2013	5-Year

148	13.6389	121.23	0.1	0.37	-0.27	Yolanda/ November 9, 2013	5-Year
149	13.643056	121.21	0	3.53	-3.53	Yolanda/ November 9, 2013	5-Year
150	13.64325	121.21	0	3.0799999	-3.08	Yolanda/ November 9, 2013	5-Year
151	13.644102	121.21	0	3.25	-3.25	Yolanda/ November 9, 2013	5-Year
152	13.644224	121.21	0	4.1900001	-4.19	Yolanda/ November 9, 2013	5-Year
153	13.644358	121.21	0	0.78	-0.78	Yolanda/ November 9, 2013	5-Year
154	13.644398	121.21	0	0.64	-0.64	Yolanda/ November 9, 2013	5-Year
155	13.644572	121.21	0	4.2800002	-4.28	Yolanda/ November 9, 2013	5-Year
156	13.644671	121.21	0	3.9400001	-3.94	Yolanda/ November 9, 2013	5-Year
157	13.644761	121.21	0	3.95	-3.95	Yolanda/ November 9, 2013	5-Year
158	13.645114	121.21	0	3.3299999	-3.33	Yolanda/ November 9, 2013	5-Year
159	13.645456	121.21	0	3.4000001	-3.4	Yolanda/ November 9, 2013	5-Year
160	13.645527	121.21	0	4.4400001	-4.44	Yolanda/ November 9, 2013	5-Year
161	13.6458	121.21	0	3.26	-3.26	Yolanda/ November 9, 2013	5-Year
162	13.645805	121.21	0.2	4.8200002	-4.62	Yolanda/ November 9, 2013	5-Year
163	13.645918	121.21	0	4.9200001	-4.92	Yolanda/ November 9, 2013	5-Year
164	13.645918	121.21	0.2	3.54	-3.34	Yolanda/ November 9, 2013	5-Year
165	13.647114	121.21	0	5.0500002	-5.05	Yolanda/ November 9, 2013	5-Year
166	13.647351	121.21	0.5	5.2199998	-4.72	Yolanda/ November 9, 2013	5-Year
167	13.654671	121.22	0.6	0.03	0.57	Yolanda/ November 9, 2013	5-Year
168	13.654834	121.22	0.5	2.9300001	-2.43	Yolanda/ November 9, 2013	5-Year
169	13.656888	121.22	0.1	1.55	-1.45	Yolanda/ November 9, 2013	5-Year
170	13.665109	121.23	2.5	3.3900001	-0.89	Yolanda/ November 9, 2013	5-Year
171	13.665789	121.23	0.1	0.72	-0.62	Yolanda/ November 9, 2013	5-Year

Annex 12. Educational Institutions Affected in Rosario-Lobo Floodplain

Table A-12.1 Educational Institutions in Lobo, Batangas affected by flooding in Rosario-Lobo Floodplain

Batangas				
Lobo				
Building Name	Barangay	Rainfall Scenario		
		5-year	25-year	100-year
BALATBAT ELEM. SCHOOL	Balatbat	None	None	None
MASAGUITSIT-BANALO NATIONAL HIGH SCHOOL	Fabrica	None	None	None
MASAGUITSIT ELEM. SCHOOL	Fabrica	None	Low	Low
MASAGUITSIT ELEM. SCHOOL STAGE	Fabrica	None	None	None
DAY CARE CENTER	Lagadlarin	Low	Medium	Medium
LAGADLARIN-OLO OLO ELEM. SCHOOL	Lagadlarin	Low	Medium	Medium
LOBO INSTITUTE INC.	Lagadlarin	Low	Medium	Medium
DAY CARE CENTER	Mabilog Na Bundok	Low	Low	Low
BATANGAS STATE UNIVERSITY	Masaguitsit	Low	Medium	Medium
MASAGUITSIT-BANALO NATIONAL HIGH SCHOOL	Masaguitsit	None	None	None
MASAGUITSIT ELEM. SCHOOL	Masaguitsit	None	Low	Low
MASAGUITSIT ELEM. SCHOOL STAGE	Masaguitsit	None	None	None
DAY CARE CENTER	Nagtalongtong	None	Medium	High
DAY CARE CENTER	Nagtoctoc	High	High	High
NAGTALUNTONG ELEM. SCHOOL	Nagtoctoc	None	None	None
DAY CARE CENTER	Olo-Olo	Medium	High	High
MABILOG NA BUNDOK ELEM. SCHOOL	Olo-Olo	Low	Medium	Medium
LOBO CENTRAL SCHOOL	Poblacion	None	None	Low
LORD IMMANUEL INSTITUTE FOUNDATION INC.	Poblacion	Low	Low	Low
DAY CARE CENTER	Soloc	None	None	None

Annex 13. Health Institutions Affected in Rosario-Lobo Floodplain

Table A-13.1 Health Institutions in Lobo, Batangas affected by flooding in Rosario-Lobo Floodplain

Batangas				
Lobo				
Building Name	Barangay	Rainfall Scenario		
		5-year	25-year	100-year
HEALTH CENTER	Fabrica	None	None	None
LOBO MUNICIPAL HOSPITAL	Fabrica	None	None	None
MULTIPURPOSE HALL	Olo-Olo	None	None	Low
LOBO HEALTH CENTER	Poblacion	None	Low	Low
HEALTH CENTER	Soloc	None	None	None
HEALTH CENTER	Tayuman	Low	Medium	Medium